CHARACTERIZATION OF KINESIN MOTOR PROTEINS AND EVOLUTION OF A MEIOTIC DRIVE ELEMENT IN ZEA MAYS

by

DAVID MICHAEL HIGGINS

(Under the Direction of R. Kelly Dawe)

ABSTRACT

Kinesins are microtubule motor proteins responsible for a diverse set of functions within cells. One particular subfamily of kinesins, kinesin-14A, is implicated in organization of the microtubule spindle and chromosome segregation during cell division. In this dissertation, we characterized two members of the kinesin-14A subfamily in the crop plant *Zea mays* (maize).

Using a candidate gene based approach, we identified the underlying gene of the *divergent spindle1* (*dv1*) locus to be a member of the kinesin-14A subfamily and provided additional evidence through identification of a second, new allele within the same gene. Loss of function of *dv1* results in wider, longer spindles in male meiocytes in maize. Live cell imaging indicates *dv1* functions late in metaphase to focus the spindle pole, but also suggests a role in prometaphase as well.

Previous work identified *kinesin driver* (*Kindr)*, a novel kinesin-14 unique to maize which is implicated in the abnormal chromosome 10 (Ab10) meiotic drive system. Plants carrying an RNAi-induced knockdown of *Kindr* expression lost the drive phenotype, indicating this gene is necessary for meiotic drive. Transcriptome sequencing

of several but not all mutant Ab10 lines deficient for the drive phenotype show reduced expression of *Kindr*, indicating this gene is not sufficient for meiotic drive. Both immunolocalization and a fluorescent protein tag were used to image *KINDR* localization within cells.

Further study of the Ab10 system was focused on identifying the deleterious effects preventing it from reaching fixation in populations. No evidence was found to suggest Ab10 transmission is inhibited through pollen. Ab10 homozygotes have reduced pollen viability, seed count, and seed weight than wild type siblings, suggesting a homozygous disadvantage to carrying Ab10. Deleterious SNPs were identified in the inverted shared region between Ab10 and normal chromosome 10 which may be responsible for decreased fitness. Variations in rates of drive and *Kindr* expression were identified in a diversity panel of maize carrying Ab10. A phylogeny of Ab10 haplotypes indicates recombination between these chromosomes in nature.

INDEX WORDS: kinesin motor protein, cell division, microtubule organization, meiotic drive, abnormal chromosome 10

CHARACTERIZATION OF KINESIN MOTOR PROTEINS AND EVOLUTION OF A MEIOTIC DRIVE ELEMENT IN ZEA MAYS

by

DAVID MICHAEL HIGGINS

BS, North Carolina State University, 2012

A Dissertation Submitted to the Graduate Faculty of The University of Georgia in Partial Fulfillment of the Requirements for the Degree

DOCTOR OF PHILOSOPHY

ATHENS, GEORGIA

2017

CHARACTERIZATION OF KINESIN MOTOR PROTEINS AND EVOLUTION OF A MEIOTIC DRIVE ELEMENT IN ZEA MAYS

by

DAVID MICHAEL HIGGINS

Major Professor:	R. Kelly Dawe
Committee:	Marcus Fechheimer
	Wolfgang Lukowitz
	Richard Meagher
	Xiaoyu Zhang

Electronic Version Approved:

Suzanne Barbour
Dean of the Graduate School
The University of Georgia
May 2017

ACKNOWLEDGEMENTS

I would like to thank my advisor R. Kelly Dawe for his steady mentorship and constant support in all aspects of my doctoral training. In addition, I would like to thank the members of my dissertation committee Marcus Fechheimer, Wolfgang Lukowitz, Richard Meagher, Xiaoyu Zhang, and former committee members Jim Leebens-Mack and David Nelson for their research advice and critique of my dissertation projects, always aimed at making me a more capable, successful scientist.

I would like to acknowledge fellow members of the Dawe Lab for their contributions to my projects at lab group meetings as well as assistance at the bench. In particular, I would like to thank Jonathan Gent and Natalie Nannas, two postdoctoral researchers whose knowledge of biology contributed a lot to my training and mentorship.

I would like to acknowledge my graduate student peers in the Plant Biology and Genetics departments for providing immeasurable academic and personal support throughout the completion of my degree.

This work was funded by a grant from the Graduate School at the University of Georgia, a Palfrey Research Grant from the Department of Plant Biology at the University of Georgia, and the National Science Foundation.

TABLE OF CONTENTS

LIST OF TABLES

Page

LIST OF FIGURES

Page

CHAPTER 1

INTRODUCTION AND LITERATURE REVIEW

The diverse forms of eukaryotic life are grounded in the complexity of their cells. In the transition from the prokaryotic to eukaryotic habit, cellular tasks were compartmentalized into specialized structures called organelles. The size of cells grew along with the size of their genomes which evolved from a circular piece of DNA to linear DNA molecules called chromosomes. Underlying the development of these new cellular structures is the need for a cell to organize these components so that it may optimize their benefits for survival.

The cytoskeleton is a complex network of proteins that are present in all forms of eukaryotic life. These cable-like structures provide a scaffold throughout the cell while also serving as an avenue for the movement of molecules and organelles. There are two classes of structures that together comprise the cytoskeleton. The first, known as microfilaments, are thread-like structures comprised of polymerized actin proteins. The second class of structures are known as microtubules.

As their name implies, microtubules are cylindrical, tube-like structures composed of polymerized monomers of the tubulin protein family. Two subunits known as α-tubulin and β-tubulin first form a dimer pair before polymerizing into the larger microtubule structure. Polymerization is favored by the binding of a guanosine triphosphate (GTP) cofactor to the α/β dimer (Nogales et al., 1998). Activation with GTP

promotes assembly of the tubulin subunits into the canonical hollow cylindrical structure which is consistently 24nm in diameter (Ledbetter and Porter, 1963). If the GTP cap is maintained, the microtubule will continue to grow and elongate in a process known as nucleation. However, if the GTP cap is hydrolyzed to guanosine diphosphate (GDP), the microtubule will quickly depolymerize in a process known as microtubule catastrophe (as reviewed in Howard and Hyman, 2009). It is important to note that microtubules exhibit directionality with one exhibiting dynamic growth and shrinking known as the plus end and one end which is relatively more stable known as the minus end (Allen and Borisy, 1974).

The polarity of microtubules caused by the alternating alignment of α- and β-tubulin subunits is not insignificant. Proteins known as plus-end tracking proteins (+TIPs) specifically bind to the plus end of microtubules. Localization of specific proteins to the plus-end of microtubules allows the cell to immediately respond and 'rescue' microtubules undergoing catastrophe (Komarova et al., 2002). Directionality is also recognized by kinesins, a class of motor enzymes that are able to move along the length of microtubules which will be discussed later.

ROLES OF MICROTUBULES

Microtubules play a number of roles in maintaining homeostasis in eukaryotic cells. As mentioned previously, one of their key roles is to serve as a guide for transportation of cellular components. The yeast *Saccharomyces cerevisiae* forms a protrusion called a shmoo as it begins searching for a mate. Microtubules originating from the nuclear envelope specifically bind at this site, positioning and adjusting the

location of the nucleus for its eventual fusion with its mate (Maddox et al., 1999). The classic structure of an animal neuron cell is to have a large cell body with a narrow protrusion called an axon. Microtubules in neurons nucleate from the cell body (minus-end) through the axon (plus-end) to dendrites which interact with neighboring neurons to transmit electrochemical signals. Axonal transport was shown to decrease following inhibition of kinesins, implicating a role for microtubules as networks for transportation (Amaratunga et al., 1993). Microtubules are critical for the structure and function of flagella, whip-like projections of motile cells. In these organelles, pairs of microtubules form a ring along the length of the flagella; regulated sliding of individual microtubule pairs causes the structure to rotate and propel the cell through its environment (structure reviewed in Luck, 1984). In plants, the formation of cell walls has also been shown to be associated with microtubules. The localization of cellulose synthase, an enzyme which produces the cell wall component cellulose, is directly coordinated by microtubules (Paredez et al., 2006). This targeted deposition of cell wall components allows plant cells to take on specific shapes, such as long and narrow pipe-like cells of the vascular tissue.

Perhaps the most critical role of microtubules is also a conserved process among all eukaryotes: cell division. As cells enter mitosis and prepare to divide, microtubules reorganize from their interphase network into a cone-shaped structure known as a spindle. Minus-ends gather together at the point of the spindle while plus-ends nucleate toward the condensed chromosomes, attaching at kinetochores in prophase. Spindles adjust the positions of the chromosomes until they are aligned in metaphase. The chromosome pairs are then split apart and moved along microtubules in opposite

direction in anaphase before two new daughter cells are formed in telophase and cytokinesis.

Although some slight variation exists between different cell types and different organisms, the roles that microtubules play in interphase and cell division as a cellular transportation network are highly conserved across eukaryotes. Despite this conservation, the manner in which microtubule nucleation is organized is not consistent between yeast, animals, and plants. Each of these types of organisms have developed their own unique microtubule organizing centers (MTOCs) that are structurally distinct from one another and are outlined below.

SPINDLE POLE BODIES AND CENTROSOMES

The spindle pole body (SPB) in budding yeast (*S. cerevisiae*) is perhaps the most well understood MTOC. The SPB is a complex of proteins embedded in the nuclear envelope and is distinguished from animal and plant cells in that it is capable of nucleating microtubules in two opposite directions: centrifugally into the cytoplasm and centripetally into the nucleus.

The structure of the SPB has been well characterized using electron microscopy, revealing stacks of protein layers aligned into discs (O'Toole et al., 1999). At the core of the structure of stable stacks is a layer known as the central plaque comprised of spindle pole component 42 (Spc42), Spc29, and Calmodulin1 (Cmd1) whose interactions were identified using fluorescence tagging and Förster resonance energy transfer (FRET) (Muller et al., 2005). These proteins form a core lattice that is bound to the nuclear envelope through interactions with Bbp1, Mps2, and ultimately the integral membrane

protein Mps3 (Jaspersen et al., 2006). The two surfaces of this lattice are polarized by different interactions on either face. The cytoplasmic face binds three additional components Cnm67, Nud1 and Spc72 at Spc42 (Gruneberg et al., 2000). The nuclear face of the central plaque binds Spc110, an α-coiled-coil protein (Elliott et al., 1999). Both Spc72 (cytosolic) and Spc110 (nuclear) are capable of binding the same γ-tubulin complex comprised of Tub4, Spc97, and Spc98 the immediate site of microtubule nucleation (Knop and Schiebel, 1997;1998).

The centrosome is the major MTOC of animal cells. The mature centrosome is made of two bundles of microtubules called centrioles which are positioned at roughly a 90 degree angle to one another. Only one centriole of the pair, called the mother centriole, is capable of nucleating microtubules. While the canonical structure of the SPB is a series of layers, the structure of centrioles can be better described as a ring of pipes bound together in a barrel configuration. Differences have arisen in individual species, but the standard arrangement of microtubules in the centriole follows a 9*3 arrangement, where microtubules are grouped in triplet with nine sets of triplets forming the centriole. The ring of microtubule triplets is bound in its center to centrin, a calcium-binding protein is required for centrosome duplication (Salisbury et al., 2002). A member of the tubulin family called δ-tubulin is implicated in the assembly of the 9*3 structure; centrioles in mutants deficient in this gene have pairs of microtubules rather than triplets incorporated into centrioles of basal bodies accompanying their flagella (Dutcher and Trabuco, 1998). Glutamylation and other post-translational modifications mark the centriole to further stabilize the structure The end result is a highly durable structure which allows the centrioles to maintain their shape and functionality under a number of

stresses, including treatment with microtubule depolymerizing agents (Osborn and Weber, 1976).

Immediately surrounding the two centrioles is a less-structured region termed the pericentriolar material (PCM) from which microtubules nucleate. One of the original studies on the PCM in hamster ovary cells demonstrated that PCMs were typically limited to the nucleation of 24 independent microtubules (Gould and Borisy, 1977). However, upon incubation with an excess of tubulin dimers, centrosomes were observed that had nucleated more than 200 microtubules, indicating that the natural limit of microtubules is set by tubulin availability and not centrosome structure (Gould and Borisy, 1977). Modern studies shown that the protein ninein, a minus-end directed protein serves to anchor microtubules at the centrosome as well as recruit the γ-tubulin complex responsible for microtubule nucleation (Delgehyr et al., 2005).

MICROTUBULE ORGANIZATION IN PLANT CELLS

Although both SPBs and centrosomes are clearly linked to microtubule nucleation and organization, neither structure is required for eukaryotic life. It has been shown that centrosomes are required for setting up spindle poles during animal cell division (Zhang and Nicklas, 1995), but removing the centrosome from the spindle in anaphase does not affect spindle morphology or chromosome segregation (Nicklas et al., 1989). SBPs and centrosomes share the same function, but the large differences in their structure (membrane-bound stacks versus cytosolic barrels) imply that there is no best way to organize microtubules in cells. This inference can be extended to plants which have no single conserved organizing center for microtubules.

Many plant species have lost the centrosome structure throughout their evolution, but not all. Two of the more basal orders of gymnosperms (gingkoes and cycads) have maintained flagellated sperm and assemble centrioles in these specific cells (Southworth and Cresti, 1997). Marshall (2009) points out that the loss of centrioles throughout eukaryotic lineages is directly linked to the loss of cilia. While angiosperms and gymnosperms have lost cilia, mosses, ferns, and algae have all maintained these structures (Marshall, 2009).

Plant cells in some of the more basal lineages (including mosses and lycopods) maintain a single large chloroplast rather than numerous smaller ones per cell. Microtubules nucleate from the surface of the chloroplast and division of this single plastid is coordinated with division of the whole cell (Brown and Lemmon, 1997). The two chloroplasts move apart upon splitting and serve as a point of spindle pole organization for cell division, ensuring the daughter cells will each get one chloroplast along with one full set of chromosomes (Brown and Lemmon, 2001).

It has long been established that higher plant cells are able to organize microtubule spindle poles without centrosomes (Pickett-Heaps, 1969). Microtubule nucleation is associated with a number of different sites in four different 'arrays' throughout the plant cell cycle. In interphase, the cortical microtubule array is highly unstructured. Microtubule minus-ends are unanchored and slowly depolymerize as the plus-ends grow in a process called microtubule treadmilling (Shaw et al., 2003). As the cell enters G2, microtubules organize around the nucleus in the second array known as the preprophase band. Microtubule nucleation occurs *in vitro* around isolated plant nuclei (Stoppin et al., 1994), implicating the surface of the nucleus as a MTOC for this array. As

the cell enters mitosis, microtubules organize into spindle poles, the third array. Finally, during telophase, microtubules nucleate from the phragmoplast, the growing cell plate between the two daughter cells. The location of the phragmoplast is closely associated with the former location of the preprophase band. Although mutant plants lacking proper preprophase band formation have abnormally placed phragmoplasts, neither structure appears to be necessary for formation of the other (Azimzadeh et al., 2008).

While plant cells lack a single MTOC, they've maintained many components from the yeast SPB and animal centrosomes, the most abundant being γ-tubulin and its associated proteins (Stearns et al., 1991). Knockouts in γ-tubulin cause a variety of defects in microtubule organization, including spindle formation and nuclear migration in yeast (Sobel and Snyder, 1995) and failure of chromosome segregation in *Drosophila melanogaster* (Sunkel et al., 1995). γ-tubulin is localized in MTOCs, including each of the four arrays in plants at different stages of the cell cycle (Liu et al., 1993). γ-tubulin knockouts in plants cause a number of similar phenotypes to the ones seen in yeast and animals. Dividing cells lacking γ-tubulin in *Arabidopsis thaliana* have curved, bent, and even shrunken spindles in meiosis (Pastuglia et al., 2006). The mitotic divisions of pollen development after meiosis are further affected, with a significant number of pollen having altered number of nuclei (Pastuglia et al., 2006), indicating that γ-tubulin has essential roles in both mitotic and meiotic spindle formation.

It is possible that the release of microtubule organization from a single structure in plants offers an evolutionary advantage to their growth habit. This relaxation of organization, particularly in interphase, allows for more careful control of cell wall deposition, particularly important in producing the long, tubular cells of roots and shoots.

These new freedoms also bring new challenges; without a single center taking control of microtubules, the challenge of organization in cell division seems much greater. One observation is that plant genomes contain a much higher number of kinesin motor proteins than animals or yeast (Reddy and Day, 2001). Particularly given that plants lack dynein, the other major class of microtubule motor proteins (Lawrence et al., 2001), it is likely that these microtubule-binding motors serve critical roles in guiding formations of larger microtubule arrays (model presented in Ambrose et al., 2005).

KINESIN MOTOR PROTEINS

As previously mentioned, kinesins are a class of motor proteins capable of traveling along the length of microtubules through the hydrolysis of adenosine triphosphate (ATP). The structure of kinesins typically consists of three domains: a highly-conserved motor domain through which protein binds both ATP and the tubulin dimer, a flexible α-helix coiled-coil linker responsible for polymerization of kinesins essential for their function, and cargo-binding domain unique to the different molecules and organelles each motor is responsible for shuttling (Yang et al., 1989). Although the initial kinesin protein discovered moved exclusively toward the plus-end of microtubules (Vale et al., 1985), similar motor proteins were found which move toward the minus end (McDonald et al., 1990). It seems that the linker region plays a role in motor directionality, as a single amino acid substitution in this region of the protein causes a direction reversal in the *D. melanogaster* kinesin *ncd* (Endow and Higuchi, 2000).

Kinesins are organized phylogenetically into distinct 14 classes, each associated with different cargoes and cellular functions (Lawrence et al., 2004; as reviewed in Miki

et al., 2005). Several of these families, including kinesin-4, -5, --7, -10, and -14A have been implicated in microtubule positioning or chromosome movement. The functions of these particular families are described in detail below.

Kinesin-4 was originally named “chromokinesin” due to its ability to bind DNA *in vitro* as well as *in vivo* localization to chromatin in both interphase and mitosis (Wang and Adler, 1995). Further studies on kinesins have indicated that not all members of this class are capable of binding DNA, nor is that ability unique to members of this class (see kinesin-10), and it is now suggested that the term chromokinesin be phased out in favor of the more general family name kinesin-4 (Miki et al., 2005). Members of this family establish a connection between chromosomes and the microtubule spindles; the human kinesin-4 KIF4A is required for both the organization of the microtubule spindle as well as the integrity of the chromosomes even before nuclear envelope breakdown (Mazumdar et al., 2004). A further study indicates KIF4A directly interacts with condensin I and is necessary for its loading onto chromosomes during their condensation in prophase and prometaphase (Takahashi et al., 2016).

The first member of the kinesin-5 subfamily was identified in *Aspergillus nidulans*, mutants of which had errors in SPB migration and subsequent spindle formation (Enos and Morris, 1990). Electron microscopy determined KRP130, a *D. melanogaster* kinesin-5, to function as a homotetramer with four catalytic motors positioned on the outside of the X-shaped structure hypothesized to crosslink and slide antiparallel microtubules at the middle of the spindle pole (Kashina et al., 1996). Loss-of-function of the *Caenorhabditis elegans* kinesin-5 results in longer spindles, suggesting this crosslinking activity serves as a brake for an otherwise fast-acting process (Saunders

et al., 2007). The restriction of spindle elongation was further validated in mammalian cells using small molecule inhibitors of kinesin-5 (Collins et al., 2014).

The kinesin-7 subfamily is enriched in plants and responsible for organization of microtubules in phragmoplast following chromosome segregation. Mutations in HINKEL, an *A. thaliana* kinesin-7, result in errors in cytokinesis, including enlarged cells, incomplete cell walls, and multinucleate daughter cells (Strompen et al., 2002). HINKEL co-localizes with ANP MAP kinase kinase kinase and activates it to begin a phosphorylation cascade responsible for signaling cytokinesis (Takahashi et al., 2010). An ortholog of HINKEL called TETRASPORE is specifically required for cytokinesis in the male gametophyte, with the four products of meiosis sharing a combined cytoplasm in these mutants (Spielman et al., 1997; Yang et al., 2003). Studies of the *Physcomitrella patens* homolog of these genes show that kinesin-7s also affect chromosome alignment and is localized at the spindle midzone as early as metaphase, and maintained at this site throughout cell division and early cytokinesis to establish the phragmoplast (Naito and Goshima, 2015).

The most widely-studied member of the kinesin-10 subfamily is *kinesin-like DNA binding protein* (*Kid*) in *D. melanogaster,* so named for its ability to directly bind DNA *in vitro* and chromosomes during interphase and mitosis (Tokai et al., 1996). *Kid* is required for regulating spindle size, with *Kid*-deficient knockouts having shorter spindles (Tokai-Nishizumi et al., 2005), opposite of the phenotype that is observed in members of the kinesin-5 subfamily (Saunders et al., 2007). *Kid* is also a major component of the generation of the polar ejection force responsible for aligning chromosomes along the

metaphase plate (Brouhard and Hunt, 2005), and directly interacts with key cell cycle regulator cyclin-dependent kinase 1 (Soeda et al., 2016).

KINESIN-14A SUBFAMILY

The defining feature of the kinesin-14A subfamily is its unique position of the motor domain. The motor domain is most commonly located at the N-terminus of kinesin proteins, but the motors of kinesin-14As are found at the C-terminal end. Associated with this reversal in protein structure is a reversal in their directionality. Functional studies of members of this class, including the *D. melanogaster* gene *nonclaret disjunctional* (*ncd*) and the *A. thaliana* gene *AtKin14b*, have shown that these proteins are minus-end directed and move specifically toward the non-polymerizing ends of microtubules, located at the spindle poles during cell division (Walker et al., 1990; Ambrose et al., 2005).

Mutations in kinesin-14As result in defects in chromosome segregation and microtubule spindle organization, particularly in cells which lack a structural MTOC. The *ncd* locus has long been known to result in chromosome abnormalities through the female meiocytes, unusual animal cells in that they lack centrosomes (Sturtevant, 1929; Davis, 1969). It wasn't until DNA sequencing technology became available that the gene at this locus was discovered to encode for a kinesin motor (Endow et al., 1990), only months after the canonical kinesin heavy chain was first identified (Yang et al., 1989). *Ncd* is capable of bundling microtubules *in vitro* (McDonald et al., 1990) and deletion mutants result in serious defects in spindle organization in meiosis I (Hatsumi and Endow, 1992).

The *S. cerevisiae* kinesin-14A known as *KAR3* was identified around the same time as *ncd*, with loss of mutants showing similar defects in spindle organization as well as errors in nuclear fusion following conjugation (Meluh and Rose, 1990). The localization of *KAR3* is dependent on binding with one of two non-motor interacting partners *CIK1* (Page et al., 1994) or *VIK1* (Manning et al., 1999) at different stages of mitosis. Loss of the *KAR3*/*CIK1* complex results in a delayed entry into anaphase following DNA replication under stressful conditions due to errors in establishing a connection between kinetochores and microtubules (Liu et al., 2011b).

The prevailing model for kinesin-14A function is that it serves to cross-link antiparallel microtubules at the spindle midzone as it begins to form, sliding them past one another and gathering askew microtubules into a focused spindle point (Ambrose et al., 2005; Fink et al., 2009; Hepperla et al., 2014). Recent studies have also demonstrated that the members of this class in *S. pombe* trigger the release of γ-tubulin from associated proteins, inhibiting microtubule nucleation (Olmsted et al., 2013). Interestingly, a member of the kinesin-5 family counters this inhibition also through binding, indicating kinesins affect microtubule formation in addition to microtubule organization (Olmsted et al., 2014).

The purpose of this study is to better understand how members of the kinesin-14A subfamily affect spindle formation and chromosome segregation in plants. In **Chapter 2** of the dissertation, the underlying gene of a locus affecting spindle organization in *Zea mays* (maize) is identified as a kinesin-14A. Through a candidate gene approach, targeted sequencing identified a premature stop mutation in the maize gene GRMZM2G114861 in the *divergent spindle-1* (*dv1*) background. Further evidence

linking this gene to the phenotype is provided through quantitative PCR and a second *dv1* allele. The effects of loss of kinesin-14A on spindle structure and chromosome segregation is further quantified through both fixed cell immunolocalization as well as live cell imaging. In **Chapter 3** of the dissertation, a novel member of the kinesin-14A subfamily implicated in the maize abnormal chromosome 10 meiotic drive system is characterized. It was determined through whole transcriptome sequencing of meiotic drive mutants and an RNA interference targeted knockdown that this gene, known as *kinesin driver* (*kindr),* is necessary but not sufficient for the meiotic drive phenotype. The results of efforts to localize KINDR protein within cells are also presented.

MEIOTIC DRIVE

The processes of microtubule organization and chromosome segregation are complex – it seems necessary that an intricate network of genes and proteins are required for the faithful duplication and segregation of the genome into identical daughter cells. When considering the process of cell division, it is important not to "lose the forest for the trees," and forget about the consequences of each of these proteins acting in synchrony. That the products of mitosis carry the same set of chromosomes is essential to the survival of an organism; errors in mitosis result in mosaicism and aneuploidy, one of the most common features of cancerous tumors in humans (Kops et al., 2005). It is equally important for the products of meiosis to carry not just a complete complement of genes, but that the arrangement of alleles is shuffled as well. That alleles are inherited with equal, Mendelian likelihood is essential for natural selection to act in an effective manner (Austin and Trivers, 2006).

Although Mendelian inheritance benefits populations, there exist selfish elements which undercut this process for their own gain. While typical inheritance of a heterozygous locus in a genome is 50:50, these special loci are passed on at a greater rate over their benign counterparts at rates ranging from 51:49 all the way to 100:0 (Austin and Trivers, 2006). This process is known as meiotic drive (Sandler and Novitski, 1957). Meiotic drive systems have been identified in animals, fungi, and plants, indicating they have evolved multiple times. The drive systems most characterized are linked to visible phenotypes which aided in their oftentimes serendipitous discovery. It's possible that meiotic drive could be a more common occurrence than we know based on the limits of what we observe. There are two general mechanisms by which selfish elements achieve drive: interference and gonotaxis.

Meiotic drive elements which function by interference eliminate their competing meiotic products without the element during gametogenesis. The most widely characterized elements of this type are the *Segregation Distortion* (*SD*) locus in *D. melanogaster* and the *t*-haplotype in *Mus musculus*. Both of these systems work in a similar manner. The driving versions of chromosomes carry a lethal killer gene which eliminates developing sperm cells but are resistant themselves. The resistance and killer loci are in tight genetic linkage due to chromosomal inversions, allowing the drive element to destroy competing sperm carrying its competitor chromosomes while protecting itself, enhancing its transmission to about 90% in *t* mice (Ardlie and Silver, 1996) and up to 95% in *SD* flies (Temin et al., 1991). In the *t*-haplotype, the killer can be one of three different recessive mutations that result in embryo lethality when homozygous (Lyon, 1991). The resistance locus, *Tcr*, encodes a novel gene with

homology to a sperm motility kinase (Herrmann et al., 1999). The mechanism of resistance is still unknown, but male mice with the genotype *t*/+ produce sperm with equal numbers of each chromosome, though wild type sperm are dysfunctional with motility defects (Olds-Clarke and Johnson, 1993). In *SD*, the role of the killer is played by *Sd-RanGAP*, a truncated and mislocalized form of a protein involved in nuclear transport (Merrill et al., 1999). Sperm cells from fathers carrying *Sd-RanGAP*/+ fail to fully develop, unless they also carry *Responder*, a region of satellite DNA which provides resistance through a yet unknown function (Wu et al., 1988).

Other meiotic drive systems operate by less antagonistic means. Drive systems which exhibit gonotaxis depend upon the often asymmetric nature of female meiosis. In both plants and animals, only one of the four products of female meiosis will go on to become a viable egg, the other three daughter cells are non-functional and abort. The chromosome that is loaded into this viable egg is typically random, but an adaptive drive element capable of ending in this cell more frequently will be more likely to be passed on. By far the most widely studied drive element of this type is the abnormal chromosome 10 system in *Z. mays.* In maize, female parents heterozygous for the abnormal chromosome 10 will pass on this chromosome at rates between 70-80%. The selfish element achieves this through the activation of normally inert heterochromatic knobs into neocentromeres which move toward the spindle pole ahead of regular centromeres. This activity allows abnormal chromosome 10 and all knob-linked portions of the genome, to be preferentially localized in one of the two outermost cells at the end of meiosis, and thus in the one daughter cell which becomes an egg (Rhoades, 1952).

In **Chapter 4** of the dissertation, the diversity of abnormal chromosome 10 is assessed through whole transcriptome sequencing to better understand the evolutionary consequences of carrying this meiotic drive element. No evidence collected from transmission rates or pollen viability supports the hypothesis that abnormal chromosome 10 is inherited less frequently as a non-driving male parent. To the contrary, a dramatic reduction in seed set and seed size was observed in abnormal chromosome 10 homozygotes, suggesting a homozygous disadvantage for plants carrying the drive element. Alleles with deleterious effects in the inverted shared region were identified which may contribute to this decrease in fitness. Rates of drive measured for chromosomes collected from different regions of Central and South America are largely uniform and do not correlate with expression of *Kindr*. In addition, a new phylogeny of abnormal chromosome 10 based on genes in the shared region is presented.

WORKS CITED

Allen, C., and Borisy, G.G. (1974). Structural polarity and directional growth of microtubules of *Chlamydomonas* flagella. *J. Cell Sci.* 14**,** 523-549.

Amaratunga, A., Morin, P.J., Kosik, K.S., and Fine, R.E. (1993). Inhibition of Kinesin Synthesis and Rapid Anterograde Axonal Transport *in Vivo* by an Antisense Oligonucleotide. *Journal of Biological Chemistry* 268**,** 17427-17430.

Ambrose, J.C., Li, W., Marcus, A., Ma, H., and Cyr, R. (2005). A minus-end-directed kinesin with plus-end tracking protein activity is involved in spindle morphogenesis. *Mol Biol Cell* 16**,** 1584-1592.

Ardlie, K.G., and Silver, L.M. (1996). Low Frequency of Mouse t Haplotypes in Wild Populations Is Not Explained by Modifiers of Meiotic Drive. *Genetics* 144**,** 1787-1797.

Austin, B., and Trivers, R. (2006). *Genes in Conflict.* Harvard University Press.

Azimzadeh, J., Nacry, P., Christodoulidou, A., Drevensek, S., Camilleri, C., Amiour, N., Parcy, F., Pastuglia, M., and Bouchez, D. (2008). Arabidopsis TONNEAU1 Proteins Are Essential for Preprophase Band Formation and Interact with Centrin. *The Plant Cell Online* 20**,** 2146-2159.

Brouhard, G.J., and Hunt, A.J. (2005). Microtubule movements on the arms of mitotic chromosomes: polar ejection forces quantified in vitro. *Proceedings of the National Academy of Sciences of the United States of America* 102**,** 13903-13908.

Brown, R.C., and Lemmon, B.E. (1997). The quadripolar microtubule system in lower land plants. *Journal of Plant Research* 110**,** 93-106.
Brown, R.C., and Lemmon, B.E. (2001). Sporogenesis in Eusporangiate Ferns: I. monoplastidic Meiosis in Angiopteris (Marattiales). *Journal of Plant Research* 114**,** 223-235.
Collins, E., Mann, B.J., and Wadsworth, P. (2014). Eg5 restricts anaphase B spindle elongation in mammalian cells. *Cytoskeleton* 71**,** 136-144.
Davis, D. (1969). Chromosome behavior under the influence of claret-nondisjunctional in Drosophila melanogaster. *Genetics* 61**,** 577.
Delgehyr, N., Sillibourne, J., and Bornens, M. (2005). Microtubule nucleation and anchoring at the centrosome are independent processes linked by ninein function. *Journal of Cell Science* 118**,** 1565-1575.
Dutcher, S.K., and Trabuco, E.C. (1998). The UNI3 Gene Is Required for Assembly of Basal Bodies of Chlamydomonas and Encodes δ-Tubulin, a New Member of the Tubulin Superfamily. *Molecular Biology of the Cell* 9**,** 1293-1308.
Elliott, S., Knop, M., Schlenstedt, G., and Schiebel, E. (1999). Spc29p is a component of the Spc110p subcomplex and is essential for spindle pole body duplication. *Proceedings of the National Academy of Sciences* 96**,** 6205-6210.
Endow, S., and Higuchi, H. (2000). A mutant of the motor protein kinesin that moves in both directions on microtubules. *Nature* 406**,** 913-916.
Endow, S.A., Henikoff, S., and Soler-Niedziela, L. (1990). Mediation of meiotic and early mitotic chromosome segregation in Drosophilia by a protein related to kinesin. *Nature* 345**,** 81.
Enos, A.P., and Morris, N.R. (1990). Mutation of a gene that encodes a kinesin-like protein blocks nuclear division in A. nidulans. *Cell* 60**,** 1019-1027.
Fink, G., Hajdo, L., Skowronek, K.J., Reuther, C., Kasprzak, A.A., and Diez, S. (2009). The mitotic kinesin-14 Ncd drives directional microtubule-microtubule sliding. *Nat Cell Biol* 11**,** 717-723.
Gould, R.R., and Borisy, G.G. (1977). The pericentriolar material in Chinese hamster ovary cells nucleates microtubule formation. *Journal of Cell Biology* 73**,** 601-615.
Gruneberg, U., Campbell, K., Simpson, C., Grindlay, J., and Schiebel, E. (2000). Nud1p links astral microtubule organization and the control of exit from mitosis. *The EMBO Journal* 19**,** 6475-6488.
Hatsumi, M., and Endow, S. (1992). Mutants of the microtubule motor protein, nonclaret disjunctional, affect spindle structure and chromosome movement in meiosis and mitosis. *Journal of Cell Science* 101**,** 547-559.
Hepperla, A.J., Willey, P.T., Coombes, C.E., Schuster, B.M., Gerami-Nejad, M., Mcclellan, M., Mukherjee, S., Fox, J., Winey, M., and Odde, D.J. (2014). Minus-End-Directed Kinesin-14 Motors Align Antiparallel Microtubules to Control Metaphase Spindle Length. *Developmental cell* 31**,** 61-72.
Herrmann, B.G., Koschorz, B., Wertz, K., Mclaughlin, K.J., and Kispert, A. (1999). A protein kinase encoded by the t complex responder gene causes non-mendelian inheritance. *Nature* 402**,** 141-146.
Howard, J., and Hyman, A.A. (2009). Growth, fluctuation and switching at microtubule plus ends. *Nature Reviews Molecular Cell Biology* 10**,** 569-574.

Jaspersen, S.L., Martin, A.E., Glazko, G., Giddings, T.H., Morgan, G., Mushegian, A., and Winey, M. (2006). The Sad1-UNC-84 homology domain in Mps3 interacts with Mps2 to connect the spindle pole body with the nuclear envelope. *The Journal of Cell Biology* 174**,** 665-675.

Kashina, A., Baskin, R., Cole, D., Wedaman, K., Saxton, W., and Scholey, J.M. (1996). A bipolar kinesin. *Nature* 379**,** 270.

Knop, M., and Schiebel, E. (1997). Spc98p and Spc97p of the yeast γ-tubulin complex mediate binding to the spindle pole body via their interaction with Spc110p. *The EMBO Journal* 16**,** 6985-6995.

Knop, M., and Schiebel, E. (1998). Receptors determine the cellular localization of a γ-tubulin complex and thereby the site of microtubule formation. *The EMBO journal* 17**,** 3952-3967.

Komarova, Y.A., Akhmanova, A.S., Kojima, S., Galjart, N., and Borisy, G.G. (2002). Cytoplasmic linker proteins promote microtubule rescue *in vivo*. *Journal of Cell Biology* 159.

Kops, G.J.P.L., Weaver, B.a.A., and Cleveland, D.W. (2005). On the road to cancer: aneuploidy and the mitotic checkpoint. *Nat Rev Cancer* 5**,** 773-785.

Lawrence, C.J., Dawe, R.K., Christie, K.R., Cleveland, D.W., Dawson, S.C., Endow, S.A., Goldstein, L.S., Goodson, H.V., Hirokawa, N., Howard, J., Malmberg, R.L., Mcintosh, J.R., Miki, H., Mitchison, T.J., Okada, Y., Reddy, A.S., Saxton, W.M., Schliwa, M., Scholey, J.M., Vale, R.D., Walczak, C.E., and Wordeman, L. (2004). A standardized kinesin nomenclature. *J Cell Biol* 167**,** 19-22.

Lawrence, C.J., Morris, N.R., Meagher, R.B., and Dawe, R.K. (2001). Dyneins Have Run Their Course in Plant Lineage. *Traffic* 2**,** 362-363.

Ledbetter, M.C., and Porter, K.R. (1963). A"Microtubule" in Plant Cell Fine Structure. *Journal of Cell Biology* 19**,** 239-250.

Liu, B., Marc, J., Joshi, H.C., and Palevitz, B.A. (1993). A gamma-tubulin-related protein associated with the microtubule arrays of higher plants in a cell cycle-dependent manner. *J Cell Sci* 104 (Pt 4)**,** 1217-1228.

Liu, H., Jin, F., Liang, F., Tian, X., and Wang, Y. (2011). The Cik1/Kar3 Motor Complex Is Required for the Proper Kinetochore–Microtubule Interaction After Stressful DNA Replication. *Genetics* 187**,** 397-407.

Luck, D.J.L. (1984). Genetic and Biochemical Dissection of the Eucaryotic Flagellum. *Journal of Cell Biology* 98**,** 789-794.

Lyon, M.F. (1991). The genetic basis of transmission-ratio distortion and male sterility due to the t complex. *The American Naturalist* 137**,** 349-358.

Maddox, P., Chin, E., Mallavarapu, A., Yeh, E., Salmon, E.D., and Bloom, K. (1999). Microtubule Dynamics from Mating through the First Zygotic Division in the Budding Yeast Saccharomyces cerevisiae. *The Journal of Cell Biology* 144**,** 977-987.

Manning, B.D., Barrett, J.G., Wallace, J.A., Granok, H., and Snyder, M. (1999). Differential regulation of the Kar3p kinesin-related protein by two associated proteins, Cik1p and Vik1p. *The Journal of cell biology* 144**,** 1219-1233.

Marshall, W.F. (2009). Centriole Evolution. *Current Opinion in Cell Biology* 21**,** 14-19.

Mazumdar, M., Sundareshan, S., and Misteli, T. (2004). Human chromokinesin KIF4A functions in chromosome condensation and segregation. *The Journal of cell biology* 166**,** 613-620.
Mcdonald, H.B., Stewart, R.J., and Goldstein, L.S. (1990). The kinesin-like ncd protein of Drosophila is a minus end-directed microtubule motor. *Cell* 63**,** 1159-1165.
Meluh, P.B., and Rose, M.D. (1990). KAR3, a kinesin-related gene required for yeast nuclear fusion. *Cell* 60**,** 1029-1041.
Merrill, C., Bayraktaroglu, L., Kusano, A., and Ganetzky, B. (1999). Truncated RanGAP encoded by the Segregation Distorter locus of Drosophila. *Science* 283**,** 1742-1745.
Miki, H., Okada, Y., and Hirokawa, N. (2005). Analysis of the kinesin superfamily: insights into structure and function. *Trends in Cell Biology* 15**,** 467-476.
Muller, E.G.D., Snydsman, B.E., Novik, I., Hailey, D.W., Gestaut, D.R., Niemann, C.A., O'toole, E.T., Giddings, T.H., Sundin, B.A., and Davis, T.N. (2005). The Organization of the Core Proteins of the Yeast Spindle Pole Body. *Molecular Biology of the Cell* 16**,** 3341-3352.
Naito, H., and Goshima, G. (2015). NACK kinesin is required for metaphase chromosome alignment and cytokinesis in the moss Physcomitrella patens. *Cell structure and function* 40**,** 31-41.
Nicklas, R.B., Lee, G.M., Rieder, C.L., and Rupp, G. (1989). Mechanically cut mitotic spindles: clean cuts and stable microtubules. *Journal of Cell Science* 94**,** 415-423.
Nogales, E., Wolf, S.G., and Downing, K.H. (1998). Structure of the alpha-beta tubulin dimer by electron crystallography. *Nature* 391**,** 199-203.
O'toole, E.T., Winey, M., and Mcintosh, J.R. (1999). High-Voltage Electron Tomography of Spindle Pole Bodies and Early Mitotic Spindles in the Yeast Saccharomyces cerevisiae. *Molecular Biology of the Cell* 10**,** 2017-2031.
Olds-Clarke, P., and Johnson, L.R. (1993). t Haplotypes in the Mouse Compromise Sperm Flagellar Function. *Developmental Biology* 155**,** 14-25.
Olmsted, Z.T., Colliver, A.G., Riehlman, T.D., and Paluh, J.L. (2014). Kinesin-14 and kinesin-5 antagonistically regulate microtubule nucleation by γ-TuRC in yeast and human cells. *Nature Communications* 5.
Olmsted, Z.T., Riehlman, T.D., Branca, C.N., Colliver, A.G., Cruz, L.O., and Paluh, J.L. (2013). Kinesin-14 Pkl1 targets γ-tubulin for release from the γ-tubulin ring complex (γ-TuRC). *Cell Cycle* 12**,** 842.
Osborn, M., and Weber, K. (1976). Cytoplasmic microtubules in tissue culture cells appear to grow from an organizing structure towards the plasma membrane. *Proc Natl Acad Sci U S A* 73**,** 867-871.
Page, B.D., Satterwhite, L.L., Rose, M.D., and Snyder, M. (1994). Localization of the Kar3 kinesin heavy chain-related protein requires the Cik1 interacting protein. *The Journal of Cell Biology* 124**,** 507-519.
Paredez, A.R., Somerville, C.R., and Ehrhardt, D.W. (2006). Visualization of Cellulose Synthase Demonstrates Functional Association with Microtubules. *Science* 312**,** 1491-1495.
Pastuglia, M., Azimzadeh, J., Goussot, M., Camilleri, C., Belcram, K., Evrard, J.L., Schmit, A.C., Guerche, P., and Bouchez, D. (2006). Gamma-tubulin is essential

for microtubule organization and development in Arabidopsis. *Plant Cell* 18**,** 1412-1425.
Pickett-Heaps, J.D. (1969). The evolution of the mitotic apparatus: an attempt at comparative ultrastructural cytology in dividing plant cells. *Cytobios* 3**,** 257-280.
Reddy, A.S., and Day, I.S. (2001). Kinesins in the Arabidopsis genome: a comparative analysis among eukaryotes. *BMC genomics* 2**,** 2.
Rhoades, M.M. (1952). "Preferential Segregation in Maize", in: *Heterosis.* (ed.) J.W. Gowen. Iowa State College Press).
Salisbury, J.L., Suino, K.M., Busby, R., and Springett, M. (2002). Centrin-2 is required for centriole duplication in mammalian cells. *Curr Biol* 12**,** 1287-1292.
Sandler, L., and Novitski, E. (1957). Meiotic drive as an evolutionary force. *The American Naturalist* 91**,** 105-110.
Saunders, A.M., Powers, J., Strome, S., and Saxton, W.M. (2007). Kinesin-5 acts as a brake in anaphase spindle elongation. *Current Biology* 17**,** R453-R454.
Shaw, S.L., Kamyar, R., and Ehrhardt, D.W. (2003). Sustained Microtubule Treadmilling in Arabidopsis Cortical Arrays. *Science* 300**,** 1715-1718.
Sobel, S.G., and Snyder, M. (1995). A highly divergent gamma-tubulin gene is essential for cell growth and proper microtubule organization in Saccharomyces cerevisiae. *The Journal of Cell Biology* 131**,** 1775-1788.
Soeda, S., Yamada-Nomoto, K., and Ohsugi, M. (2016). The microtubule-binding and coiled-coil domains of Kid are required to turn off the polar ejection force at anaphase. *J Cell Sci* 129**,** 3609-3619.
Southworth, D., and Cresti, M. (1997). Comparison of flagellated and nonflagellated sperm in plants. *American Journal of Botany* 84**,** 1301.
Spielman, M., Preuss, D., Li, F.-L., Browne, W.E., Scott, R.J., and Dickinson, H.G. (1997). TETRASPORE is required for male meiotic cytokinesis in Arabidopsis thaliana. *Development* 124**,** 2645-2657.
Stearns, T., Evans, L., and Kirschner, M. (1991). gamma-Tubulin is a highly conserved component of the centrosome. *Cell* 65.
Stoppin, V., Vantard, M., Schmit, A.C., and Lambert, A.M. (1994). Isolated Plant Nuclei Nucleate Microtubule Assembly: The Nuclear Surface in Higher Plants Has Centrosome-like Activity. *The Plant Cell Online* 6**,** 1099-1106.
Strompen, G., El Kasmi, F., Richter, S., Lukowitz, W., Assaad, F.F., Jürgens, G., and Mayer, U. (2002). The Arabidopsis HINKEL gene encodes a kinesin-related protein involved in cytokinesis and is expressed in a cell cycle-dependent manner. *Current Biology* 12**,** 153-158.
Sturtevant, A.H. (1929). The claret mutant type of Drosophila simulans: a study of chromosome elimination and of cell-lineage. *Z. wiss. Zool* 135**,** 323-356.
Sunkel, C., Gomes, R., Sampaio, P., Perdigao, J., and Gonzalez, C. (1995). Gamma-tubulin is required for the structure and function of the microtubule organizing centre in Drosophila neuroblasts. *The EMBO journal* 14**,** 28.
Takahashi, M., Wakai, T., and Hirota, T. (2016). Condensin I-mediated mitotic chromosome assembly requires association with chromokinesin KIF4A. *Genes & Development* 30**,** 1931-1936.
Takahashi, Y., Soyano, T., Kosetsu, K., Sasabe, M., and Machida, Y. (2010). HINKEL kinesin, ANP MAPKKKs and MKK6/ANQ MAPKK, which phosphorylates and

activates MPK4 MAPK, constitute a pathway that is required for cytokinesis in Arabidopsis thaliana. *Plant and cell physiology* 51**,** 1766-1776.

Temin, R.G., Ganetzky, B., Powers, P.A., Lyttle, T.W., Pimpinelli, S., Dimitri, P., Chung, I.W., and Hiraizumi, Y. (1991). Segregation Distortion in Drosophila melanogaster: Genetic and Molecular Analyses. *The American Naturalist* 137**,** 287-331.

Tokai-Nishizumi, N., Ohsugi, M., Suzuki, E., and Yamamoto, T. (2005). The chromokinesin Kid is required for maintenance of proper metaphase spindle size. *Molecular biology of the cell* 16**,** 5455-5463.

Tokai, N., Fujimoto-Nishiyama, A., Toyoshima, Y., Yonemura, S., Tsukita, S., Inoue, J., and Yamamota, T. (1996). Kid, a novel kinesin-like DNA binding protein, is localized to chromosomes and the mitotic spindle. *The EMBO journal* 15**,** 457.

Vale, R.D., Reese, T.S., and Sheetz, M.P. (1985). Identification of a novel force-generating protein, kinesin, involved in microtubule-based motility. *Cell* 42**,** 39-50.

Walker, R.A., Salmon, E.D., and Endow, S.A. (1990). The Drosophila Claret Segregation Protein Is a Minus-End Directed Motor Molecule. *Nature* 347**,** 780-782.

Wang, S.-Z., and Adler, R. (1995). Chromokinesin: a DNA-binding, kinesin-like nuclear protein. *Journal of Cell Biology* 128**,** 761-768.

Wu, C.-I., Lyttle, T.W., Wu, M.-L., and Lin, G.-F. (1988). Association between a satellite DNA sequence and the Responder of Segregation Distorter in D. melanogaster. *Cell* 54**,** 179-189.

Yang, C.Y., Spielman, M., Coles, J., Li, Y., Ghelani, S., Bourdon, V., Brown, R., Lemmon, B., Scott, R.J., and Dickinson, H. (2003). TETRASPORE encodes a kinesin required for male meiotic cytokinesis in Arabidopsis. *The Plant Journal* 34**,** 229-240.

Yang, J.T., Laymon, R.A., and Goldstein, L.S. (1989). A three-domain structure of kinesin heavy chain revealed by DNA sequence and microtubule binding analyses. *Cell* 56**,** 879-889.

Zhang, D., and Nicklas, R.B. (1995). The impact of chromosomes and centrosomes on spindle assembly as observed in living cells. *Journal of Cell Biology* 129**,** 1287-1300.

CHAPTER 2

THE MAIZE DIVERGENT SPINDLE-1 (DV1) GENE ENCODES A KINESIN-14A MOTOR PROTEIN REQUIRED FOR MEIOTIC SPINDLE POLE ORGANIZATION[1]

[1] Higgins, D.M.; Nannas, N.J.; and R.K. Dawe. 2016. *Frontiers in Plant Science*. 7:1277. Reprinted here with permission of the publisher.

ABSTRACT

The classic maize mutant *divergent spindle-1* (*dv1*) causes failures in meiotic spindle assembly and a decrease in pollen viability. By analyzing two independent *dv1* alleles we demonstrate that this phenotype is caused by mutations in a member of the kinesin-14A subfamily, a class of C-terminal, minus-end directed microtubule motors. Further analysis demonstrates that defects in early spindle assembly are rare, but that later stages of spindle organization promoting the formation of finely focused spindle poles are strongly dependent on *Dv1*. Anaphase is error-prone in *dv1* lines but not severely so, and the majority of cells show normal chromosome segregation. Live-cell imaging of wild type and mutant plants carrying CFP-tagged β-tubulin confirm that meiosis in *dv1* lines fails primarily at the pole-sharpening phase of spindle assembly. These data indicate that plant kinesin-14A proteins help to enforce bipolarity by focusing spindle poles and that this stage of spindle assembly is not required for transition through the spindle checkpoint but improves the accuracy of chromosome segregation.

INTRODUCTION

The plant cytoskeleton, comprised of actin-based microfilaments and tubulin-based microtubules, is involved in a number of critical cellular processes, including cell elongation, cell wall deposition, and cell division. Microtubules are hollow tube-shaped structures comprised of polymerized dimers of α- and β-tubulin and are polarized into dynamically growing and shrinking plus ends as well as relatively stable minus ends. This polar quality of microtubules is important in a number of their roles in plant cells, including meiosis, the process by which diploid somatic cells undergo reductional division to form haploid gametes. During prophase of meiosis I, microtubules circle the nuclear envelope as the chromosomes inside begin to recombine and condense. As the nuclear envelope breaks down, the minus ends of microtubules organize into the spindle structure while their plus ends attach to kinetochores and position chromosomes in the metaphase plate (reviewed in Howard and Hyman, 2003). Chromosomes are then retracted along the microtubules during anaphase before forming new nuclei in telophase. Organisms have evolved different structures known as microtubule organizing centers (MTOCs) to assist in this process. These include the spindle pole body in budding yeast (reviewed in Kilmartin, 2014) and centrosomes in animals (reviewed in Conduit et al., 2015).

Microtubules in plant cells are not organized by a single structure and are instead nucleated as one of four different arrays throughout the plant cell cycle (reviewed in Lloyd and Chan, 2006;McMichael and Bednarek, 2013). During interphase, cortical microtubules are nucleated from multiple, mobile points along the inner surface of the plasma membrane (Chan et al., 2003). Some of these microtubules are capable of slowly

depolymerizing at their minus ends while their plus ends elongate in a process known as microtubule treadmilling (Shaw et al., 2003). As the cell prepares to undergo division, microtubules collect around the nucleus. In mitosis, they organize as a ring-shaped structure known as the preprophase band, the location of which predicts the ultimate plate of cell division (Mineyuki, 1999). As the nuclear envelope breaks down at the beginning of cell division, so do the microtubules of the preprophase band which collect in the nuclear space and form a chaotic bipolar array which is then focused and oriented into the spindle (Shamina, 2005). Following anaphase, microtubules nucleate in a flat disc called the phragmoplast between the divided chromosome masses in order to establish the cell membrane and cell wall between the two new daughter cells (Liu et al., 2011a). Overall, the cells of flowering plants have unique methods of organizing and nucleating their microtubules compared to other eukaryotes, particularly as they pertain to the spindle structure, the mechanisms of which are still unknown (Zhang and Dawe, 2011).

Zea mays (maize) has served as a model for plant cytogenetics research for over a century and a number of meiotic mutants have been identified (Carlson, 1988). One such mutant, *divergent spindle-1* (*dv1*), is deficient in meiotic spindle formation in meiocytes. In wild type meiotic cells, microtubules form a bipolar spindle with organized, focused poles. Cells carrying the mutant *dv1* fail to complete this process with their spindle microtubules remaining unorganized and divergent from one another (Clark, 1940). Chromosomes are retracted along these divergent microtubules during anaphase, causing aberrant chromosome segregation and pollen abortion rates ranging from 56% to 90% in extreme situations (Clark, 1943;Staiger and Cande, 1990). Phenotypically, plants carrying the *dv1* mutation are indistinguishable from wild type siblings, indicating that

dv1 does not cause deleterious effects of mitosis (Staiger and Cande, 1990). Additionally, there is no observed effect on seed set, suggesting the effects of *dv1* are limited to male meiosis and are not present in female meiocytes (Clark, 1940).

Further analysis of *dv1* using immunofluorescence indicated that meiocytes carrying the mutation do not exhibit a microtubule phenotype during prophase, only as the nuclear envelope begins to break down and the spindle starts to organize (Staiger and Cande, 1990). Additional characterization demonstrated a plasticity of the spindle phenotype of *dv1* plants grown under altered light and temperature conditions resulting in a radial spindle phenotype (Shamina et al., 2000). The *dv1* mutation also has effects on the nuclear envelope, resulting in an abnormal breakdown during prometaphase, leaving fragments of the membrane among the chromosome bivalents (Shamina et al., 2000). A recent study supports this view, showing that *dv1* affects localization of the protein SUN2 that is involved in tethering telomeres to the nuclear envelope (Murphy et al., 2014).

Kinesins are a large superfamily of proteins that are known to be involved in multiple stages of mitosis (reviewed in Hirokawa and Noda, 2008), making them excellent candidates for the gene underlying the *dv1* phenotype. Kinesins were first identified from the extract of squid giant axons by their ability to generate force through binding and releasing microtubules with their highly-conserved motor domain (Vale et al., 1985;Hirokawa et al., 1989). The kinesin superfamily is divided into 14 distinct subfamilies (Lawrence et al., 2004). Each of these subfamilies is distinguished by the unique cargo bound at their tail domains, allowing different kinesins to transport a variety of proteins, vesicles, and organelles throughout the cell (reviewed in Hirokawa et al., 2009). The motor activity of most kinesins is plus end directed, moving only from the

minus end of microtubules toward the plus end. The kinesin-14 subfamily is unique in that its members are minus-end directed.

The kinesin-14A subfamily contains multiple examples of genes that are involved in organizing spindle poles from species as diverse as *Saccharomyces cerevisiae* (Meluh and Rose, 1990), *Drosophila melanogaster* (McDonald et al., 1990;Walker et al., 1990), *Xenopus laevis* (Walczak et al., 1997), and *Arabidopsis thaliana* (Mitsui et al., 1993). Although their specific phenotypes vary slightly, knockout mutants display errors in cell division, spindle structure and organization of spindle poles (Matthies et al., 1996;Chen et al., 2002). The *Arabidopsis* genome encodes two kinesin-14A genes: Atk5/AtKIN14b (Ambrose and Cyr, 2007), which affects mitotic spindle pole formation, and Atk1/AtKIN14a (Chen et al., 2002), which primarily affects meiotic spindle pole formation and chromosome segregation, similar to maize *dv1* (Quan et al., 2008).

Although the *dv1* mutant was first identified over 75 years ago (Clark, 1940) and has been the subject of several studies since then (Staiger and Cande, 1990; Shamina et al., 2000; Murphy et al., 2014), the gene responsible for its phenotype has never been identified. In this paper, we identify two different members of the kinesin-14A subfamily in maize and demonstrate that the *Dv1* gene encodes one of these proteins through sequencing, quantification of transcripts, and allelism tests of two alleles we identify as *dv1-1* and *dv1-IG*. In addition, we further characterize the effects of *dv1* through by quantifying spindle shape in the *dv1* mutant using immunolocalization, examining the link between errors in meiosis and pollen viability, and documenting the effects of *dv1* on spindle assembly and chromosome segregation *in vivo* through live cell imaging. Overall, we find that *Dv1* is not required for the formation of bipolar spindles but is specifically

required for focusing the spindle pole to a fine point. These data suggest that in plant cells, as in animal oocytes lacking centrosomes (Matthies et al., 1996;Walczak et al., 1998), kinesin-14A proteins serve the primary function of organizing spindle poles.

MATERIALS AND METHODS

Maize Tissue & DNA Extraction

Maize stocks for *dv1-1* and *dv-IG* were received from the Maize Genetics Cooperation Stock Center (University of Illinois). The inbred A619 used in the EMS mutagenesis that led to the identification *dv1-IG* was received from Jay Hollick (Ohio State University). Seeds carrying the CFP-tubulin transgene were received from Anne Sylvester (University of Wyoming). DNA extractions were carried out on leaf tissue using a CTAB protocol with ethanol precipitation (Clarke, 2009).

DNA Sequencing, dv1 *Allele Genotyping, & qRT-PCR*

Genomic DNA was amplified using the Phusion High-Fidelity PCR Kit (New England Biolabs, Ipswich, MA) with the primers outlined in Table 2.1. PCR products were purified for sequencing using the QIAquick PCR Purification Kit (QIAGEN, Germantown, MD). Sanger sequencing was completed at the Georgia Genomics Facility (Athens, GA). Reads were aligned to the B73v3 maize reference genome using the software Geneious (v8.0, Biomatters Ltd., Auckland, New Zealand).

For subsequent studies, *dv1-1* and *dv1-IG* were differentiated from wild type alleles using PCR and restriction digest. Amplification of maize genomic DNA using the *dv1-1* genotyping primers (Table 2.1) produces a PCR product of 235 bp. When this

product is digested with the restriction endonuclease MseI (New England Biolabs), the wild type copy remains uncut while *dv1-1* is cleaved into two pieces of sizes 152 bp and 83 bp. Likewise, *dv1-IG* genotyping primers (Table 2.1) produce a product of 533bp. When digested with the enzyme NsiI (New England Biolabs), the *dv1-IG* allele remains uncut while the wild type allele will be cleaved into two pieces of sizes 272 bp and 261 bp.

For quantification of *dv1* transcripts, RNA was extracted from meiotic anthers using the RNeasy Plant Mini Kit (QIAGEN, Germantown, MD) from which cDNA was generated using the SuperScript III First-Strand Synthesis System for RT-PCR (Thermo Fisher Scientific, Waltham, MA). cDNA was quantified using a Qubit 3.0 Fluorometer (Thermo Fisher Scientific) and equal amounts of template were used for a qRT-PCR reaction with Power SYBR Green PCR Master Mix (Thermo Fisher Scientific). Primers used for *dv1* quantification are given in Table 2.1 while primers for reference gene Membrane protein PB1A10.07c (MEP) were previously published (Manoli et al., 2012). Quantification of transcripts was carried out using the $2^{-\Delta\Delta C_T}$ method (Livak and Schmittgen, 2001).

Meiocyte Immunolocalization

Immunolocalization of maize meiocytes was carried out using an altered version of the protocol by Staiger and Cande (1990). Whole anthers containing meiocytes at metaphase were dissected from florets and fixed in 4% paraformaldehyde in PHEMS buffer for 60 minutes. Fixed anthers were washed in PBS and meiocytes were extruded onto coverslips coated in poly-L-lysine. Coverslips were spun in a swinging bucket

centrifuge at 100g for 1 minute to affix meiocytes. Meiocytes were incubated for one hour in a permeabilization solution (1% Triton X-100 in PBS with 1mM EDTA) before being blocked in 10% goat serum for 90 minutes. Meiocytes were incubated with a monoclonal antibody against sea urchin α-tubulin (Asai et al., 1982) at 37°C overnight. Coverslips were again blocked with 10% goat serum, followed by incubation with Rhodamine-conjugated AffiniPure Goat Anti-Mouse IgG (H+L) secondary antibodies (Jackson ImmunoResearch Inc., West Grove, PA) for 150 minutes. Washed coverslips were mounted in ProLong Gold with DAPI (Thermo Fisher Scientific). Slides were viewed on a Zeiss Axio Imager.M1 fluorescence microscope with a 63x Plan-APO Chromat oil objective. Images were collected using the Slidebook software package (Intelligent Imaging Innovations, Denver, CO) at exposure times ranging from 0.1-1 seconds. Spindle measurements were collected using the Line tool in the Slidebook software. Statistical significance was determined through an ANOVA using the R package "agricolae" (De Mendiburu, 2014).

Immunolocalization for scoring the multinucleate daughter cells was conducted in the same manner as described above with a primary antibody specific to CENP-C (Dawe et al., 1999) and fluorescein-conjugated AffiniPure Goat Anti-Mouse IgG (H+L) secondary antibodies (Jackson ImmunoResearch Inc.).

Pollen Viability

Fresh pollen was collected from dehiscent tassels and stained using a modified version of Alexander's stain (Alexander, 1969;Peterson et al., 2010). Slides were viewed on a Zeiss Axiophot light microscope using a 10x Plan-NEOFLUAR objective lens. A

total of 500 pollen grains from each plant were scored for viability based on color. Statistical significance was determined through an ANOVA using the R package "agricolae" (De Mendiburu, 2014)

Live Meiotic Imaging and Analysis

Cells in metaphase I were extruded from immature maize tassels as previously described (Yu et al., 1997) into a meiocyte-specific live cell imaging medium (De La Peña, 1986;Yu et al., 1997) that contained a final concentration of 2μM SYTO12 Green DNA dye (Invitrogen Molecular Probes, Grand Island, NY). Coverslips were sealed and slides imaged using the same microscope, objective and software used for immunolocalization. Images were collected at 5-minute intervals in 3-dimensions using a 20μm Z range and step size of 1μm. In order to minimize photo-bleaching, exposure times were kept brief (30ms for SYTO12 and 50ms for CFP) and binning was increased (2x2). Chromosome offset and anaphase movements were measured using Slidebook; the three-dimensional coordinates of the center of spindle and chromosome masses were extracted using the object statistics function. Chromosome offset was measured by calculating the distance between the chromosome and spindle coordinates. Anaphase distances were calculated as the three-dimensional distance between the chromosomes at different time points, and anaphase rate was calculated as this distance divided by time.

RESULTS

Identification of mutations associated with the dv1 *phenotype*

Based on the observation that the *dv1* phenotype in maize (Figure 2.1A, 2.1B) is similar to mutations in members of the kinesin-14A subfamily in other species (Matthies et al., 1996;Chen et al., 2002), we hypothesized that the gene underlying the *dv1* phenotype may be a member of this subfamily as well. The sequences of genes of this subclass were collected from different species, including the *Arabidopsis* genes AtKIN14a (Chen et al., 2002) and AtKIN14b (Ambrose et al., 2005), the *Drosophila melanogaster* gene NCD (McDonald et al., 1990) and the *Xenopus laevis* gene XCTK2 (Walczak et al., 1997). In addition, we extracted a complete list of maize genes containing the kinesin motor domain from the maize B73 reference genome (Schnable et al., 2009). The coding sequences (CDS) of these genes were aligned using the MUSCLE algorithm (Edgar, 2004) and assembled into a gene tree using RAxML (Stamatakis, 2006) in order to identify members of the kinesin-14A subfamily in maize. The resulting tree identified two maize genes that cluster with the kinesin-14As of other species (Figure 2.2). These two genes are GRMZM2G114861 and GRMZM2G436981, previously annotated as *ZmKin6* and *ZmKin11* respectively (Lawrence et al., 2002). Transcriptome data on these two genes indicates that the expression of *ZmKin6* in meiotic anthers is 5.18-fold higher than *ZmKin11* (Sekhon et al., 2011, accessed via Maize eFP Browser). Given this large difference in expression in the tissue that shows the *dv1* phenotype, we focused our efforts on sequencing and characterizing *ZmKin6* in the *dv1* background. We generated primer pairs (Table 2.1) for Sanger sequencing across the exons of *ZmKin6* in a maize line that contained the reference *dv1* allele identified by Clark (1940), which

we refer to as *dv1-1*. We identified two single nucleotide polymorphisms (SNPs) in the *dv1-1* allele of *ZmKin6* (Supplemental Data). One SNP produces a premature termination codon (PTC) in the sixth exon of the predicted peptide (Figure 2.1E). As this mutation is upstream of the kinesin motor domain, any mRNA that is produced is likely to be nonfunctional. The second SNP causes a transversion in the eleventh exon, downstream of the PTC and likely to be of no consequence. We also assayed mRNA from the mutant to determine whether nonsense mediated decay, a mechanism that eliminates transcripts carrying deleterious alleles, causes a reduction in the level of ZmKin6 transcript. We outcrossed *dv1-1* to the maize inbred B73 and self-crossed to create a segregating F2 population with *dv1-1*/*dv1-1*, *dv1-1*/+, and wild type genotypes. Quantitative RT-PCR on meiotic anthers from each of these indicates that expression of *dv1* in the *dv1-1*/+ genotype is approximately 30% of wild type while *dv1-1/dv1-1* is 5% of wild type (Figure 2.1C).

We also received from Inna Golubovskaya (University of California, Berkeley, retired) an independently-generated mutant line that shows a similar phenotype as *dv1* (Cande and Freeling, 2011). We renamed this previously unpublished mutant, originally referred to as 'divergent EMS new' *dv1-IG* in her honor. The same primers used to identify the *dv1-1* allele were used to sequence across the *ZmKin6* gene in *dv1-IG* and the A619 inbred from which *dv1-IG* was derived. We identified eight SNPs that differentiated the *dv1-IG* allele from the B73 reference (Supplemental Data). Seven of these were silent mutations found in both *dv1-IG* and the progenitor A619. However, the eighth is unique to the *dv1-IG* allele and results in a transition of the 494th amino acid from a cysteine to a tyrosine residue (Figure 2.1E). This mutation is in the highly

conserved kinesin motor domain, within five amino acid residues of the ATP-binding pocket (Kull et al., 1996;Sablin et al., 1996). We used the software tool PROVEAN to predict the effects of this mutation based on levels of conservation between homologous genes in other species (Choi et al., 2012;Choi and Chan, 2015). PROVEAN generates an alignment of homologous genes and returns a value between +4 and -13, representing a range of predictions for a given mutation to be somewhere between neutral and highly deleterious respectively (Choi et al., 2012). Based on the high levels conservation of this site across plant species, the PROVEAN software predicts that the *dv1-IG* allele of *ZmKin6* would be deleterious with a score of -10.789 (Figure 2.3). We conducted an allelism test by crossing a line homozygous for the *dv1-1* allele with a line heterozygous for the *dv1-IG* allele. The heteroallelic progeny (*dv1-1/dv1-IG*) showed a clearly divergent spindle phenotype (Figure 2.1D, n=6). Taken together, these data indicate that *ZmKin6* is the *Dv1* gene.

The dv1-1 *allele affects meiotic spindle shape and length as a homozygote and heterozygote*

The segregating F2 population described above was also used for a more thorough imaging analysis of homozygous mutant (*dv1-1*/*dv1-1*), heterozygous (*dv1-1*/+), and wild type (B73) siblings. Spindle shape was quantified by measuring the width of the metaphase plate (W_C), the length of the half-spindle (L), and the width of the spindle at 75% of the length of the half-spindle (W_S) (Figure 2.4A). The metaphase plate was found to be significantly wider in *dv1-1* mutants than wild type or heterozygous siblings (Figure 2.4B, α=0.05). Half-spindle length was determined to be significantly longer in plants

carrying *dv1-1* as both a heterozygote and a homozygote (Figure 2.4C, α=0.05). Due to the differences in W_C, we opted to correct the comparison of W_S measurements by the width of the chromosomes. The resulting ratio of spindle width to metaphase plate width (W_S/W_C) represents how tightly focused the spindle is: a value closer to 1 indicates that the spindle microtubules have not converged while a value closer to 0 indicates a very narrow, tightly organized spindle (Figure 2.4A). When spindle width was measured at the distance of 75% along its half-length, spindle shape was significantly more diverged in *dv1-1* mutants than in either wild type or heterozygous siblings. However we also observed that heterozygotes displayed an intermediate phenotype suggestive of partial dominance (Figure 2.4D). Our data show that the mode of inheritance for the effects of *dv1-1* varies for different phenotypes (Table 2.2).

Errors in chromosome segregation and pollen viability

Prior data suggest that a small percentage of *dv1* cells contain severely perturbed spindles (Staiger and Cande, 1990). We also observed similar phenotypes. For instance, some spindles appear to be dividing into parts, with separate spindles parallel to one another (Figure 2.5A, 2.5B). We also observed prometaphase cells with entirely separate spindles oriented in different directions in both the *dv1-1* (Figure 2.5C) and *dv1-IG* homozygotes (Figure 2.5D). Multiple mini-spindles within a single cell have been reported in meiosis II of the *Arabidopsis AtKin14A* mutant, similar to what we have observed here (Chen et al., 2002). One particularly abnormal spindle showed the opposite phenotype, with congressed chromosomes but a very distinct, tri-polar spindle (Figure

2.5E). These extreme phenotypes were only observed in homozygous mutants, suggesting the heterozygous genotype is not sufficient to produce such aberrant spindles.

Although such severe spindle defects seem likely to lead to errors in chromosome segregation, we rarely observed lagging chromosomes at anaphase (Figure 2.5F). One way to assay chromosome loss during meiosis is to score at the tetrad stage where lost chromosomes are visible as "mininuclei" that are separated from primary telophase nuclei (Figure 2.5G). We therefore analyzed tetrad-stage cells derived from the same F2 siblings segregating for *dv1-1*. Kinetochores were visualized using an antibody to Centromere Protein C (CENP-C) as a means to distinguish chromosomes from one another (Dawe et al., 1999). Less than one percent of *dv1-1* cells at the tetrad stage (3 of 434 counted) showed a multinucleate phenotype, demonstrating that while meiotic spindle shape is clearly aberrant in *dv1-1* plants, the majority of cells segregate chromosomes correctly.

The *dv1* mutant is known to affect pollen viability (Clark, 1940). This phenotype could be caused by loss of chromosomes from aberrant meioses, errors in the mitotic cell divisions that precede pollen formation, or some other cause. It has been shown that mature pollen collected from *dv1-1* plants often contain fewer nuclei than expected (one or two nuclei instead of three), and that pollen with an abnormal number of nuclei are less likely to germinate (Clark, 1943). We stained pollen from the same F2 population using a modified version of Alexander's stain that differentiates viable pollen from empty exine (Peterson et al., 2010). Mean pollen viability was significantly lower in *dv1-1* mutants, showing a reduction from 97.7% in wild type to 86.8% in mutant plants (Figure 2.5H, α=0.05). The viability of pollen in the *dv1-1*/+ heterozygote was an intermediate

value of 94.3% that was not significantly different from either wild type or *dv1-1* mutants (Figure 2.5H, α=0.05). These results suggest that the effects of *dv1-1* on pollen viability are not necessarily an outcome of spindle defects in meiosis and may be caused by errors in the mitotic divisions during gametophyte development.

Live cell imaging of dv1 *implicates specific roles for kinesin-14As in spindle assembly*

The static images provided by fixed specimens have limited value when studying a dynamic process such as spindle assembly. To observe the *dv1-1* phenotype in live cells, we crossed *dv1-1* into a maize line containing a version of β-tubulin tagged with cyan fluorescent protein (Mohanty et al., 2009). Meiocytes carrying the CFP-tubulin transgene were extruded from anthers into a growth medium containing SYTO12, a fluorophore that stains DNA in live cells (Yu et al., 1997), allowing for two-color imaging of spindle microtubules and chromosomes. Viable cells in prometaphase and metaphase are difficult to find and rarely continue through anaphase under observation; however, we were able to image several live meiocytes from wild type, *dv1-1/+*, and *dv1-1* plants.

In wild type cells, prometaphase chromosomes begin in close proximity to one another and only mild adjustments are needed to align them in the metaphase plate (Figure 2.6A). In contrast, the chromosomes of a *dv1-1* cell begin much further apart and require more dramatic movement to form a metaphase plate (Figure 2.6B). Separate microtubule spindles attach to distinct groups of chromosomes and then fold and connect with one another as the chromosomes begin to congress (Figure 2.6B). These data

corroborate the findings from our immunolocalization imaging showing multiple smaller spindles forming in *dv1-1* mutants (Figure 2.5C, 2.5D).

Additional live cell imaging shows chromosome and spindle dynamics in metaphase and anaphase. As a wild type cell prepares to enter anaphase, the poles of the metaphase spindle focus from a rounded tip to a pointed tip before the chromosomes divide (Figure 2.6C). A heterozygous *dv1-1/+* cell shows a similar phenotype with the spindle tips curling along the edge of the cell (Figure 2.6D). A third series of images from a *dv1-1* homozygote shows that the spindle pole never becomes fully focused before anaphase begins. (Figure 2.6E). While chromosome segregation toward the poles is uniform in both the wild type and *dv1-1/+* cells, lagging chromosomes were observed in the *dv1-1* homozygote, a phenotype seen in fixed cells as well (Figure 2.6F).

To quantify the observed effects of *dv1-1* on spindle morphogenesis, we measured three separate phenotypes: chromosome congression, anaphase segregation distance and rate of chromosome movement. Due to difficulty of capturing living meiocytes undergoing division, the sample size is low and not amenable to statistical analysis (n = 4 to 12 per genotype). We defined chromosome offset as the distance between the center of the spindle and the center of the mass of chromosomes at metaphase. This value accesses how well the chromosomes are congressed and aligned in the middle of the spindle. The trends from our data suggest that *dv1-1* negatively affects the cell's ability to organize and collect chromosomes on the spindle (Figure 2.6F). Anaphase A is the movement of the chromosomes from the metaphase plate towards the poles, and is the result of the retraction of chromosomes along the kinetochore microtubules. The trends in our data show that chromosomes move slightly farther in both the *dv1-1/+* and *dv1-1* genotypes

(Figure 2.6G). The rate of chromosome movement in anaphase A is very uniform across all three genotypes (Figure 2.6H), suggesting that the difference in anaphase A distance is due to movement over a longer time rather than a faster movement. The genotypes with farther moving chromosomes are the same as those with longer spindles *(dv1-1 and dv1-1/+*, Figure 2.4C) and the possible relationship between these phenotypes is discussed below.

DISCUSSION

We demonstrate that the maize *Dv1* locus encodes the kinesin-14A gene GRMZM2G114861, previously described as *ZmKin6* (Lawrence et al., 2002). The reference allele *dv1-1* contains a stop codon in the middle of the gene that results nonsense mediated decay of the transcript while a second allele *dv1-IG* contains a deleterious mutation in the conserved motor domain. Both alleles affect spindle shape (Figure 2.4D) and pollen viability (Figure 2.5H). The fact that kinesin-14A mutants in other species have very similar phenotypes to *dv1* (Matthies et al., 1996;Chen et al., 2002;Ambrose and Cyr, 2007) provides further evidence supporting this conclusion.

Our quantitative analysis of spindle shape suggests that *dv1* affects both the width and length of the half-spindle, with the effect on half-spindle length being genetically dominant (Table 2.2). The large decrease in *Dv1* expression observed in heterozygous lines (Figure 2.1C) suggests that the semi-dominant effects we observed may be due to haploinsufficiency. We also found that pollen viability is reduced in both *dv1* homozygotes and heterozygotes (Table 2.2) although the effects on pollen viability were not as severe as those previously described by either Clark (as low as 10% viable, 1943)

or Staiger and Cande (approximately 44% viable, 1990). Shamina and coworkers (2000) demonstrated a dramatic effect on spindle shape in *dv1* plants grown under altered light and temperature conditions, suggesting that the *dv1* phenotype may depend heavily on genetic background and environmental conditions.

Our data support the prevailing view that the major role of C-terminal kinesins such as DV1 in spindle assembly is to gather microtubules and focus the spindle poles (Sharp et al., 2000). The model presented by Hepperla et al. (2014) suggests that kinesin-14 motors are capable of cross-linking antiparallel microtubules from the two different spindle poles, allowing them to tighten and slide along one another. Measurements of wild type and *dv1-1* spindles indicate that mutant spindles are wider at both the metaphase plate (Figure 2.4B) and 75% along the length of the half-spindle (Figure 2.4D), supporting a role for kinesin-14As in pulling microtubules together. Our measurements of half-spindle length indicate *dv1-1* mutants have longer spindles than wild type (Figure 2.4C), contrary to findings of other kinesin-14A studies in mitotic cells of humans (Cai et al., 2009) and yeast (Troxell et al., 2001). The *Arabidopsis* homolog *AtKin14B* showed no effect on spindle length at metaphase in mitotic tissues (Ambrose and Cyr, 2007). Our finding of increased spindle length could be the result of the lack of a canonical MTOC in plant cells, a unique effect of meiosis, or some factor of both. Overall, microtubules in wild type cells and *dv1-1* cells appear similar early in metaphase, where spindles are only loosely focused. It is only later in organization of the spindle structure that the phenotype becomes obvious, as wild type cells proceed to form tightly focused poles, but *dv1-1* spindles remain in a loosely focused state.

While DV1 is not strictly required for the separation of chromosomes, we observed negative effects in anaphase such as lagging chromosomes in the *dv1-1* mutant (Figure 2.5F, Figure 2.6E). Homozygous *dv1-1* plants nevertheless produced ample functional pollen (Figure 2.5H) and assays for micronuclei (Figure 2.5G) showed that errors in chromosome segregation are rare. One explanation for the limited phenotypic consequences of *dv1* may be genetic redundancy, as the second kinesin-14A gene in maize GRMZM2G436981 (Lawrence et al., 2002) is expressed at a low level in anthers (Sekhon et al., 2011) and may be involved in spindle morphogenesis as well.

While the major effects of *dv1* on microtubule organization are not visible until late in the organization of the meiotic spindle, *dv1-1* has been shown to have effects on nuclear envelope prior to its breakdown at the onset of metaphase. The localization of ZmSUN2, a protein that functions as a part of complex that bridges chromatin and the cytoskeleton during meiotic prophase is aberrant in *dv1-1* mutants (Murphy et al., 2014) and fragments of the nuclear envelope remain among the chromosomes as late as metaphase (Shamina et al., 2000). A survey of male meiosis in several species of land plants indicates that the male meiotic spindle is derived from a “chaotic array” of bipolar microtubules which crash into the nuclear space following envelope breakdown (Shamina, 2005). Our movies of wild type meiocytes match this observation with a single large spindle quickly forming and focusing (Figure 2.6A, 2.6C). In *dv1-1* cells, we observed several small spindles independently forming around separate groups of chromosomes which were then pulled together (Figure 2.5A, 2.5C, 2.5D, 2.6B). Perhaps poor collection of the chromosome bivalents in the nucleus during prophase, a result of mislocalization of SUN2 in the absence of DV1 (Murphy et al., 2014), causes

chromosomes to be more dispersed following nuclear envelope breakdown. Live cell imaging shows that meiocytes are capable of at least partially correcting this error (Figure 2.6B), but nuclear envelope defects could be partially responsible for the some of the spindle phenotypes observed in *dv1* meiocytes, such as the increased size of the metaphase plate (Figure 2.4B) and decreased chromosome alignment on the spindle (Figure 2.6F). Future studies on the physical interactions between DV1 and other proteins at the surface of the nucleus are needed to explore this potential mechanism.

In animals where centrosomes facilitate spindle formation, the minus-end directed motor dynein has a key role is focusing spindle poles (Sharp et al., 2000). However, the oocytes of many animals are anastral, lacking centrosomes, and form by a mechanism whereby the kinesin superfamily of proteins has a more prominent role in organizing poles (Walczak et al., 1998). Higher plants lack dynein (Lawrence et al., 2001) and their spindles are presumed to form by a mechanism similar to animal anastral spindles, thus relying more heavily on the activity of kinesins (Bannigan et al., 2008;Zhang and Dawe, 2011). Our data on *dv1* provides direct supporting evidence for this model of kinesin-driven spindle assembly. While still able to form a metaphase plate and bundle microtubules, reduction of kinesin-14A inhibits the formation of the spindle poles, causing a mild reduction in the accuracy of chromosome segregation and viability of resulting daughter cells.

ACKNOWLEDGEMENTS

We thank Lisa Kanizay for initiating this project and for providing the images in Figures 3C and G. We thank Amy Hodges and Caroline Jackson for technical support,

and Jay Hollick for providing the A619 inbred. Funding was provided by grants from the National Science Foundation to NJN (1400616) and RKD (1412063). The authors declare no conflicts of interest.

WORKS CITED

Alexander, M. (1969). Differential staining of aborted and nonaborted pollen. *Stain technology* 44**,** 117-122.

Ambrose, J.C., and Cyr, R. (2007). The kinesin ATK5 functions in early spindle assembly in Arabidopsis. *The Plant Cell* 19**,** 226-236.

Ambrose, J.C., Li, W., Marcus, A., Ma, H., and Cyr, R. (2005). A minus-end-directed kinesin with plus-end tracking protein activity is involved in spindle morphogenesis. *Mol Biol Cell* 16**,** 1584-1592.

Asai, D.J., Thompson, W.C., Wilson, L., and Brokaw, C.J. (1982). Two different monoclonal antibodies to alpha-tubulin inhibit the bending of reactivated sea urchin spermatozoa. *Cell motility* 2**,** 599-614.

Bannigan, A., Lizotte-Waniewski, M., Riley, M., and Baskin, T.I. (2008). Emerging molecular mechanisms that power and regulate the anastral mitotic spindle of flowering plants. *Cell motility and the cytoskeleton* 65**,** 1-11.

Cai, S., Weaver, L.N., Ems-Mcclung, S.C., and Walczak, C.E. (2009). Kinesin-14 family proteins HSET/XCTK2 control spindle length by cross-linking and sliding microtubules. *Mol Biol Cell* 20**,** 1348-1359.

Cande, W.Z., and Freeling, M. (2011). Inna Golubovskaya: the life of a geneticist studying meiosis. *Genetics* 188**,** 491-498.

Carlson, W.R., Sprague, G., and Dudley, J. (1988). The Cytogenetics of Corn. *Corn and Corn Improvement. Third Edition.***,** 259-343.

Chan, J., Calder, G.M., Doonan, J.H., and Lloyd, C.W. (2003). EB1 reveals mobile microtubule nucleation sites in Arabidopsis. *Nat Cell Biol* 5**,** 967-971.

Chen, C., Marcus, A., Li, W., Hu, Y., Calzada, J.-P.V., Grossniklaus, U., Cyr, R.J., and Ma, H. (2002). The *Arabidopsis ATK1* gene is required for spindle morphogenesis in male meiosis. *Development* 129**,** 2401-2409.

Choi, Y., and Chan, A.P. (2015). PROVEAN web server: a tool to predict the functional effect of amino acid substitutions and indels. *Bioinformatics* 31**,** 2745-2747.

Choi, Y., Sims, G.E., Murphy, S., Miller, J.R., and Chan, A.P. (2012). Predicting the Functional Effect of Amino Acid Substitutions and Indels. *PLoS ONE* 7**,** e46688.

Clark, F.J. (1940). Cytogenetic Studies of Divergent Meiotic Spindle Formation in Zea Mays. *American Journal of Botany* 27**,** 547-559.

Clark, F.J. (1943). The Germination Capacity of Maize Pollen Having Aberrant Nuclei. *Bulletin of the Torrey Botanical Club* 70**,** 449-456.

Clarke, J.D. (2009). Cetyltrimethyl ammonium bromide (CTAB) DNA miniprep for plant DNA isolation. *Cold Spring Harbor Protocols* 2009**,** pdb. prot5177.

Conduit, P.T., Wainman, A., and Raff, J.W. (2015). Centrosome function and assembly in animal cells. *Nat Rev Mol Cell Biol* 16**,** 611-624.

Dawe, R.K., Reed, L.M., Yu, H.-G., Muszynski, M.G., and Hiatt, E.N. (1999). A maize homolog of mammalian CENPC is a constitutive component of the inner kinetochore. *The Plant Cell* 11**,** 1227-1238.

De La Peña, A. (1986). 'In vitro' culture of isolated meiocytes of rye, Secale cereale L. *Environmental and Experimental Botany* 26**,** 17-23.

De Mendiburu, F. (2014). Agricolae: statistical procedures for agricultural research. *R package version* 1**,** 1-6.

Edgar, R.C. (2004). MUSCLE: multiple sequence alignment with high accuracy and high throughput. *Nucleic Acids Research* 32**,** 1792-1797.

Hepperla, A.J., Willey, P.T., Coombes, C.E., Schuster, B.M., Gerami-Nejad, M., Mcclellan, M., Mukherjee, S., Fox, J., Winey, M., and Odde, D.J. (2014). Minus-End-Directed Kinesin-14 Motors Align Antiparallel Microtubules to Control Metaphase Spindle Length. *Developmental cell* 31**,** 61-72.

Hirokawa, N., and Noda, Y. (2008). Intracellular transport and kinesin superfamily proteins, KIFs: structure, function, and dynamics. *Physiological reviews* 88**,** 1089-1118.

Hirokawa, N., Noda, Y., Tanaka, Y., and Niwa, S. (2009). Kinesin superfamily motor proteins and intracellular transport. *Nat Rev Mol Cell Biol* 10**,** 682-696.

Hirokawa, N., Pfister, K.K., Yorifuji, H., Wagner, M.C., Brady, S.T., and Bloom, G.S. (1989). Submolecular domains of bovine brain kinesin identified by electron microscopy and monoclonal antibody decoration. *Cell* 56**,** 867-878.

Howard, J., and Hyman, A.A. (2003). Dynamics and mechanics of the microtubule plus end. *Nature* 422**,** 753-758.

Kilmartin, J.V. (2014). Lessons from yeast: the spindle pole body and the centrosome. *Philosophical Transactions of the Royal Society of London B: Biological Sciences* 369**,** 20130456.

Kull, F.J., Sablin, E.P., Lau, R., Fletterick, R.J., and Vale, R.D. (1996). Crystal structure of the kinesin motor domain reveals a structural similarity to myosin. *Nature* 380**,** 550.

Lawrence, C.J., Dawe, R.K., Christie, K.R., Cleveland, D.W., Dawson, S.C., Endow, S.A., Goldstein, L.S., Goodson, H.V., Hirokawa, N., Howard, J., Malmberg, R.L., Mcintosh, J.R., Miki, H., Mitchison, T.J., Okada, Y., Reddy, A.S., Saxton, W.M., Schliwa, M., Scholey, J.M., Vale, R.D., Walczak, C.E., and Wordeman, L. (2004). A standardized kinesin nomenclature. *J Cell Biol* 167**,** 19-22.

Lawrence, C.J., Malmberg, R.L., Muszynski, M.G., and Dawe, R.K. (2002). Maximum likelihood methods reveal conservation of function among closely related kinesin families. *J Mol Evol* 54**,** 42-53.

Lawrence, C.J., Morris, N.R., Meagher, R.B., and Dawe, R.K. (2001). Dyneins Have Run Their Course in Plant Lineage. *Traffic* 2**,** 362-363.

Liu, B., Hotta, T., Ho, C.-M.K., and Lee, Y.-R.J. (2011). "Microtubule Organization in the Phragmoplast," in *The Plant Cytoskeleton*, ed. B. Liu. (New York, NY: Springer New York), 207-225.

Livak, K.J., and Schmittgen, T.D. (2001). Analysis of relative gene expression data using real-time quantitative PCR and the $2^{-\Delta\Delta CT}$ method. *methods* 25**,** 402-408.

Lloyd, C.W., and Chan, J. (2006). Not so divided: the common basis of plant and animal cell division. *Nature Reviews Molecular Cell Biology* 7**,** 147-152.

Manoli, A., Sturaro, A., Trevisan, S., Quaggiotti, S., and Nonis, A. (2012). Evaluation of candidate reference genes for qPCR in maize. *Journal of Plant Physiology* 169**,** 807-815.

Matthies, H.J., Mcdonald, H.B., Goldstein, L.S., and Theurkauf, W.E. (1996). Anastral meiotic spindle morphogenesis: role of the non-claret disjunctional kinesin-like protein. *The Journal of Cell Biology* 134**,** 455-464.

Mcdonald, H.B., Stewart, R.J., and Goldstein, L.S. (1990). The kinesin-like ncd protein of Drosophila is a minus end-directed microtubule motor. *Cell* 63**,** 1159-1165.

Mcmichael, C.M., and Bednarek, S.Y. (2013). Cytoskeletal and membrane dynamics during higher plant cytokinesis. *New Phytologist* 197**,** 1039-1057.

Meluh, P.B., and Rose, M.D. (1990). KAR3, a kinesin-related gene required for yeast nuclear fusion. *Cell* 60**,** 1029-1041.

Mineyuki, Y. (1999). "The Preprophase Band of Microtubules: Its Function as a Cytokinetic Apparatus in Higher Plants," in *International Review of Cytology,* ed. W.J. Kwang. Academic Press), 1-49.

Mitsui, H., Yamaguchi-Shinozaki, K., Shinozaki, K., Nishikawa, K., and Takahashi, H. (1993). Identification of a gene family (kat) encoding kinesin-like proteins in Arabidopsis thaliana and the characterization of secondary structure of KatA. *Molecular and General Genetics MGG* 238**,** 362-368.

Mohanty, A., Luo, A., Deblasio, S., Ling, X., Yang, Y., Tuthill, D.E., Williams, K.E., Hill, D., Zadrozny, T., Chan, A., Sylvester, A.W., and Jackson, D. (2009). Advancing cell biology and functional genomics in maize using fluorescent protein-tagged lines. *Plant Physiol* 149**,** 601-605.

Murphy, S.P., Gumber, H.K., Mao, Y., and Bass, H.W. (2014). A dynamic meiotic SUN belt includes the zygotene-stage telomere bouquet and is disrupted in chromosome segregation mutants of maize (Zea mays L.). *Frontiers in Plant Science* 5**,** 314.

Peterson, R., Slovin, J.P., and Chen, C. (2010). A simplified method for differential staining of aborted and non-aborted pollen grains. *International Journal of Plant Biology* 1.

Quan, L., Xiao, R., Li, W., Oh, S.A., Kong, H., Ambrose, J.C., Malcos, J.L., Cyr, R., Twell, D., and Ma, H. (2008). Functional divergence of the duplicated AtKIN14a and AtKIN14b genes: critical roles in Arabidopsis meiosis and gametophyte development. *Plant J* 53**,** 1013-1026.

Sablin, E.P., Kull, F.J., Cooke, R., Vale, R.D., and Fletterick, R.J. (1996). Crystal structure of the motor domain of the kinesin-related motor ncd. *Nature* 380**,** 555-559.

Schnable, P.S., Ware, D., Fulton, R.S., Stein, J.C., Wei, F., Pasternak, S., Liang, C., Zhang, J., Fulton, L., Graves, T.A., Minx, P., Reily, A.D., Courtney, L., Kruchowski, S.S., Tomlinson, C., Strong, C., Delehaunty, K., Fronick, C., Courtney, B., Rock, S.M., Belter, E., Du, F., Kim, K., Abbott, R.M., Cotton, M., Levy, A., Marchetto, P., Ochoa, K., Jackson, S.M., Gillam, B., Chen, W., Yan, L., Higginbotham, J., Cardenas, M., Waligorski, J., Applebaum, E., Phelps, L., Falcone, J., Kanchi, K., Thane, T., Scimone, A., Thane, N., Henke, J., Wang, T.,

Ruppert, J., Shah, N., Rotter, K., Hodges, J., Ingenthron, E., Cordes, M., Kohlberg, S., Sgro, J., Delgado, B., Mead, K., Chinwalla, A., Leonard, S., Crouse, K., Collura, K., Kudrna, D., Currie, J., He, R., Angelova, A., Rajasekar, S., Mueller, T., Lomeli, R., Scara, G., Ko, A., Delaney, K., Wissotski, M., Lopez, G., Campos, D., Braidotti, M., Ashley, E., Golser, W., Kim, H., Lee, S., Lin, J., Dujmic, Z., Kim, W., Talag, J., Zuccolo, A., Fan, C., Sebastian, A., Kramer, M., Spiegel, L., Nascimento, L., Zutavern, T., Miller, B., Ambroise, C., Muller, S., Spooner, W., Narechania, A., Ren, L., Wei, S., Kumari, S., Faga, B., Levy, M.J., Mcmahan, L., Van Buren, P., Vaughn, M.W., et al. (2009). The B73 Maize Genome: Complexity, Diversity, and Dynamics. *Science* 326**,** 1112-1115.

Sekhon, R.S., Lin, H., Childs, K.L., Hansey, C.N., Buell, C.R., De Leon, N., and Kaeppler, S.M. (2011). Genome-wide atlas of transcription during maize development. *The Plant Journal* 66**,** 553-563.

Shamina, N., Dorogova, N., and Trunova, S. (2000). Radial Spindle and the Phenotype of the Maize Meiotic Mutant, DV. *Cell Biology International* 24**,** 729-736.

Shamina, N.V. (2005). Formation of division spindles in higher plant meiosis. *Cell Biology International* 29**,** 307-318.

Sharp, D.J., Rogers, G.C., and Scholey, J.M. (2000). Microtubule motors in mitosis. *Nature* 407**,** 41-47.

Shaw, S.L., Kamyar, R., and Ehrhardt, D.W. (2003). Sustained Microtubule Treadmilling in Arabidopsis Cortical Arrays. *Science* 300**,** 1715-1718.

Staiger, C.J., and Cande, W.Z. (1990). Microtubule Distribution in dv, a Maize Meiotic Mutant Defective in the Prophase to Metaphase Transition. *Developmental Biology* 138**,** 231-242.

Stamatakis, A. (2006). RAxML-VI-HPC: maximum likelihood-based phylogenetic analyses with thousands of taxa and mixed models. *Bioinformatics* 22**,** 2688-2690.

Troxell, C.L., Sweezy, M.A., West, R.R., Reed, K.D., Carson, B.D., Pidoux, A.L., Cande, W.Z., and Mcintosh, J.R. (2001). pkl1(+)and klp2(+): Two kinesins of the Kar3 subfamily in fission yeast perform different functions in both mitosis and meiosis. *Mol Biol Cell* 12**,** 3476-3488.

Vale, R.D., Reese, T.S., and Sheetz, M.P. (1985). Identification of a novel force-generating protein, kinesin, involved in microtubule-based motility. *Cell* 42**,** 39-50.

Walczak, C., Verma, S., and Mitchison, T. (1997). XCTK2: A Kinesin-related Protein That Promotes Mitotic Spindle Assembly in *Xenopus laevis* Egg Extracts. *Journal of Cell Biology* 136**,** 859-870.

Walczak, C.E., Vernos, I., Mitchison, T.J., Karsenti, E., and Heald, R. (1998). A model for the proposed roles of different microtubule-based motor proteins in establishing spindle bipolarity. *Current biology* 8**,** 903-913.

Walker, R.A., Salmon, E.D., and Endow, S.A. (1990). The Drosophila Claret Segregation Protein Is a Minus-End Directed Motor Molecule. *Nature* 347**,** 780-782.

Yu, H.-G., Hiatt, E.N., Chan, A., Sweeney, M., and Dawe, R.K. (1997). Neocentromere-mediated Chromosome Movement in Maize. *The Journal of Cell Biology* 139**,** 831-840.

Zhang, H., and Dawe, R.K. (2011). Mechanisms of plant spindle formation. C*hromosome research* 19**,** 335-344.

Table 2.1 Complete list of DNA primers used in Chapter 2.

Primer Name	Sequence (5' -> 3')	Locus (5')
	Identification of SNPs in ZmKin6	
ZMKin6 LP-Flank	TCTGTTTGGGTCCACGAGTT	7625686
ZMKin6 LP-1	GCGGTAAGTAGGCTGTGAATTG	7626440
ZMKin6 LP-2	ACCCAAGTCTGCTACACCAA	7626878
ZMKin6 LP-3	ACGTGGTCATCTCCTTTTGC	7627369
ZMKin6 LP-4	ACCTACTCTGGGATGCTTTCTC	7628098
ZMKin6 LP-5	TCCTTGAGATTCTAGAAACCGAC	7628403
ZMKin6 LP-6	TGCCTTACTCATCATGTTGGG	7628878
ZMKin6 LP-7	GAGGCCGATTGTTAACTAGAGAG	7629345
ZMKin6 LP-8	TTGGTGCGGAATCTTTCACA	7629886
ZMKin6 LP-9	TGCTGAGCTGGGCCTCTG	7630907
ZMKin6 LP-10	CCTCCCACTGAACTCGATCA	7631368
ZMKin6 LP-11	GGGGTGGGATGGAGTGAA	7631908
ZMKin6 RP-1	AGCTATATCTTCACTTTGCAGCC	7627271
ZMKin6 RP-2	TGGATCTAACGAGGTAGAATGGA	7627794
ZMKin6 RP-3	CGTGATTTGTTAGCACCTGGT	7628260
ZMKin6 RP-4	CGGAAGGTGCCTCTATCTCT	7629263
ZMKin6 RP-5	TCGGACATTTCAAAAGCAGCT	7629769
ZMKin6 RP-6	CCGTCTGAAGTTTTACATGCT	7630765
ZMKin6 RP-7	ATTGATGCGGATTTGTCGG	7631265
ZMKin6 RP-8	CCACCCTCGCCTTCTCTC	7631780
ZMKin6 RP-Flank	TGCTCCATCCATTACGAGCT	7632062
	Genotyping of the dv1-1 Allele	
dv1-1 Geno LP	TGAAGGAAGAGCTCAGGAAAGA	7630054
dv1-1 Geno RP	GCCCGATAGTTACCCAGAAC	7629820
	Genotyping of the dv1-IG Allele	
dv1-IG Geno LP	TCCAACATTGATGCCTGCAC	7628280
dv1-IG Geno RP	TTTGTGCCCTCCAAGACATT	7628812
	Quantification of dv1 Transcripts	
dv1 qRT-PCR FP	AAGATATCTGGATCTAACGAGAACA	7627802
dv1 qRT-PCR RP	TTGACTGAGTTTCCTTCAAGC	7627436

Table 2.2 Summary of the modes of inheritance on different *dv1-1* phenotypes.

Phenotype	Mode of Inheritance
Spindle Length (L)	DOMINANT
Metaphase Plate Width (Wc)	RECESSIVE
Spindle Shape (Ws/Wc)	RECESSIVE
Pollen Viability	SEMI-DOMINANT

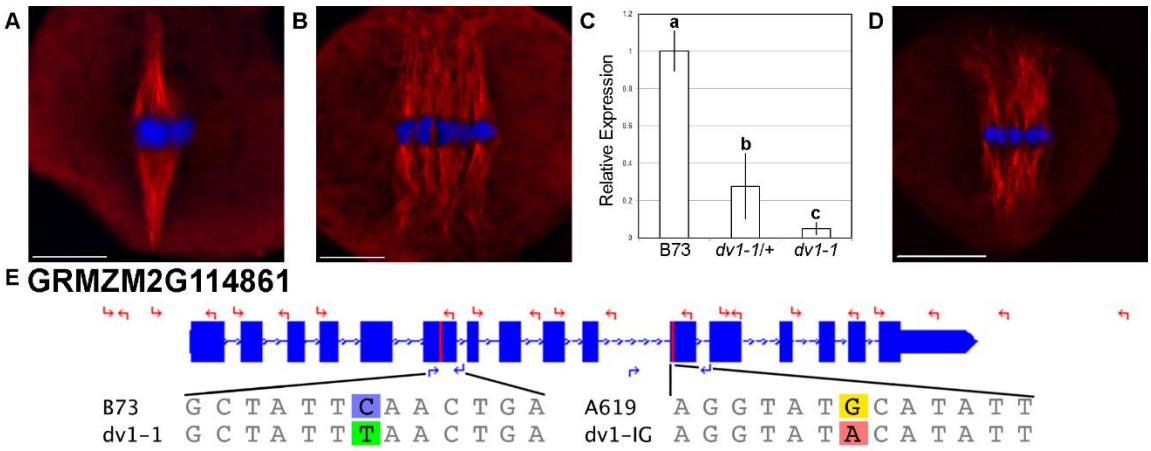

Figure 2.1 Two alleles of *dv1* show a divergent spindle phenotype.

Meiocytes were stained using immunofluorescence with a primary antibody specific to α-tubulin. Scale bars for each image represent 10 μm.

(A) Wild type spindle showing highly focused spindle poles;

(B) *dv1-1/dv1-1* spindle showing splayed, divergent poles;

(C) Expression of the *dv1-1* allele of ZmKin6 adjusted to the B73 wild type allele. Error bars represent 95% confidence intervals, groups of significant difference are designated with lowercase letters;

(D) *dv1-1/dv1-IG* heteroallelic mutant is similar to the *dv1-1* homozygote;

(E) Gene model of *ZmKin6* highlighting the location of the two *dv1* alleles, the *dv1-1* stop codon in the sixth exon and the *dv1-IG* transversion in the motor domain. Coordinates along chromosome 2 are shown above. The locations of sequencing primers are shown with red arrows while the locations of genotyping primers are shown with blue arrows. The reference and mutant sequences of each allele are shown below the gene diagram.

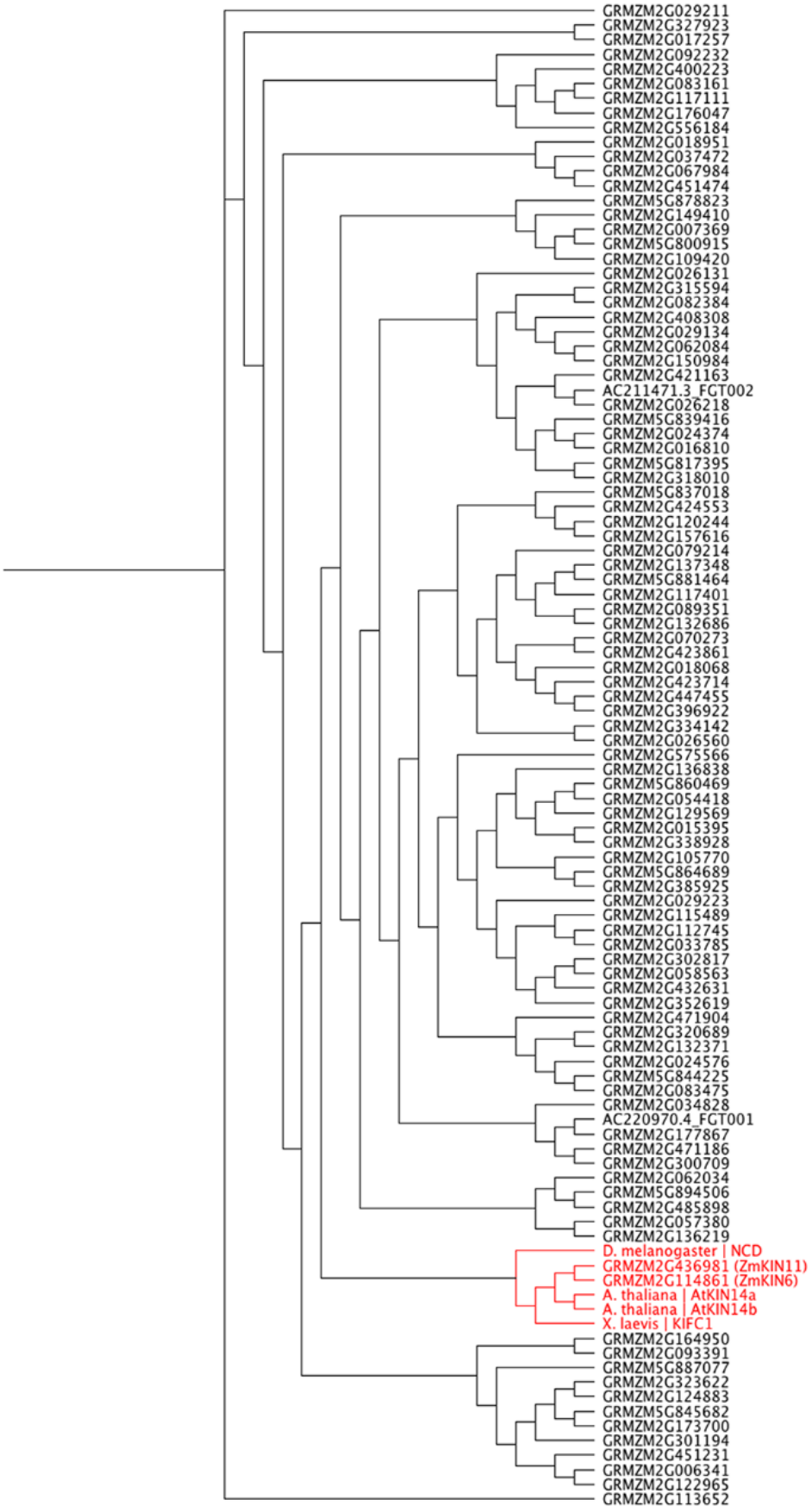
GRMZM2G029211
GRMZM2G327923
GRMZM2G017257
GRMZM2G092232
GRMZM2G400223
GRMZM2G083161
GRMZM2G117111
GRMZM2G176047
GRMZM2G556184
GRMZM2G018951
GRMZM2G037472
GRMZM2G067984
GRMZM2G451474
GRMZM5G878823
GRMZM2G149410
GRMZM2G007369
GRMZM5G800915
GRMZM2G109420
GRMZM2G026131
GRMZM2G315594
GRMZM2G082384
GRMZM2G408308
GRMZM2G029134
GRMZM2G062084
GRMZM2G150984
GRMZM2G421163
AC211471.3_FGT002
GRMZM2G026218
GRMZM5G839416
GRMZM2G024374
GRMZM2G016810
GRMZM5G817395
GRMZM2G318010
GRMZM5G837018
GRMZM2G424553
GRMZM2G120244
GRMZM2G157616
GRMZM2G079214
GRMZM2G137348
GRMZM5G881464
GRMZM2G117401
GRMZM2G089351
GRMZM2G132686
GRMZM2G070273
GRMZM2G423861
GRMZM2G018068
GRMZM2G423714
GRMZM2G447455
GRMZM2G396922
GRMZM2G334142
GRMZM2G026560
GRMZM2G575566
GRMZM2G136838
GRMZM5G860469
GRMZM2G054418
GRMZM2G129569
GRMZM2G015395
GRMZM2G338928
GRMZM2G105770
GRMZM5G864689
GRMZM2G385925
GRMZM2G029223
GRMZM2G115489
GRMZM2G112745
GRMZM2G033785
GRMZM2G302817
GRMZM2G058563
GRMZM2G432631
GRMZM2G352619
GRMZM2G471904
GRMZM2G320689
GRMZM2G132371
GRMZM2G024576
GRMZM5G844225
GRMZM2G083475
GRMZM2G034828
AC220970.4_FGT001
GRMZM2G177867
GRMZM2G471186
GRMZM2G300709
GRMZM2G062034
GRMZM5G894506
GRMZM2G485898
GRMZM2G057380
GRMZM2G136219
D. melanogaster | NCD
GRMZM2G436981 (ZmKIN11)
GRMZM2G114861 (ZmKIN6)
A. thaliana | AtKIN14a
A. thaliana | AtKIN14b
X. laevis | KIFC1
GRMZM2G164950
GRMZM2G093391
GRMZM5G887077
GRMZM2G323622
GRMZM2G124883
GRMZM5G845682
GRMZM2G173700
GRMZM2G301194
GRMZM2G451231
GRMZM2G006341
GRMZM2G122965
GRMZM2G113652

Figure 2.2 Alignment of maize kinesins reveals two members of the kinesin-14A subfamily.

Coding sequences were aligned using the MUSCLE algorithm. All genes shown are from the *Zea mays* B73 reference genome unless a different species name is given. Two maize genes appear with other members of the kinesin-14A subfamily (highlighted in red) and were identified as candidates for *Dv1*. The figure was generated using the software Geneious (v8.0).

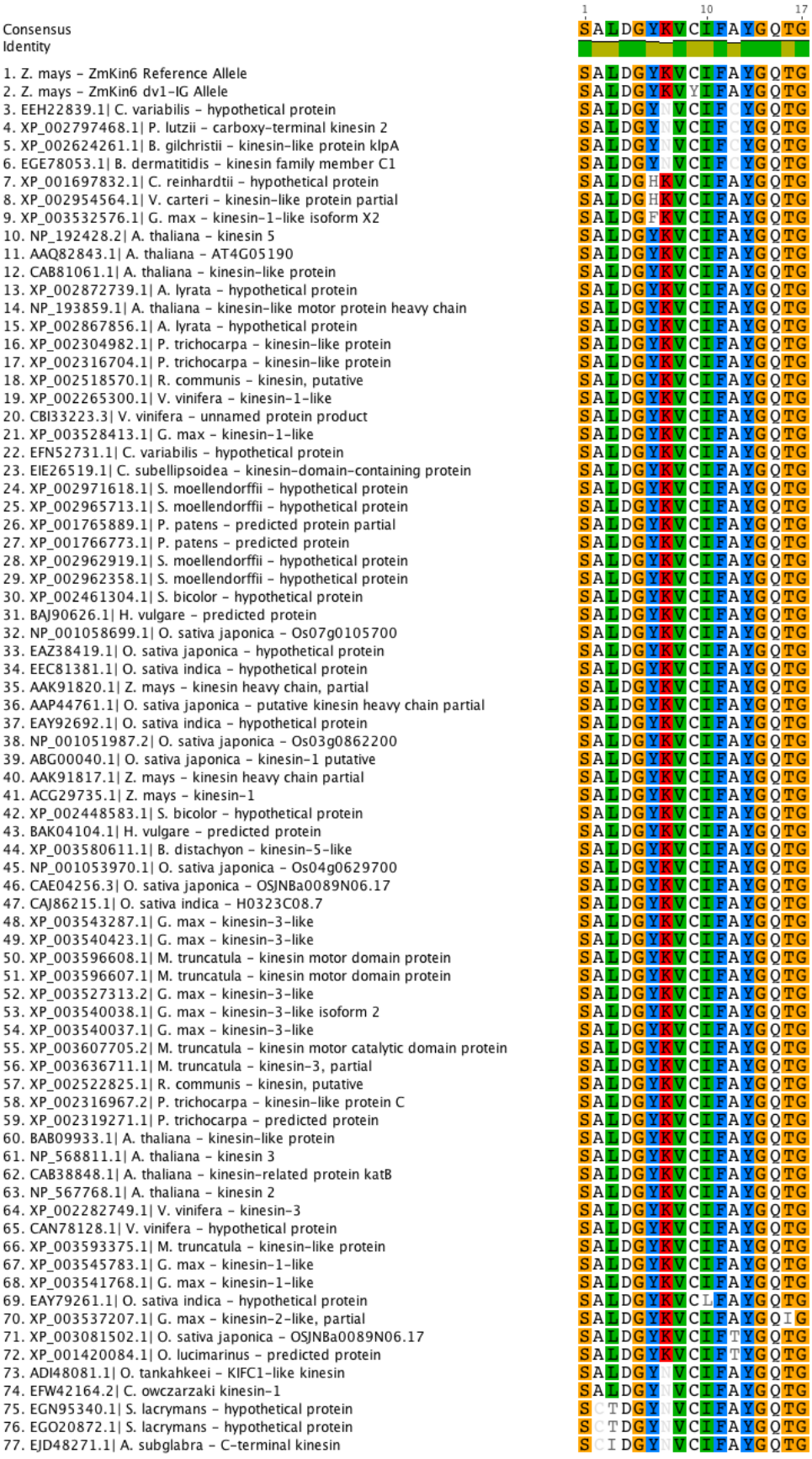
1
10
17
Consensus
Identity
1. Z. mays - ZmKin6 Reference Allele
2. Z. mays - ZmKin6 dv1-IG Allele
3. EEH22839.1| C. variabilis - hypothetical protein
4. XP_002797468.1| P. lutzii - carboxy-terminal kinesin 2
5. XP_002624261.1| B. gilchristii - kinesin-like protein klpA
6. EGE78053.1| B. dermatitidis - kinesin family member C1
7. XP_001697832.1| C. reinhardtii - hypothetical protein
8. XP_002954564.1| V. carteri - kinesin-like protein partial
9. XP_003532576.1| G. max - kinesin-1-like isoform X2
10. NP_192428.2| A. thaliana - kinesin 5
11. AAQ82843.1| A. thaliana - AT4G05190
12. CAB81061.1| A. thaliana - kinesin-like protein
13. XP_002872739.1| A. lyrata - hypothetical protein
14. NP_193859.1| A. thaliana - kinesin-like motor protein heavy chain
15. XP_002867856.1| A. lyrata - hypothetical protein
16. XP_002304982.1| P. trichocarpa - kinesin-like protein
17. XP_002316704.1| P. trichocarpa - kinesin-like protein
18. XP_002518570.1| R. communis - kinesin, putative
19. XP_002265300.1| V. vinifera - kinesin-1-like
20. CBI33223.3| V. vinifera - unnamed protein product
21. XP_003528413.1| G. max - kinesin-1-like
22. EFN52731.1| C. variabilis - hypothetical protein
23. EIE26519.1| C. subellipsoidea - kinesin-domain-containing protein
24. XP_002971618.1| S. moellendorffii - hypothetical protein
25. XP_002965713.1| S. moellendorffii - hypothetical protein
26. XP_001765889.1| P. patens - predicted protein partial
27. XP_001766773.1| P. patens - predicted protein
28. XP_002962919.1| S. moellendorffii - hypothetical protein
29. XP_002962358.1| S. moellendorffii - hypothetical protein
30. XP_002461304.1| S. bicolor - hypothetical protein
31. BAJ90626.1| H. vulgare - predicted protein
32. NP_001058699.1| O. sativa japonica - Os07g0105700
33. EAZ38419.1| O. sativa japonica - hypothetical protein
34. EEC81381.1| O. sativa indica - hypothetical protein
35. AAK91820.1| Z. mays - kinesin heavy chain, partial
36. AAP44761.1| O. sativa japonica - putative kinesin heavy chain partial
37. EAY92692.1| O. sativa indica - hypothetical protein
38. NP_001051987.2| O. sativa japonica - Os03g0862200
39. ABG00040.1| O. sativa japonica - kinesin-1 putative
40. AAK91817.1| Z. mays - kinesin heavy chain partial
41. ACG29735.1| Z. mays - kinesin-1
42. XP_002448583.1| S. bicolor - hypothetical protein
43. BAK04104.1| H. vulgare - predicted protein
44. XP_003580611.1| B. distachyon - kinesin-5-like
45. NP_001053970.1| O. sativa japonica - Os04g0629700
46. CAE04256.3| O. sativa japonica - OSJNBa0089N06.17
47. CAJ86215.1| O. sativa indica - H0323C08.7
48. XP_003543287.1| G. max - kinesin-3-like
49. XP_003540423.1| G. max - kinesin-3-like
50. XP_003596608.1| M. truncatula - kinesin motor domain protein
51. XP_003596607.1| M. truncatula - kinesin motor domain protein
52. XP_003527313.2| G. max - kinesin-3-like
53. XP_003540038.1| G. max - kinesin-3-like isoform 2
54. XP_003540037.1| G. max - kinesin-3-like
55. XP_003607705.2| M. truncatula - kinesin motor catalytic domain protein
56. XP_003636711.1| M. truncatula - kinesin-3, partial
57. XP_002522825.1| R. communis - kinesin, putative
58. XP_002316967.2| P. trichocarpa - kinesin-like protein C
59. XP_002319271.1| P. trichocarpa - predicted protein
60. BAB09933.1| A. thaliana - kinesin-like protein
61. NP_568811.1| A. thaliana - kinesin 3
62. CAB38848.1| A. thaliana - kinesin-related protein katB
63. NP_567768.1| A. thaliana - kinesin 2
64. XP_002282749.1| V. vinifera - kinesin-3
65. CAN78128.1| V. vinifera - hypothetical protein
66. XP_003593375.1| M. truncatula - kinesin-like protein
67. XP_003545783.1| G. max - kinesin-1-like
68. XP_003541768.1| G. max - kinesin-1-like
69. EAY79261.1| O. sativa indica - hypothetical protein
70. XP_003537207.1| G. max - kinesin-2-like, partial
71. XP_003081502.1| O. sativa japonica - OSJNBa0089N06.17
72. XP_001420084.1| O. lucimarinus - predicted protein
73. ADI48081.1| O. tankahkeei - KIFC1-like kinesin
74. EFW42164.2| C. owczarzaki kinesin-1
75. EGN95340.1| S. lacrymans - hypothetical protein
76. EGO20872.1| S. lacrymans - hypothetical protein
77. EJD48271.1| A. subglabra - C-terminal kinesin

Figure 2.3 PROVEAN output indicates the residue at which the *dv1-IG* mutation occurs is highly conserved.

The PROVEAN software identified 75 GenBank entries that show homology to the *Dv1* sequence. GenBank IDs are listed for each entry along with their species and given annotation. A portion of the PROVEAN alignment is shown at the right. Amino acid sequences for the B73 reference and *dv1-IG* allele are listed at the top. This cysteine in the middle of the alignment (residue 494) is conserved across the sample of plant, algae, and animal sequences. However, the *dv1-IG* allele codes for a tyrosine at this position. The figure was generated using the software Geneious (v8.0).

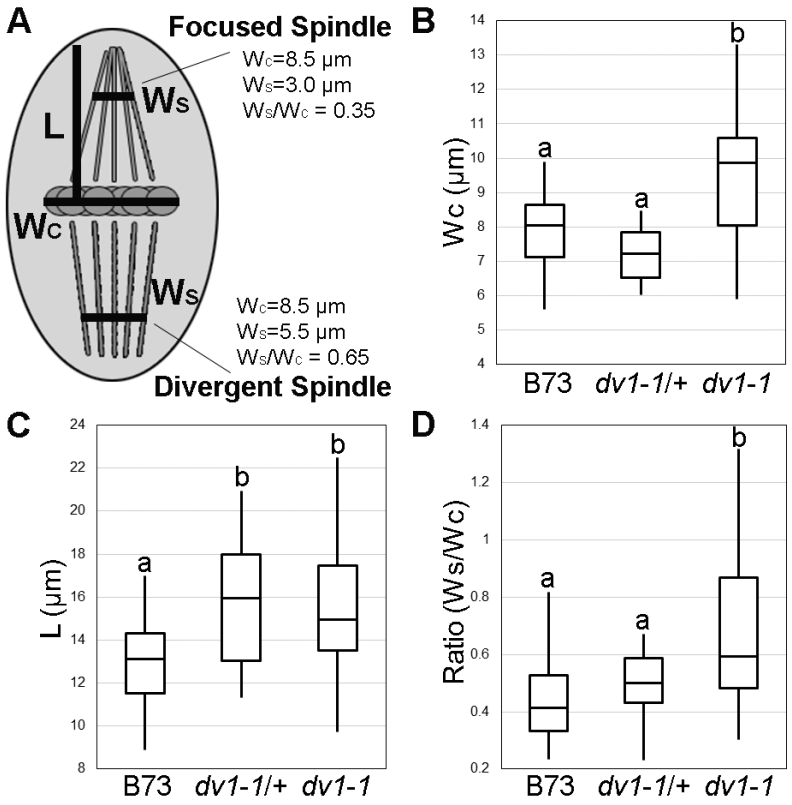

Figure 2.4 Quantification of the *dv1-1* phenotype on spindle shape and pollen viability.

Spindles were visualized using immunofluorescence as shown in Figure 2.1. Measurements were taken using the Slidebook 6 digital microscopy software package (Intelligent Imaging Innovations, Denver, CO). Lowercase letters in B, C, and D represent groups of significant difference as determined using ANOVA at α=0.05. (A) Schematic of measurements taken, including width of the metaphase plate (W_C), length of the half-spindle from metaphase plate to pole (L) and width of the spindle at 75% of length L (W_S). The ratio of W_S/W_C can be used to quantify spindle shape as either focused (shown in the top half-spindle) or divergent (bottom half-spindle); (B) Width of the metaphase plate (µm) is significantly higher in plants homozygous for *dv1-1* than either wild type or heterozygous plants;

(C) Length of the half-spindle (μm) is significantly larger than wild type in both *dv1-1* homozygotes and heterozygotes;

(D) The ratio of spindle width at the metaphase plate to spindle width near the poles, a proxy for spindle shape and degree of pole focus, is significantly higher in *dv1-1* plants while heterozygotes displayed an intermediate phenotype.

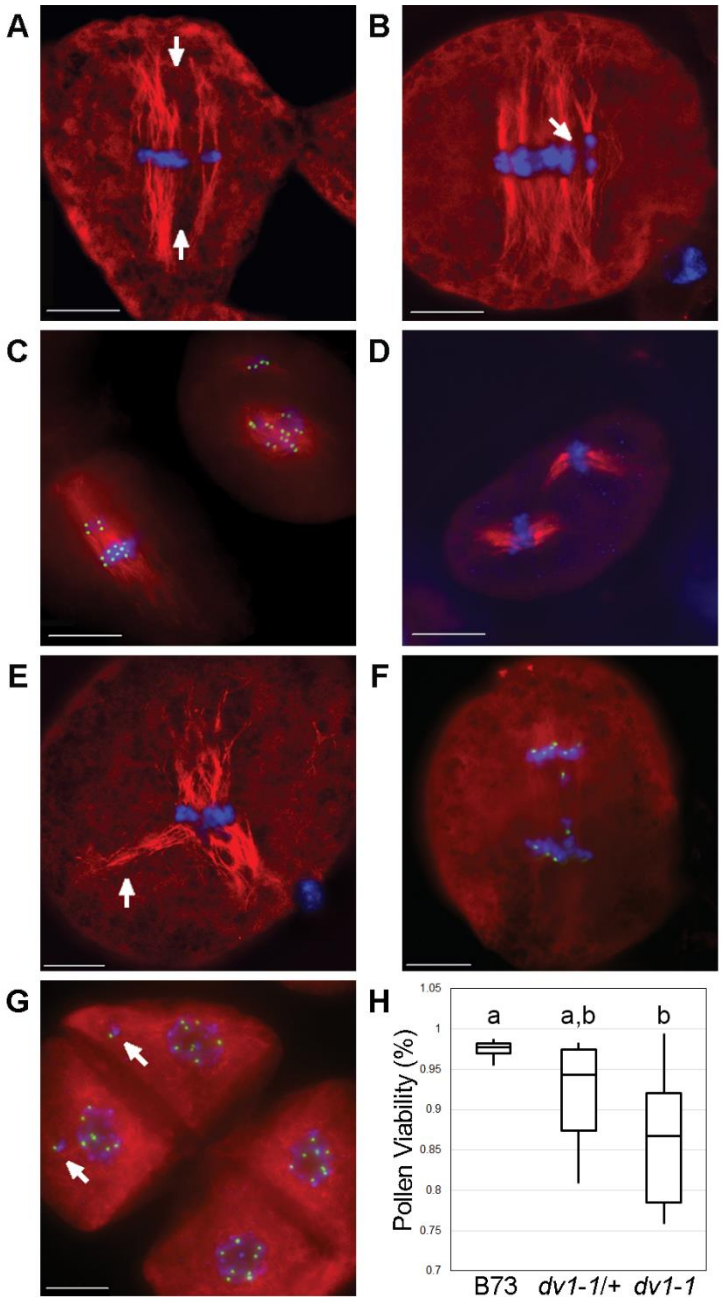

Figure 2.5 Rarely-observed severe effects of *dv1-1* include multiple spindles and multinucleate daughter cells.

Meiocytes were stained using immunofluorescence with a primary antibody specific to α-tubulin shown in red and CENP-C shown in green. DNA (DAPI) is shown in blue. Scale bars for each image represent 10 μm.

(A) Multi-spindle *dv1-1* cell with metaphase alignment errors. Poor congression of chromosomes along the metaphase plate in a *dv1-1* cell with parallel spindles in metaphase separated by space (arrows);

(B) Early anaphase of a similar *dv1-1* cell with parallel spindles and chromosomes separated by space (arrow);

(C) Cells with severe errors in spindle assembly. Cell on the left appears to be a fusion of a small and a large spindle in the process of correction. Cell on the right shows two distinct spindles, the larger of which appears as a chaotic array of early prometaphase;

(D) Two separate spindles of approximately the same size in a *dv1-IG* cell;

(E) Tri-polar spindle of a *dv1-1* cell at metaphase showing separated microtubules (arrow) with congressed chromosomes;

(F) Lagging chromosomes during anaphase in a *dv1-1* cell;

(G) Tetrad-stage cells showing examples of mininuclei (arrows), isolated chromosomes not a part of the nucleus;

(H) Pollen shows a decreased viability in both *dv1-1* homozygotes and heterozygotes. Groups of statistical significance are designated with lowercase letters (n=7-10 plants per genotype, 500 pollen grains per plant; $\alpha=0.05$).

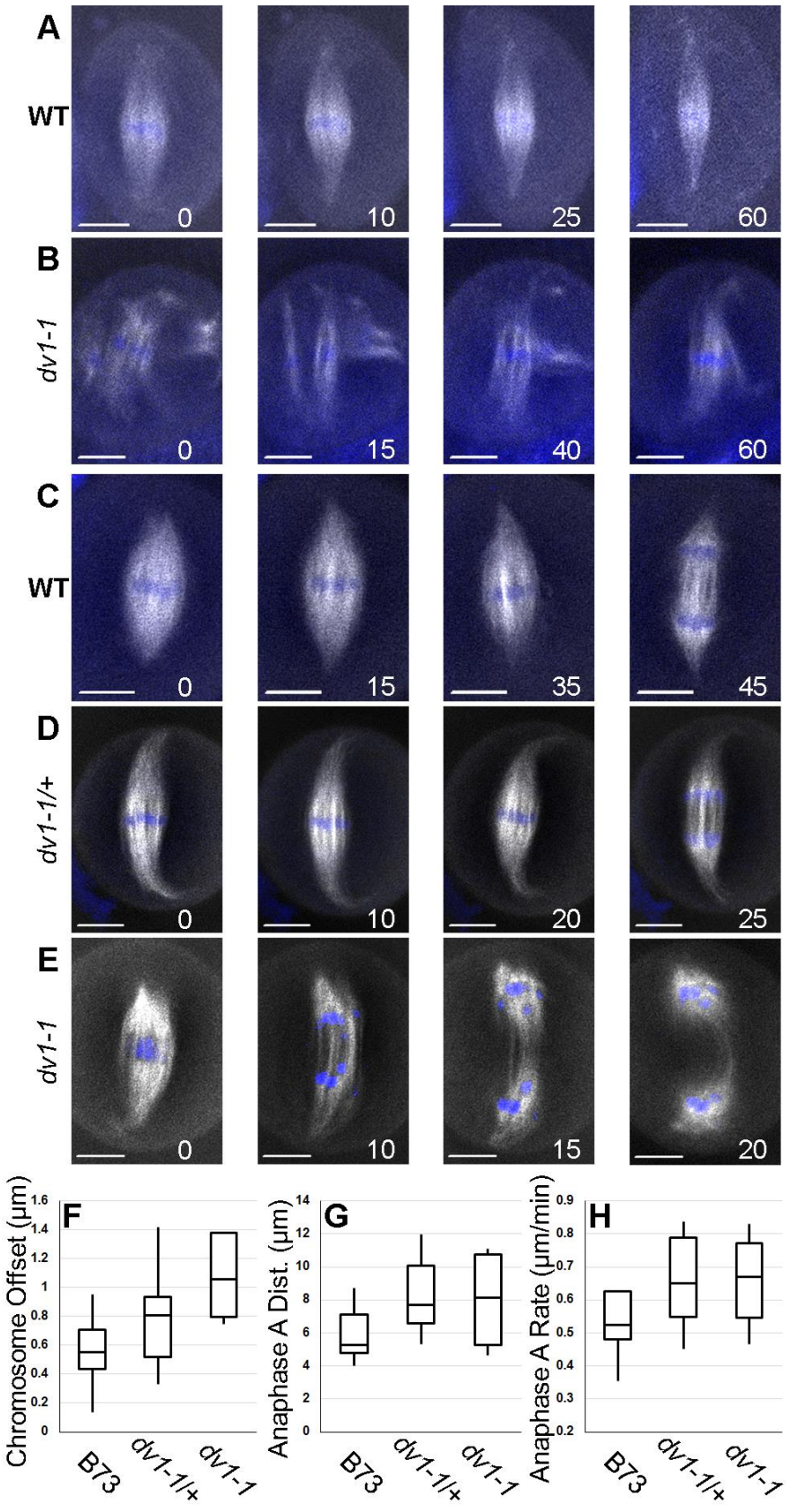
A
WT
0
10
25
60
B
dv1-1
0
15
40
60
C
WT
0
15
35
45
D
dv1-1/+
0
10
20
25
E
dv1-1
0
10
15
20
F
Chromosome Offset (µm)
1.6
1.4
1.2
1
0.8
0.6
0.4
0.2
0
B73
dv1-1/+
dv1-1
G
Anaphase A Dist. (µm)
14
12
10
8
6
4
2
0
B73
dv1-1/+
dv1-1
H
Anaphase A Rate (µm/min)
0.9
0.8
0.7
0.6
0.5
0.4
0.3
0.2
B73
dv1-1/+
dv1-1

Figure 2.6 Live cell imaging demonstrates a role for *Dv1* in prometaphase and metaphase.

Images captured from a line carrying a β-tubulin transgene tagged with a cyan fluorescent protein (shown in white) and incubated with SYTO12 which stains chromosomes (shown in blue). Images presented are sequential frames from the movie with minutes since the original capture shown in the lower right of each image. Scale bars for each image represent 10 μm.

(A) Chromosomes in a wild type cell begin loosely collected in a metaphase plate and then compress as the spindle narrows throughout metaphase;

(B) Chromosomes in a *dv1-1* cell are highly unorganized in prometaphase with three separate mini-spindles around different chromosome groups which are then brought together;

(C) The spindle poles of a wild type cell begin rounded, then sharpen and elongate before the cell enters anaphase;

(D) The spindle pole of a heterozygous cell shows highly focused spindles which curl along the edge of the cell as it enters anaphase;

(E) The spindle pole of a *dv1-1* cell is highly unorganized in metaphase and anaphase chromosome movement is uneven with several lagging chromosomes;

(F) Measurement of chromosome offset, the distance between the center of the chromosome mass and the spindle appears to be larger in the *dv1-1* homozygote than other genotypes;

(G) Distance of chromosomes moved in anaphase A appears to be larger in the *dv1-1* heterozygotes and homozygotes;

(H) Rate of chromosome movement in anaphase A is not significantly different between the three genotypes.

SUPPLEMENTAL DATA

Sequence of B73 Reference Allele of dv1

ATGGGTTACAACAAGGCGACGCCGCGCCGGAACGTGCTATCGGCTCTCAACAACGCCGAGGC
CAACGGGGGGACGCCGTCCGTGCCGGCGGATGGCGGCGGCGGCGGCGGCGCGGCGGAGGCG
GCGCCCGTGATCGAGTTCAGTGGGAGGGAGGATGTGGAGCGCTTGCTCGCCGAGAAAATGAA
GGGCAAAAGCAAGAACGATTTCAAGGGGAGAGTCGATCAGATGAGCGACTACATCAAGAAG
CTCAGGGCGTGCATCCGGTGGTACATGGAGCTGGAGGATGGCTATTTGGCTGAGCAGGAGAA
GCTCCTAGGTGCTATGGATTCTGAGAACACCCGTCATACCGAGTTGGAGGCCCAGCTCAGCAC
TGCTATTGAAGAGCTGAAAGCCACTAACTTGGACTTGACAAGGCGTTGTGAGTCTCTAGAGGA
GAGCTTCAACAAGGAGAAGTCTGAAAAACTGATCGCTGTGGAGTCCTACGAGAAAGAAAAGC
AGGAAAGGGAATCCGCTGAGAGTTCACGAGATGTACTAACTGTGGACCTAGAAAGGGTCACT
CATGATGCTAAGCGGTTTAGCGAGCAGCTAAAAATGGTCCAAGACACTAATAAAAGGCTTCA
AGAATACAACACCAGCCTGCAACAATACAACAGTAACCTTCAGGCTGATGCCTCGAAGAGTG
GTGAGACCATCTCAAAACTTCAGAAAGAGAAGAGTGCCATGATGGAAACTATGGCTACTCTG
AGAGAGTGTAACAGCTCAATGGGCAATCAGCTTGAATCTTCTAGAGTTTCTCAACAAGAAGCT
ATTAGAGTGAAGGAAGAGCTCAGGAAAGAAGTGGAGTGCCTTAGAGTTGAGTTGAAGCAAGT
TAGAGATGATCGTGATCATTCAGCTATTCAACTGAACAGTTTGAACATTGAACTTGGTAATTA
CAAGGAACAGATTGGTAAAACTTCAAAAGAATGTGAAAGATTCCGCACCAAAGTATCTGAAC
TTGAGGAAACATGCAGTACACAACAAGAACAGATTCGGACATTTCAAAAGCAGCTTGCAGTT
GCGACTGAGAAGTTGAAGCTTGCTGATGTAACTGCGATAGAGGCGATGACTGGTTATGAAGA
ACAGAAGGAGAAAATAAAATACCTTGAGGAGCGTTTAGCACAGGCAGAGTCTCAAATTGTTG
AAGGCGACGAGTTACGGAAAAAACTGCACAACACTATATTGGAACTGAAAGGAAACATTAGG
GTTTTTTGTAGAGTTCGACCACTTCTTCGATTTGAGGGTGATTCCAATGGTCCGGAAGGTGCCT
CTATCTCTTTTCCAACATCTGTAGAGTCTACTGGACGTAGCATTGATTTGATAAACCAAGGGC
AAAAGCTCTCCTTCTCATATGACAAGGTTTTTGACCATGGTGCGTCACAGGAAGATGTGTTTG
TGGAAATATCGCAACTAGTCCAAAGTGCCCTTGATGGGTACAAGGTATGCATATTTGCATATG
GTCAAACTGGATCTGGTAAAACTTATACAATGATGGGTAAACCAGGAAATGATCAAAAAGGG
ATAATACCTCGTTCTTTGGAGCAAATTTTCAAGACCAGTCGGTTTCTAGAATCTCAAGGATGG
AATTATTCCATGCAAGCATCAATGTTGGAAATATACAATGAGACCATTCGTGATTTGTTAGCA
CCTGGTCGGTCTAACAGTTTTGAGTCTAGTAAACAATGCACTATAAAGCATGACCCTCATGGG
AATATTGTGTCGGACCTTACAATTATTGATGTCTTTGGTATTGCTGATGTGACTAGTCTACTAG
AGAAAGCATCCCAGAGTAGGTCTGTGGGTAAGACTCAGATGAATGAACAGTCGTCCAGAAGT
CATTTTGTATTCACATTAAAGATATCTGGATCTAACGAGAACACAGGCCAAAATGTCCAAGGA
GTCCTTAACTTGATTGATTTAGCTGGGAGTGAGCGTCTTGCTAAAAGTGGCTCCACAGGTGAT
CGCTTGAAGGAAACTCAGTCAATCAATAAAAGCTTGTCGGCTTTGAGCGATGTAATCTTCGCG
ATCGCAAAAGGAGATGACCACGTTCCGTTCAGAAATTCAAAACTTACATACCTATTGCAGCCT
TGCCTTGGAGGTGACTCGAAAGCTCTCATGTTTGTCAACATTTCACCGGAGGCATCCTCCGTTG
GTGAGACGATATGCTCGTTGAGGTTTGCTTCAAGGGTGAATGCTTGTGAGATTGGAATACCAA
GACGTCACACATAA

Sequence of dv1-1 Allele of dv1

ATGGGTTACAACAAGGCGACGCCGCGCCGGAACGTGCTATCGGCTCTCAACAACGCCGAGGC
CAACGGGGGGACGCCGTCCGTGCCGGCGGATGGCGGCGGCGGCGGCGGCGCGGCGGAGGCG
GCGCCCGTGATCGAGTTCAGTGGGAGGGAGGATGTGGAGCGCTTGCTCGCCGAGAAAATGAA
GGGCAAAAGCAAGAACGATTTCAAGGGGAGAGTCGATCAGATGAGCGACTACATCAAGAAG
CTCAGGGCGTGCATCCGGTGGTACATGGAGCTGGAGGATGGCTATTTGGCTGAGCAGGAGAA
GCTCCTAGGTGCTATGGATTCTGAGAACACCCGTCATACCGAGTTGGAGGCCCAGCTCAGCAC
TGCTATTGAAGAGCTGAAAGCCACTAACTTGGACTTGACAAGGCGTTGTGAGTCTCTAGAGGA
GAGCTTCAACAAGGAGAAGTCTGAAAAACTGATCGCTGTGGAGTCCTACGAGAAAGAAAAGC
AGGAAAGGGAATCCGCTGAGAGTTCACGAGATGTACTAACTGTGGACCTAGAAAGGGTCACT
CATGATGCTAAGCGGTTTAGCGAGCAGCTAAAAATGGTCCAAGACACTAATAAAAGGCTTCA

AGAATACAACACCAGCCTGCAACAATACAACAGTAACCTTCAGGCTGATGCCTCGAAGAGTG
GTGAGACCATCTCAAAACTTCAGAAAGAGAAGAGTGCCATGATGGAAACTATGGCTACTCTG
AGAGAGTGTAACAGCTCAATGGGCAATCAGCTTGAATCTTCTAGAGTTTCTCAACAAGAAGCT
ATTAGAGTGAAGGAAGAGCTCAGGAAAGAAGTGGAGTGCCTTAGAGTTGAGTTGAAGCAAGT
TAGAGATGATCGTGATCATTCAGCTATTTAACTGAACAGTTTGAACATTGAACTTGGTAATTA
CAAGGAACAGATTGGTAAAACTTCAAAAGAATGTGAAAGATTCCGCACCAAAGTATCTGAAC
TTGAGGAAACATGCAGTACACAACAAGAACAGATTCGGACATTTCAAAAGCAGCTTGCAGTT
GCGACTGAGAAGTTGAAGCTTGCTGATGTAACTGCGATAGAGGCGATGACTGGTTATGAAGA
ACAGAAGGAGAAAATAAAATACCTTGAGGAGCGTTTAGCACAGGCAGAGTCTCAAATTGTTG
AAGGCGACGAGTTACGGAAAAAACTGCACAACACTATATTGGAACTGAAAGGAAACATTAGG
GTTTTTTGTAGAGTTCGACCACTTCTTCGATTTGAGGGTGATTCCAATGGTCCGGAAGGTGCCT
CTATCTCTTTTCCAACATCTGTAGAGTCTACTGGACGTAGCATTGATTTGATAAACCAAGGGC
AAAAGCTCTCCTTCTCATATGACAAGGTTTTTGACCATGGTGCGTCACAGGAAGATGTGTTTG
TGGAAATATCGCAACTAGTCCAAAGTGCCCTTGATGGGTACAAGGTATGCATATTTGCATATG
GTCAAACTGGATCTGGTAAAACTTATACAATGATGGGTAAACCAGGAAATGATCAAAAAGGG
ATAATACCTCGTTCTTTGGAGCAAATTTTCAAGACCAGTCGGTTTCTAGAATCTCAAGGATTG
AATTATTCCATGCAAGCATCAATGTTGGAAATATACAATGAGACCATTCGTGATTTGTTAGCA
CCTGGTCGGTCTAACAGTTTTGAGTCTAGTAAACAATGCACTATAAAGCATGACCCTCATGGG
AATATTGTGTCGGACCTTACAATTATTGATGTCTTTGGTATTGCTGATGTGACTAGTCTACTAG
AGAAAGCATCCCAGAGTAGGTCTGTGGGTAAGACTCAGATGAATGAACAGTCGTCCAGAAGT
CATTTTGTATTCACATTAAAGATATCTGGATCTAACGAGAACACAGGCCAAAATGTCCAAGGA
GTCCTTAACTTGATTGATTTAGCTGGGAGTGAGCGTCTTGCTAAAAGTGGCTCCACAGGTGAT
CGCTTGAAGGAAACTCAGTCAATCAATAAAAGCTTGTCGGCTTTGAGCGATGTAATCTTCGCG
ATCGCAAAAGGAGATGACCACGTTCCGTTCAGAAATTCAAAACTTACATACCTATTGCAGCCT
TGCCTTGGAGGTGACTCGAAAGCTCTCATGTTTGTCAACATTTCACCGGAGGCATCCTCCGTTG
GTGAGACGATATGCTCGTTGAGGTTTGCTTCAAGGGTGAATGCTTGTGAGATTGGAATACCAA
GACGTCACACATAA

Sequence of the A619 Reference Allele of dv1

ATGGGTTACAACAAGGCGACGCCGCGCCGGAACGTGCTATCGGCTCTCAACAACGCCGAGGC
CAACGGGGGGACGCCGTCCGTGCCGGCGGATGGCGGCGGCGGCGGCGGCGCGGCGGAGGCG
GCGCCCGTGATCGAGTTCAGTGGGAGGGAGGATGTGGAGCGCTTGCTCGCCGAGAAAATGAA
GGGCAAAAGCAAGAACGATTTCAAGGGGAGAGTCGATCAGATGAGCGACTACATCAAGAAG
CTCAGGGCGTGCATCCGGTGGTACATGGAGCTGGAGGATGGCTATTTGGCTGAGCAGGAGAA
GCTCCTAGGTGCTATGGATTCTGAGAACACCCGTCATACCGAGTTGGAGGCCCAGCTCAGCAC
TGCTATTGAAGAGCTGAAAGCCACTAACTTGGACTTGACAAGGCGTTGTGAGTCTCTAGAGGA
GAGCTTCAACAAGGAGAAGTCTGAAAAACTGATCGCTGTGGAGTCGTACGAGAAAGAAAAGC
AGGAAAGGGAATCAGCTGAGAGTTCACGAGATGTACTAACTGTGGACCTAGAAAGGGTCACT
CATGATGCTAAGCGGTTTAGCGAGCAGCTAAAAATGGTCCAAGACACTAATAAAAGGCTTCA
AGAATACAACACCAGCCTGCAACAATACAACAGTAACCTTCAGGCTGATGCCTCGAAGAGTG
GTGAGACCATCTCAAAACTTCAGAAAGAGAAGAGTGCCATGATGGAAACTATGGCTACTCTG
AGAGAGTGTAACAGCTCAATGGGCAATCAGCTTGAATCTTCTAGAGTTTCTCAACAAGAAGCT
ATTAGAGTGAAGGAAGAGCTCAGGAAAGAAGTGGAGTGCCTTAGAGTTGAGTTGAAGCAAGT
TAGAGATGATCGTGATCATTCAGCTATTCAACTGAACAGTTTGAACATTGAACTTGGTAATTA
CAAGGAACAGATTGGTAAAACTTCAAAAGAATGTGAAAGATTCCGCACCAAAGTATCTGAAC
TTGAGGAAACATGCAGTACACAACAAGAACAGATTCGGACATTTCAAAAGCAGCTTGCAGTT
GCGACTGAGAAGTTGAAGCTTGCTGATGTAACTGCGATAGAGGCGATGACTGGATATGAAGA
ACAGAAGGAGAAAATAAAATACCTTGAGGAGCGTTTAGCACAGGCAGAGTCTCAAATTGTTG
AAGGCGACGAGTTACGGAAAAAACTGCACAACACTATATTGGAACTGAAAGGAAACATTAGG
GTTTTTTGTAGAGTTCGACCACTTCTTCGATTTGAGGGTGATTCCAATGGTCCGGAAGGTGCCT
CTATCTCTTTTCCAACATCTGTAGAGTCTACTGGACGTAGCATTGATTTGATAAACCAAGGGC
AAAAGCTCTCCTTCTCATATGACAAGGTTTTTGACCATGGTGCGTCACAGGAAGATGTGTTTG
TGGAAATATCGCAACTAGTCCAAAGTGCCCTTGATGGGTACAAGGTATGCATATTTGCATATG
GTCAAACTGGATCTGGTAAAACTTATACAATGATGGGTAAACCAGGAAATGATCAAAAAGGG

ATAATACCTCGTTCTTTGGAGCAAATTTTCAAGACCAGTCGGTTTCTAGAATCTCAAGGATGG
AATTATTCCATGCAAGCATCAATGTTGGAAATATACAATGAGACCATTCGTGATTTGTTAGCA
CCTGGTCGGTCTAACAGTTTTGAGTCTAGTAAACAATGCACTATTAAGCATGACCCTCATGGG
AATATTGTGTCGGACCTTACAATTATTGATGTCTTTGGTATTGCTGATGTGACTAGTCTACTAG
AGAAAGCATCCCAGAGTAGGTCTGTGGGTAAGACTCAGATGAACGAACAGTCATCCAGAAGT
CATTTTGTATTCACATTAAAGATATCTGGATCTAATGAGAACACAGGCCAAAATGTCCAAGGA
GTCCTTAACTTGATTGATTTAGCTGGGAGTGAGCGTCTTGCTAAAAGTGGCTCCACAGGTGAT
CGCTTGAAGGAAACTCAGTCAATCAATAAAAGCTTGTCGGCTTTGAGCGATGTAATCTTCGCG
ATCGCAAAAGGAGATGACCACGTTCCGTTCAGAAATTCAAAACTTACATACCTATTGCAGCCT
TGCCTTGGAGGTGACTCGAAAGCTCTCATGTTTGTCAACATTTCACCTGAGGCATCCTCCGTTG
GTGAGACGATATGCTCGTTGAGGTTTGCTTCAAGGGTGAATGCTTGTGAGATTGGAATACCAA
GACGTCACACATAA

Sequence of the dv1-IG Allele of dv1

ATGGGTTACAACAAGGCGACGCCGCGCCGGAACGTGCTATCGGCTCTCAACAACGCCGAGGC
CAACGGGGGGACGCCGTCCGTGCCGGCGGATGGCGGCGGCGGCGGCGGCGCGGCGGAGGCG
GCGCCCGTGATCGAGTTCAGTGGGAGGGAGGATGTGGAGCGCTTGCTCGCCGAGAAAATGAA
GGGCAAAAGCAAGAACGATTTCAAGGGGAGAGTCGATCAGATGAGCGACTACATCAAGAAG
CTCAGGGCGTGCATCCGGTGGTACATGGAGCTGGAGGATGGCTATTTGGCTGAGCAGGAGAA
GCTCCTAGGTGCTATGGATTCTGAGAACACCCGTCATACCGAGTTGGAGGCCCAGCTCAGCAC
TGCTATTGAAGAGCTGAAAGCCACTAACTTGGACTTGACAAGGCGTTGTGAGTCTCTAGAGGA
GAGCTTCAACAAGGAGAAGTCTGAAAAACTGATCGCTGTGGAGTCGTACGAGAAAGAAAAGC
AGGAAAGGGAATCAGCTGAGAGTTCACGAGATGTACTAACTGTGGACCTAGAAAGGGTCACT
CATGATGCTAAGCGGTTTAGCGAGCAGCTAAAAATGGTCCAAGACACTAATAAAAGGCTTCA
AGAATACAACACCAGCCTGCAACAATACAACAGTAACCTTCAGGCTGATGCCTCGAAGAGTG
GTGAGACCATCTCAAAACTTCAGAAAGAGAAGAGTGCCATGATGGAAACTATGGCTACTCTG
AGAGAGTGTAACAGCTCAATGGGCAATCAGCTTGAATCTTCTAGAGTTTCTCAACAAGAAGCT
ATTAGAGTGAAGGAAGAGCTCAGGAAAGAAGTGGAGTGCCTTAGAGTTGAGTTGAAGCAAGT
TAGAGATGATCGTGATCATTCAGCTATTCAACTGAACAGTTTGAACATTGAACTTGGTAATTA
CAAGGAACAGATTGGTAAAACTTCAAAAGAATGTGAAAGATTCCGCACCAAAGTATCTGAAC
TTGAGGAAACATGCAGTACACAACAAGAACAGATTCGGACATTTCAAAAGCAGCTTGCAGTT
GCGACTGAGAAGTTGAAGCTTGCTGATGTAACTGCGATAGAGGCGATGACTGGATATGAAGA
ACAGAAGGAGAAAATAAAATACCTTGAGGAGCGTTTAGCACAGGCAGAGTCTCAAATTGTTG
AAGGCGACGAGTTACGGAAAAAACTGCACAACACTATATTGGAACTGAAAGGAAACATTAGG
GTTTTTTGTAGAGTTCGACCACTTCTTCGATTTGAGGGTGATTCCAATGGTCCGGAAGGTGCCT
CTATCTCTTTTCCAACATCTGTAGAGTCTACTGGACGTAGCATTGATTTGATAAACCAAGGGC
AAAAGCTCTCCTTCTCATATGACAAGGTTTTTGACCATGGTGCGTCACAGGAAGATGTGTTTG
TGGAAATATCGCAACTAGTCCAAAGTGCCCTTGATGGGTACAAGGTATACATATTTGCATATG
GTCAAACTGGATCTGGTAAAACTTATACAATGATGGGTAAACCAGGAAATGATCAAAAAGGG
ATAATACCTCGTTCTTTGGAGCAAATTTTCAAGACCAGTCGGTTTCTAGAATCTCAAGGATGG
AATTATTCCATGCAAGCATCAATGTTGGAAATATACAATGAGACCATTCGTGATTTGTTAGCA
CCTGGTCGGTCTAACAGTTTTGAGTCTAGTAAACAATGCACTATTAAGCATGACCCTCATGGG
AATATTGTGTCGGACCTTACAATTATTGATGTCTTTGGTATTGCTGATGTGACTAGTCTACTAG
AGAAAGCATCCCAGAGTAGGTCTGTGGGTAAGACTCAGATGAACGAACAGTCATCCAGAAGT
CATTTTGTATTCACATTAAAGATATCTGGATCTAATGAGAACACAGGCCAAAATGTCCAAGGA
GTCCTTAACTTGATTGATTTAGCTGGGAGTGAGCGTCTTGCTAAAAGTGGCTCCACAGGTGAT
CGCTTGAAGGAAACTCAGTCAATCAATAAAAGCTTGTCGGCTTTGAGCGATGTAATCTTCGCG
ATCGCAAAAGGAGATGACCACGTTCCGTTCAGAAATTCAAAACTTACATACCTATTGCAGCCT
TGCCTTGGAGGTGACTCGAAAGCTCTCATGTTTGTCAACATTTCACCTGAGGCATCCTCCGTTG
GTGAGACGATATGCTCGTTGAGGTTTGCTTCAAGGGTGAATGCTTGTGAGATTGGAATACCAA
GACGTCACACATAA

CHAPTER 3

CHARACTERIZATION OF *KINESIN DRIVER*, A NOVEL KINESIN MOTOR PROTEIN IMPLICATED IN THE ABNORMAL CHROMOSOME 10 MEIOTIC DRIVE SYSTEM IN ZEA MAYS[2]

[2] Higgins, D.M. and R.K. Dawe. To be submitted to *G3*.

ABSTRACT

Abnormal chromosome 10 (Ab10) is a female-specific meiotic drive system in *Zea mays*. During metaphase and anaphase in plants carrying Ab10, normally inert heterochromatic knobs become activated neocentromeres and move toward the spindle poles ahead of the centromere. Based on the asymmetric nature of the female meiocytes, it is hypothesized that this neocentromere movement is responsible for the meiotic drive phenotype. Recent sequencing experiments have identified *kinesin driver* (*Kindr*), a unique gene present on the end of Ab10. In this study, we measure the expression of *Kindr* in multiple drive-deficient mutants and determined that expression of *Kindr* is not sufficient for meiotic drive while an RNAi-induced knockout indicates it is required. Additionally, we present the first efforts at localizing *KINDR in vivo,* potential alternative hypotheses for the cellular role of *Kindr*, and suggested future directions for its study.

INTRODUCTION

Chromosomes are complex macromolecules of DNA and protein which carry the complete set of genes required for development and life of an organism. Diploid organisms typically carry two pairs of each chromosome in their genome, each with mostly the same genes only slightly varied from acquired mutations over time. As the units of genetic inheritance, chromosomes are passed on from parents to offspring through a specialized type of cell division known as meiosis. They align and separate during two successive stages of metaphase and anaphase, segregating each chromosome into one of four haploid daughter cells. According to Mendel's law of segregation, either chromosome is equally likely to be transmitted to the next generation. While chromosome segregation generally adheres to this law, there are a number of systems that cause a particular locus to be more likely to be passed on to the next generation, a process known as meiotic drive (Sandler and Novitski, 1957). Meiotic drive systems have been identified in animals, fungi, and plants. Among plant systems, the maize abnormal chromosome 10 is the most widely studied but still not entirely understood.

Zea mays (maize) is a diploid grass species with two sets of ten chromosomes (2n = 2x = 20). The tenth, smallest chromosome comes in two distinct forms: the much more common normal chromosome 10 (N10) and the rarer abnormal chromosome 10 (Ab10). The difference between the two chromosome lies at the end of the long arm, where Ab10 contains several heterochromatic knobs (Longley, 1938). Marcus Rhoades was one of the first to use Ab10 in an experiment, originally designed for mapping the *colored1* locus near the end of chromosome 10, when he inadvertently discovered abnormal chromosome 10 to be a meiotic driver; female parents heterozygous for Ab10 passed on

this haplotype at a rate of 72%, greater than the 50:50 ratio expected under Mendelian inheritance (Rhoades, 1942). A follow-up cytogenetics study identified a unique phenomenon during metaphase and anaphase in Ab10 meiocytes in which chromosome arms bearing knobs streaked to the spindle poles ahead of the centromeres, calling these activated knobs "neocentromeres" (Rhoades and Vilkomerson, 1942). Further studies demonstrated that all loci linked to knobs, not just Ab10, are preferentially inherited when activated as neocentromeres (Longley, 1945).

In 1952, Rhoades presented his hypothesis linking neocentromeres with meiotic drive (Rhoades, 1952). The Rhoades Hypothesis is based on the organization of the female products of meiosis. Meiosis always produces four cells, but those cells are arranged in different orientations depending in male and female meiosis. While the products of male microsporogenesis in maize are arranged in a square planar orientation (2x2), those of the female megasporocyte are aligned in a linear orientation (1x4). In metaphase I, knobbed chromosome arms become activated neocentromeres and begin traveling towards spindle poles. The homologous chromosomes then split with the knobbed chromatid oriented outward as the cell undergoes its first division. If this orientation is maintained into the second division, with the knobbed chromosome pulled outward away from the original meiosis I division plane, it will preferentially end in the two cells on the ends of the linear tetrad. As only the basal product of megasporogenesis becomes a viable egg cell, knobbed chromosomes are transmitted at a rate greater than 1:1.

Subsequent mutagenesis screens have identified Ab10 mutants in which the meiotic drive phenotype is lost. This family of mutants known as *suppressor of meiotic*

drive (*smd*) also show a loss of neocentromere activity, clearly linking these two phenotypes (Dawe and Cande, 1996). Despite their name, neocentromeres do not recruit typical kinetochore proteins found at centromeres, indicating some alternative type of proteins are responsible for the connection between neocentromeres and the meiotic spindle (Dawe et al., 1999; Dawe and Hiatt, 2004). Through analysis of a series of terminal deletion mutants of Ab10, it was determined that there are two distinct genes at different loci along Ab10 responsible for neocentromere activity, each unique to a specific type of knob repeat (Hiatt et al., 2002). While both genes activate neocentromeres, only the one which activates knobs derived from the 180-bp repeat is necessary for meiotic drive (Kanizay et al., 2013a).

The tools to uncover the identity of these genes became available with the development of high-throughput sequencing technologies. A transcriptomics study designed to compare genes expressed in Ab10 but not a terminal deficiency line identified a novel gene we have named *kinesin driver* (*Kindr*). As its name suggests, *Kindr* has a kinesin motor domain at its C-terminus. *Kindr* is a unique gene not found elsewhere in the maize genome, its closest homolog being *ZmKin11* (Figure 3.1A). While the motor domain is conserved, the cargo-binding N-terminus is highly diverged and unique, suggesting a novel function. Both genes are members of the kinesin-14A subfamily of minus-end directed motors (as reviewed in Hirokawa et al., 2009).

Additional sequencing of a BAC library derived from an Ab10 source (Kanizay et al., 2013b) identified multiple distinct copies of *Kindr* and subsequent genome assembly mapped at least eight tandemly duplicated copies of this gene in a 1 MB window (Figure 3.1B). Given the directionality of more characterized members of the 14A-subfamily, its

derived nature, and copy number proliferation, *Kindr* represents an ideal candidate for the neocentromere activating gene. It is possible that *Kindr* binds to knobs and pulls them toward the minus-end spindle pole ahead of centromeres, as predicted by the Rhoades Hypothesis.

In this study, we carried out several experiments aimed at better understanding the role *Kindr* plays in Ab10 neocentromere activity and meiotic drive. Through analysis of whole-transcriptome sequencing data, we quantified expression of *Kindr* in five different *smd* mutants and identified which copies of the gene family are expressed. An RNAi knockdown of a *Kindr* demonstrated that *Kindr* is required for meiotic drive. Additionally, we present results from two attempts of *Kindr* localization within cells.

MATERIALS AND METHODS

Measuring Kindr *Expression by RNA-Sequencing*

Whole-transcriptome RNA-sequencing (RNA-Seq) was used to quantify the expression of *Kindr* in Ab10 and the five *smd* mutants. Anthers were dissected from developing tassels and staged for the phases of meiosis as previously described (Higgins et al., 2016). Whole anthers containing meiocytes in either meiosis I or II were ground using liquid nitrogen and mRNA extracted using the Qiagen RNeasy Plant Mini Kit (Qiagen, Germantown, MD). Sequencing libraries were generated using the KAPA Stranded RNA-Seq Kit (Kapa Biosystems, Wilmington, MA) and sequenced by 150 bp paired-end Illumina sequencing on an Illumina MiSeq at the Georgia Genomics Facility (Athens, GA).

A modified version of the maize B73 genome (AGPv3.27, Schnable et al., 2009) was used as the genomic reference for read alignment. The sequence of the ten maize chromosomes was appended with an additional 100 kb of sequence from the Ab10 distal tip centered on the E9 copy of *Kindr*. Reads were aligned using Tophat version 2.0.14 (Kim et al., 2013) and differential expression of transcripts including *Kindr* was calculated using Cufflinks and Cuffdiff version 2.2.1 (Trapnell et al., 2010) following the previously published protocol (Trapnell et al., 2012). FPKM was normalized by adjusting the Ab10 homozygous sample to 1.0 and converting the *smd* samples by the same ratio.

Relative Copy Expression in Ab10

In order to quantify the relative expression of individual *Kindr* genes, the frequency of unique SNPs appearing in the transcriptome reads was quantified. There are 17 SNPs in the transcribed regions of the eight *Kindr* genes for which we have sequence (Table 3.1). Though two pairs of *Kindr* copies are exactly identical (G11 & B1, E9 & B9), we can distinguish reads as coming from one of five sets of copies based on the relative frequency of SNPs at each locus. Aligned reads from the RNA-seq experiment above were visualized using the Integrated Genomics Viewer version 2.3 (Thorvaldsdóttir et al., 2013). Reads containing diagnostic SNPs were counted and recorded as a percentage of total reads. Data from replicates with the same genotype were averaged.

RNAi Construct Generation, Transformation, Screening

In order to test whether *Kindr* is necessary for the Ab10 meiotic drive phenotype, the expression of *Kindr* was specifically reduced using RNA interference (RNAi). Unique sequence from the first exon (Figure 3.2A) was synthesized in both the forward and reverse orientations by Genscript (Piscataway, NJ) with restriction site adapters added to each end, such that the reverse sequence was flanked with AscI and AvrII sites and the forward sequence was flanked with SacI and SpeI. Both of these sequences were cloned into the RNAi vector pMCG1005 (Li and Dawe, 2009), designed to combine the reverse and forward oriented sequences to create an mRNA hairpin structure joined by an intron spacer derived from the *waxy* gene from *Oryza sp*.

The plasmid was transformed into maize (HiII) at the Iowa State Plant Transformation Facility (Ames, IA). Plantlets from six independent transgenic events were grown to maturity and crossed to a line carrying Ab10 linked to the dominant kernel color gene *colored1 (R1)* locus. This first generation of plants, heterozygous for both *R1* and Ab10 (*R1*-Ab10/*r1*-N10) and carrying the RNAi construct was then crossed as females by an N10 tester line (*r1*-N10/*r1*-N10). The frequency of the *R1* allele as determined by kernel color in the resulting generation was used to calculate the rate of meiotic drive. The transmission rates were determined to be different from Mendelian expectation using chi-square analysis.

Kindr *Immunolocalization and Fluorescent-Protein Tagging*

In order to determine the localization of *Kindr* in meiotic cells, we carried out two separate imaging protocols: immunolocalization with a *Kindr* antibody and screening of a transgenic *Kindr* tagged with a fluorescent protein.

A peptide antibody specific to a motif in the first exon of *Kindr* corresponding to amino acids 56-67 (Ac-CSIRIERPRRPD-amide) was generated by New England Peptide, Inc. (Gardner, MA). Immunolocalization was carried out on meiotic anthers using an α-Tubulin antibody (Asai et al., 1982) and procedures described previously (Higgins et al., 2016). Images were collected using a Zeiss Axio Imager M1 fluorescence microscope with a 63x Plan-APO Chromat oil objective and the Slidebook software package (Intelligent Imaging Innovations, Denver, CO).

The second method used for studying the localization of *Kindr* was a series of fluorescent-protein tag constructs. The first consisted of the N-terminal and coiled-coil region of *Kindr* (all but the motor domain) tagged to the Citrine yellow fluorescent protein (*KindrX1-YFP*). The construct was generated by cloning the Citrine sequence from plasmid pEG101, previously used to tag the LacI gene (Zhang et al., 2012). The sequence for LacI was replaced with the *Kindr* sequence. The original promoter (35S) was determined to express poorly in meiosis (R. Kelly Dawe, personal communication) and was replaced with that of *beta tubulin1* (*Tub1*, GRMZM2G164696), the same promoter used for a cyan fluorescent protein construct of beta tubulin (CFP-Tubulin) (Mohanty et al., 2009). The final construct was assembled in the pRTF101 vector for transformation. Two additional constructs were also designed for screening *Kindr* localization: full-length versions of *Kindr* and *ZmKin11* tagged with Citrine (YFP-*Kindr*

and YFP-*Kin11*, respectively). These constructs were synthesized by Genscript and cloned under the same promoter as *KindrX1-YFP* into the pRTF101 vector.

All three plasmids were transformed into maize at the Iowa State Plant Transformation Facility. Plantlets were grown to maturity and crossed into Ab10 lines. Six transformation events for each construct were selected based on the quantity of seed produced. Root meristems, ligules, and meiocytes from this generation were screened for YFP localization using the same microscope and software described above. The *KindrX1*-YFP construct was crossed to a maize line containing the previously described CFP-Tubulin construct as well as a chromatin marker Histone H2B-mCherry (Howe et al., 2012) and the same tissues were screened.

RESULTS

Kindr *expression is variable among smd mutants*

The set of five *smd* mutants are all deficient in neocentromere activity and meiotic drive. To test whether this phenotype is associated with the loss of *Kindr* expression, we measured gene expression in meiotic anthers using RNA-Seq. Through this method, we were able to determine relative levels of expression of each gene among both homozygous (Ab10, *smd1*, *smd3*, *smd8*, *smd13*) and heterozygous (Ab10/N10, *smd1*/N10, *smd3*/N10, *smd8*/N10, *smd12*/N10) genotypes.

Results from sequencing indicate that many of the *smd* haplotypes result in a decrease in expression of *Kindr* (Figure 3.1C). In particular, *smd1*, *smd3*, and *smd12* all showed significantly lower levels of expression than the heterozygous Ab10 genotype ($p=0.011$, $p=0.004$, $p<0.001$, respectively). Contrary to this finding, both *smd8* genotypes

tested showed no significant difference in *Kindr* expression while *smd13* shows higher levels than that of Ab10 (Figure 3.1C). The results from three haplotypes correlate meiotic drive with our expectations of *Kindr* expression. Despite this, the finding that *smd8* and *smd13* lack meiotic drive while maintaining robust expression of our candidate gene indicates that the expression of *Kindr* is not sufficient for meiotic drive of Ab10.

At least four, potentially up to eight different copies of Kindr *are expressed*

Sequencing of the BAC clones unique to the Ab10 distal tip identified eight different copies of *Kindr*, with a hypothesized ninth copy based on the BioNano scaffolding (Figure 3.1B). The transcriptome analysis quantified total expression of *Kindr* in different haplotypes, but could not support conclusions about which copies of the gene are actively transcribed – it is possible that each copy is expressed at a low level, or that only one of the copies accounts for the entirety of expression. In order to measure this, we quantified the relative proportions of unique SNPs present in the transcriptome reads which mapped to *Kindr*. By manually examining the reads, we identified SNPs corresponding to four of the five different SNP profiles including C4, B2, B9/E9, G11/B1 but not B10 (Figure 3.1D). Because B9 and E9 as well as G11 and B1 are exactly identical, it is impossible to determine from which member of the gene pair the reads corresponding to those SNP profiles originated. The B2 copy had the highest proportion of expression, but it should be noted that this copy is adjacent to two for which we do not have complete sequences – F6 and the hypothesized ninth. It's possible that this relatively elevated expression could be due to the adjacent copies we are unable to measure. Given

the relative proportion of expression, it is possible that each of these eight copies are transcribed at approximately equal levels.

When completed in the *smd8* mutants, the same analysis indicates that the G11 and B1 copies of *Kindr* are not expressed in this haplotype (Figure 3.1D). This supports a previous finding that the *smd8* mutant is a terminal deletion (Jonathan Gent, personal communication), the breakage point for which we hypothesize to be somewhere between the B9 and G11 copies of *Kindr*. The *smd13* mutant shows expression of each of the four SNP profiles as observed in Ab10 in similar proportions (Figure 3.1D), indicating that the loss of meiotic drive phenotype is not due to the loss of a particular copy of *Kindr*.

RNAi knockdown of Kindr *results in a loss of meiotic drive*

While *Kindr* represents the only large open reading frame identified on the distal tip of Ab10, it is possible that other factors are responsible for the drive phenotype, especially given the results that *Kindr* is not sufficient for meiotic drive (Figure 3.1C). In order to better understand the role of *Kindr* in the meiotic drive phenotype, we generated an RNAi construct to specifically knockdown its expression. The targeting sequence was designed to match that of the first exon, the region most unique from its closest maize homolog *ZmKin11* (Figure 3.2A). This construct was transformed into plants and multiple transformation events were crossed into the Ab10 background. This generation, as well as an Ab10 control in the absence of the RNAi construct, was crossed by a recessive tester and meiotic drive was measured using the marker gene *colored1*.

Mendelian inheritance of a heterozygous element is 50%. The Ab10 control exhibited meiotic drive at a rate of 75.4% (Figure 3.2B), typical of the system (Kanizay et

al., 2013a). As multiple transgenic events often have different expression patterns, six RNAi families corresponding to different transformation events were screened for rates of transmission (Table 3.2). While four of the events (DH193, DH196, DH197, DH198) did not affect the drive phenotype, two showed a reduction (Figure 3.2B). Ab10 was transmitted in family DH194 carrying the *Kindr* RNAi construct at a rate of only 42.7%, significantly lower than what would be expected at a Mendelian rate as determined by a chi-squared analysis at p=0.01 (Figure 3.2B). Family DH195 family displayed a lower average of transmission at 66.3%, still greater than expected by Mendelian inheritance but lower than the Ab10 control (p=0.034).

Further analysis of *Kindr* expression in the RNAi families DH194, DH195, and DH197 was carried out using quantitative PCR by colleague Na Wang. Results indicate that in DH197, a family with no reduction in meiotic drive, *Kindr* expression is unaffected in the presence of the RNAi transgene (Figure 3.2C), suggesting that this RNAi construct is non-functional. Both DH194 and DH195, the families which show a reduction in Ab10 transmission, show a complete loss of *Kindr* expression (at least 99% reduction or greater) in the presence of the RNAi construct (Figure 3.2C). Overall, expression levels of *Kindr* were decreased in each of the families which showed the loss of the drive phenotype, indicating that the expression of *Kindr* is necessary for meiotic drive in Ab10. Interestingly, even when the RNAi construct is crossed out, *Kindr* expression remains at low levels in some individuals (Figure 3.2C), suggesting the RNAi construct has induced a stable epimutant of the entire *Kindr* complex which is capable of being inherited independent of the transgene which generated it.

Localization of Kindr *in meiocytes*

The results of the RNAi analysis clearly implicate *Kindr* in the Ab10 meiotic drive phenotype, but do not indicate what role the KINDR protein is playing within cells. We hypothesize that, as a motor protein, *Kindr* may be responsible for binding to heterochromatic knobs and activating neocentromeres, walking them toward spindle poles in metaphase and anaphase. To investigate this hypothesis further, we used two different imaging methods for observing the localization of proteins: immunolocalization using a KINDR peptide antibody and screening plants expressing fluorescently-tagged *Kindr* transgenes.

Using antibodies generated against a short peptide sequence in the first exon of KINDR as well as previously published α-tubulin antibodies, we carried out immunolocalization on pollen mother cells in different stages of meiosis I and II. Imaging of cells in metaphase indicate no localization of this antibody to either chromosomes or the spindle (Figure 3.3A). Cells in anaphase likewise fail to show any localization above background levels (Figure 3.3B), even when displaying clear neocentromere activity (Figure 3.3B, arrows).

The second method used to determine the localization of KINDR was a series of fluorescently-tagged transgenes. Citrine-tagged versions of the N-terminal region of *Kindr*, the full-length *Kindr* protein, and the full-length *ZmKin11* were transformed into maize. Six families for each were screened for YFP signal, including root tips, ligules, and pollen mother cells. Similar to the previous imaging method, no localization was observed in any of these tissues including meiotic cells in metaphase (Figure 3.3C). These lines were crossed into a background carrying CFP-Tubulin driven by the same

promoter to test its activity. The tubulin construct displayed vividly in meiosis (Figure 3.3D), suggesting the promoter responsible for driving expression of the YFP constructs is robust in these tissues.

DISCUSSION

Kindr *is necessary but not sufficient for meiotic drive*

Overall, our results indicate that *Kindr* is an essential part of the Ab10 meiotic drive phenotype but there are additional, currently unidentified components which also contribute. The RNAi knockdown clearly shows that with the specific loss of *Kindr* expression, the meiotic drive phenotype is lost (Figure 3.2B, 3.2C), indicating that *Kindr* is necessary for meiotic drive. The analysis of *smd* mutants further supports this, with three of the five haplotypes showing a significantly decreased level of *Kindr* expression: *smd1*, *smd3*, and *smd12* (Figure 3.1C).

Contrary to this, *Kindr* expression in *smd8* and *smd13* is either equal to or higher than that of the drive-capable Ab10 heterozygote (Figure 3.1C), indicating that the presence of the *Kindr* gene by itself is not sufficient for meiotic drive to occur. The expression of individual copies of *Kindr* in these haplotypes was checked to identify if specific copies were lost that may be essential for the phenotype. Reads from *smd13* carry SNPs from the four SNP profiles expressed in the Ab10 control (Figure 3.1D). The G11/B1 profile is absent from *smd8,* consistent with our prediction that this mutant is a terminal deletion which lacks those *Kindr* copies. It is possible that the loss of drive in *smd8* is caused by a gene or other factor located between the *Kindr* complex and the telomere, perhaps the same one for which *smd13* is deficient.

An additional experiment to test for the sufficiency of *Kindr* would be to transform a copy into a maize line without Ab10 and check for meiotic drive. Alternatively, the Ab10 mutant Df(L) could be used. Df(L) carries the heterochromatic knobs linked to *colored1* but lacks the distal tip and *Kindr* (Hiatt and Dawe, 2003), allowing drive to still be quantified using the simple, kernel color phenotype. We have already generated a transgenic YFP-*Kindr* plant which could be used for such an experiment, but at the present we have no indication it is functional (Figure 3.3C, 3.3D), casting doubt on any results derived from its use.

Previous quantification of drive-deficient Ab10 mutants showed segregation rates between 42.0% - 47.1% (Hiatt and Dawe, 2003), significantly lower than a return to Mendelian rate of 50% as might be expected. The most heavily affected RNAi family DH194 showed a similar transmission rate (x = 42.7%), suggesting that the Ab10 haplotype may be deleterious by itself without the positive effect on transmission granted by *Kindr*, a topic which will be explored in the subsequent chapter of this dissertation.

Localization of Kindr *within cells*

Neither of the two methods used for *Kindr* localization provided data suggesting the KINDR protein binds knobs and moves them toward the spindle pole (Figure 3.3). The antibody tested showed no localization to chromosomes, even when neocentromeres are observed (Figure 3.3B, arrows). Likewise, the FP-tagged proteins failed to show localization, even when constructs under the same promoter are expressed (Figure 3.3D). Given the failure of the YFP-*Kin11* control construct to express as well, it is possible that the transgenes inserted into inactive areas of the genome, reducing expression of the

constructs. The low penetrance of the RNAi phenotype (Figure 3.2B) supports the conclusion that positive transformants (as assayed by presence of the transgene in genomic DNA by PCR) may not indicate an actively transcribed construct.

It's unclear immediately what changes should be made in subsequent attempts to collect data on *Kindr* localization. Perhaps the native *Kindr* promoter should be used to ensure expression in the correct tissues, but questions then arise of which and how much of the seven promoters sequenced to include. In hindsight, given the difficulties and expense of maize transformation, it may have been more prudent to test for *Kindr* function in other assays before directly testing in our species. An *in vitro* assay for microtubule sliding (such as the one described in Ambrose and Cyr, 2007) could be used to determine if the *KINDR* motor is functional. Transient transformations of FP-tagged proteins into tobacco leaves could be used to test for proper protein folding and microtubule binding *in vivo*.

Alternative mechanisms of meiotic drive

At the onset of this study, our goals were to test whether *Kindr* fulfills the Rhoades Hypothesis of meiotic drive through the binding of knobs and moving them to the spindle pole. We determined that while the expression of *Kindr* is necessary for drive, it is not sufficient. Furthermore, our data fail to show *Kindr* localization to knobs as a direct cause of neocentromere activity. Microtubule motors act in a variety of capacities within cells. The most traditional perception of them may be as cargo-shuttling molecules along a single microtubule track, however they also have other roles and functions. While

the data presented do not disprove that *Kindr* binds knobs, here we present alternative mechanisms of meiotic drive which should also be considered.

A key component of the Rhoades Hypothesis is the conservation of chromosome orientation from the first cell division to the second. In metaphase I, recombined homologous chromosomes align along the spindle. Knobbed chromosome arms begin their poleward movement first, rotating the orientation of these chromatids to the outside of the cell. As long as this orientation is maintained, the knobbed chromosome will end in the outermost cell. However, in maize both male and female meiocytes undergo an interphase between meiosis I and II in which the nuclear envelope is reformed and the chromosomes partially decondense (Golubovskaya et al., 1992). As the cell prepares to enter metaphase II, it no longer has any obvious advantage to pull the knobbed chromosome along one spindle pole over the other and should thus transmit at a 1:1 ratio. Previous imaging of Ab10 microsporocytes indicates that knobs in meiotic interphase are kept to the side of the nucleus furthest from the original metaphase plate (Dawe and Cande, 1996). It has been shown previously that kinesin motors are capable of transmitting forces through the nuclear envelope to act on chromosome dynamics within the nucleus (Duroc et al., 2014). Perhaps *Kindr* is acting in a similar way, to hold the knobbed chromosome variants to the furthest edge of the nucleus to promote its transfer along that spindle pole.

Alternatively, *Kindr* might not be acting on chromosomes at the metaphase plate or nuclear envelope at all. Cortical dynein, a class of minus-end directed motors, act on the surface of the cell membrane to influence the position of the spindle in asymmetrical cell division (Nguyen-Ngoc et al., 2007). While plants do not have dynein (Lawrence et

al., 2001), it is possible that *KINDR* is functioning in a similar way. The divisions of the female meiocyte are highly asymmetric, with daughter cells having both unequal cell sizes and shapes (Golubovskaya et al., 1992) - perhaps *Kindr* is responsible for adjusting the location of the spindle in this cell type in order to preferentially pass on Ab10 to the basal cell of the tetrad, with neocentromeres acting as some type of consequence of this movement.

Ultimately, further studies on the Ab10 meiotic drive system should be focused on the female meiocyte. While immense progress has been made through the study of male meiocytes, this tissue is only a proxy for the one in which the phenotype is observed. The shape and resulting daughter cells are entirely different, as well as likely the expression of genes within these cells. Megasporocytes certainly offer a considerable challenge to imaging and analysis, as evidenced through the dramatically less amount of literature on it than developing pollen (Golubovskaya et al., 1992 represents one of the few examples). The best understanding of how *Kindr* impacts meiotic drive must lie in the tissue in which it occurs.

ACKNOWLEDGEMENTS

The authors would like to acknowledge Natalie Nannas for assisting with some of the molecular cloning required for constructing fluorescent protein tagged vectors as well as Na Wang for carrying out quantification of *Kindr* expression in the RNAi lines. Funding for this project was provided by the National Science Foundation (NSF-1412063). Additional funding for construct synthesis was provided by a Palfrey Research Grant from the Department of Plant Biology, University of Georgia.

WORKS CITED

Ambrose, J.C., and Cyr, R. (2007). The kinesin ATK5 functions in early spindle assembly in Arabidopsis. *The Plant Cell* 19**,** 226-236.

Asai, D.J., Thompson, W.C., Wilson, L., and Brokaw, C.J. (1982). Two different monoclonal antibodies to alpha-tubulin inhibit the bending of reactivated sea urchin spermatozoa. *Cell motility* 2**,** 599-614.

Dawe, R.K., and Cande, W.Z. (1996). Induction of centromeric activity in maize by suppressor of meiotic drive 1. *Proceedings of the National Academy of Sciences* 93**,** 8512-8517.

Dawe, R.K., and Hiatt, E.N. (2004). Plant neocentromeres: fast, focused, and driven. *Chromosome Research* 12**,** 655-669.

Dawe, R.K., Reed, L.M., Yu, H.-G., Muszynski, M.G., and Hiatt, E.N. (1999). A maize homolog of mammalian CENPC is a constitutive component of the inner kinetochore. *The Plant Cell* 11**,** 1227-1238.

Duroc, Y., Lemhemdi, A., Larchevêque, C., Hurel, A., Cuacos, M., Cromer, L., Horlow, C., Armstrong, S.J., Chelysheva, L., and Mercier, R. (2014). The kinesin AtPSS1 promotes synapsis and is required for proper crossover distribution in meiosis. *PLoS Genet* 10**,** e1004674.

Golubovskaya, I., Avalkina, N.A., and Sheridan, W.F. (1992). Effects of several meiotic mutations on female meiosis in maize. *genesis* 13**,** 411-424.

Hiatt, E.N., and Dawe, R.K. (2003). The meiotic drive system on maize abnormal chromosome 10 contains few essential genes. *Genetica* 117**,** 67-76.

Hiatt, E.N., Kentner, E.K., and Dawe, R.K. (2002). Independently regulated neocentromere activity of two classes of tandem repeat arrays. *The Plant Cell Online* 14**,** 407-420.

Higgins, D.M., Nannas, N.J., and Dawe, R.K. (2016). The maize Divergent spindle-1 (dv1) gene encodes a kinesin-14A motor protein required for meiotic spindle pole organization. *Frontiers in Plant Science* 7.

Hirokawa, N., Noda, Y., Tanaka, Y., and Niwa, S. (2009). Kinesin superfamily motor proteins and intracellular transport. *Nat Rev Mol Cell Biol* 10**,** 682-696.

Howe, E.S., Clemente, T.E., and Bass, H.W. (2012). Maize histone H2B-mCherry: a new fluorescent chromatin marker for somatic and meiotic chromosome research. *DNA and cell biology* 31**,** 925-938.

Kanizay, L.B., Albert, P.S., Birchler, J.A., and Dawe, R.K. (2013a). Intragenomic conflict between the two major knob repeats of maize. *Genetics* 194**,** 81-89.

Kanizay, L.B., Pyhajarvi, T., Lowry, E.G., Hufford, M.B., Peterson, D.G., Ross-Ibarra, J., and Dawe, R.K. (2013b). Diversity and abundance of the abnormal chromosome 10 meiotic drive complex in Zea mays. *Heredity* 110**,** 570-577.

Kim, D., Pertea, G., Trapnell, C., Pimentel, H., Kelley, R., and Salzberg, S.L. (2013). TopHat2: accurate alignment of transcriptomes in the presence of insertions, deletions and gene fusions. *Genome biology* 14**,** 1.

Lawrence, C.J., Morris, N.R., Meagher, R.B., and Dawe, R.K. (2001). Dyneins Have Run Their Course in Plant Lineage. *Traffic* 2**,** 362-363.

Li, X., and Dawe, R.K. (2009). Fused sister kinetochores initiate the reductional division in meiosis I. *Nat Cell Biol* 11**,** 1103-1108.

Longley, A.E. (1938). Chromosomes of maize from Native American Indians. *J. Agric. Res.* 56**,** 177-195.

Longley, A.E. (1945). Abnormal Segregation during Megasporogenesis in Maize. *Genetics* 30**,** 100-113.

Mohanty, A., Luo, A., Deblasio, S., Ling, X., Yang, Y., Tuthill, D.E., Williams, K.E., Hill, D., Zadrozny, T., Chan, A., Sylvester, A.W., and Jackson, D. (2009). Advancing cell biology and functional genomics in maize using fluorescent protein-tagged lines. *Plant Physiol* 149**,** 601-605.

Nguyen-Ngoc, T., Afshar, K., and Gonczy, P. (2007). Coupling of cortical dynein and G[alpha] proteins mediates spindle positioning in Caenorhabditis elegans. *Nat Cell Biol* 9**,** 1294-1302.

Rhoades, M., and Vilkomerson, H. (1942). On the anaphase movement of chromosomes. *Proceedings of the National Academy of Sciences* 28**,** 433-436.

Rhoades, M.M. (1942). Preferential Segregation in Maize. *Genetics* 27**,** 395-407.

Rhoades, M.M. (1952). "Preferential Segregation in Maize", in: *Heterosis.* (ed.) J.W. Gowen. Iowa State College Press).

Sandler, L., and Novitski, E. (1957). Meiotic drive as an evolutionary force. *The American Naturalist* 91**,** 105-110.

Schnable, P.S., Ware, D., Fulton, R.S., Stein, J.C., Wei, F., Pasternak, S., Liang, C., Zhang, J., Fulton, L., Graves, T.A., Minx, P., Reily, A.D., Courtney, L., Kruchowski, S.S., Tomlinson, C., Strong, C., Delehaunty, K., Fronick, C., Courtney, B., Rock, S.M., Belter, E., Du, F., Kim, K., Abbott, R.M., Cotton, M., Levy, A., Marchetto, P., Ochoa, K., Jackson, S.M., Gillam, B., Chen, W., Yan, L., Higginbotham, J., Cardenas, M., Waligorski, J., Applebaum, E., Phelps, L., Falcone, J., Kanchi, K., Thane, T., Scimone, A., Thane, N., Henke, J., Wang, T., Ruppert, J., Shah, N., Rotter, K., Hodges, J., Ingenthron, E., Cordes, M., Kohlberg, S., Sgro, J., Delgado, B., Mead, K., Chinwalla, A., Leonard, S., Crouse, K., Collura, K., Kudrna, D., Currie, J., He, R., Angelova, A., Rajasekar, S., Mueller, T., Lomeli, R., Scara, G., Ko, A., Delaney, K., Wissotski, M., Lopez, G., Campos, D., Braidotti, M., Ashley, E., Golser, W., Kim, H., Lee, S., Lin, J., Dujmic, Z., Kim, W., Talag, J., Zuccolo, A., Fan, C., Sebastian, A., Kramer, M., Spiegel, L., Nascimento, L., Zutavern, T., Miller, B., Ambroise, C., Muller, S., Spooner, W., Narechania, A., Ren, L., Wei, S., Kumari, S., Faga, B., Levy, M.J., Mcmahan, L., Van Buren, P., Vaughn, M.W., et al. (2009). The B73 Maize Genome: Complexity, Diversity, and Dynamics. *Science* 326**,** 1112-1115.

Thorvaldsdóttir, H., Robinson, J.T., and Mesirov, J.P. (2013). Integrative Genomics Viewer (IGV): high-performance genomics data visualization and exploration. *Briefings in bioinformatics* 14**,** 178-192.

Trapnell, C., Roberts, A., Goff, L., Pertea, G., Kim, D., Kelley, D.R., Pimentel, H., Salzberg, S.L., Rinn, J.L., and Pachter, L. (2012). Differential gene and transcript expression analysis of RNA-seq experiments with TopHat and Cufflinks. *Nat. Protocols* 7**,** 562-578.

Trapnell, C., Williams, B.A., Pertea, G., Mortazavi, A., Kwan, G., Van Baren, M.J., Salzberg, S.L., Wold, B.J., and Pachter, L. (2010). Transcript assembly and quantification by RNA-Seq reveals unannotated transcripts and isoform switching during cell differentiation. *Nature biotechnology* 28**,** 511-515.

Zhang, H., Phan, B.H., Wang, K., Artelt, B.J., Jiang, J., Parrott, W.A., and Dawe, R.K. (2012). Stable integration of an engineered megabase repeat array into the maize genome. *The Plant Journal* 70**,** 357-365.

Table 3.1 List of SNPs used to differentiate *Kindr* family members

Context	Location in Alignment	Consensus Allele	SNP	SNP in Copy
CCAXCCG	10	C	T	G11/B1
CCCXGAG	82	G	A	B10
CCCXCTC	214	G	T	G11/B1
ACCXCCG	247	C	T	B10
CATXGAT	267	A	G	G11/B1 and B10
GATXCAC	271	C	T	G11/B1 and B10
CCGXAGA	347	A	G	G11/B1 and B10
AAGXTGA	437	C	T	B10
TTAXAAT	467	A	G	B9/E9 and B2
AAGXCAG	489	G	A	B9/E9 and B2
ACAXGTT	503	G	A	G11/B1
TGAXTGA	539	C	T	G11/B1
TGAXAAA	543	A	G	G11/B1
CCTXCAG	591	T	C	B9/E9
ATGXCTA	670	T	C	C4
TTTXTTG	861	G	A	?
TGCXTAT	1062	C	T	G11/B1
CAGXCAC	1174	G	A	C4

Table 3.2 Rates of transmission of Ab10 in RNAi backgrounds

Cross	R-Ab10	r-N10	% Trans	Expected	χ^2	at p=0.01
DH193xDH200	196	95	67.35395189	145.5	35.05498	Reject - DRIVE
DH193xDH200	388	140	73.48484848	264	116.4848	Reject - DRIVE
Total DH193	**584**	**235**	**71.30647131**	**409.5**	**148.7192**	**Reject - DRIVE FOR AB10**
DH194xDH200	323	437	42.5	380	17.1	Reject - DRIVE
DH194xDH200	146	216	40.33149171	181	13.53591	Reject - DRIVE
DH194xDH200	146	171	46.05678233	158.5	1.971609	Fail to Reject - NO DRIVE
Total DH194	**615**	**824**	**42.73801251**	**719.5**	**30.35511**	**Reject - DRIVE FOR N10**
DH195xDH200	225	94	70.53291536	159.5	53.79624	Reject - DRIVE
DH195xDH200	178	72	71.2	125	44.944	Reject - DRIVE
DH195xDH200	404	136	74.81481481	270	133.0074	Reject - DRIVE
DH195xDH200	169	182	48.14814815	175.5	0.481481	Fail to Reject - NO DRIVE
DH195xDH200	92	65	58.59872611	78.5	4.643312	Fail to Reject - NO DRIVE
DH195xDH200	275	134	67.23716381	204.5	48.6088	Reject - DRIVE
Total DH195	**1343**	**683**	**66.28825271**	**1013**	**215.0049**	**Reject - DRIVE FOR AB10**
DH196xDH200	385	104	78.73210634	244.5	161.4744	Reject - DRIVE
DH196xDH200	296	67	81.54269972	181.5	144.4656	Reject - DRIVE
DH196xDH200	146	62	70.19230769	104	33.92308	Reject - DRIVE
Total DH196	**827**	**233**	**78.01886792**	**530**	**332.8642**	**Reject - DRIVE FOR AB10**
DH197xDH200	182	60	75.20661157	121	61.50413	Reject - DRIVE
DH197xDH200	446	113	79.78533095	279.5	198.3703	Reject - DRIVE
DH197xDH200	429	101	80.94339623	265	202.9887	Reject - DRIVE
DH197xDH200	403	95	80.92369478	249	190.49	Reject - DRIVE
Total DH197	**1460**	**369**	**79.82504101**	**914.5**	**650.7824**	**Reject- DRIVE FOR AB10**
DH198xDH200	394	107	78.64271457	250.5	164.4092	Reject - DRIVE
DH198xDH200	330	97	77.28337237	213.5	127.1405	Reject - DRIVE
DH198xDH200	192	44	81.3559322	118	92.81356	Reject - DRIVE
DH198xDH200	238	65	78.54785479	151.5	98.77558	Reject - DRIVE
Total DH198	**1154**	**313**	**78.66394001**	**733.5**	**482.1275**	**Reject - DRIVE FOR AB10**
DH199xDH200	241	68	77.99352751	154.5	96.85761	Reject - DRIVE
DH199xDH200	191	81	70.22058824	136	44.48529	Reject - DRIVE
DH199xDH200	142	38	78.88888889	90	60.08889	Reject - DRIVE
DH199xDH200	128	45	73.98843931	86.5	39.82081	Reject - DRIVE
DH199xDH200	398	122	76.53846154	260	146.4923	Reject - DRIVE
DH199xDH200	189	66	74.11764706	127.5	59.32941	Reject - DRIVE
Total DH199	**1289**	**420**	**75.42422469**	**854.5**	**441.873**	**Reject - DRIVE FOR AB10**

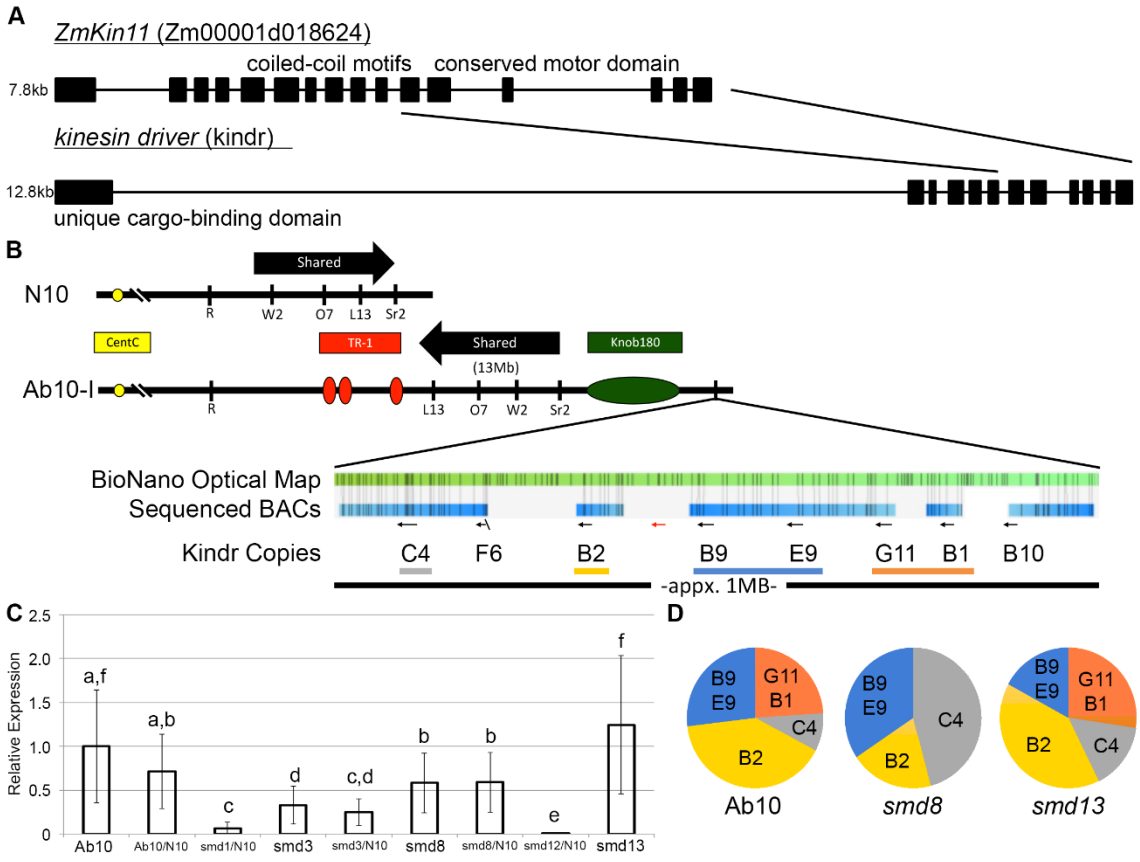

Figure 3.1 Gene models and expression of *Kindr*.

(A) Gene models of *Kindr* and *ZmKin11*, the closest homolog to *Kindr* in the maize genome. Exons are represented with filled rectangles with introns represented as solid black lines. The C-terminal motor domain shows a large degree of homology, while the N-terminal cargo-binding domain is less conserved. Total lengths (introns + exons) are presented to the left of the gene model.

(B) BioNano optical map of the Ab10 distal dip modeling where the *Kindr* complex is located. Sequenced BACs are aligned to the optical map with copies of *Kindr* labeled with black arrows. The sequence of F6 is truncated by the end of the BAC. A ninth copy (red arrow) is hypothesized based on homology of the optical map pattern around B2.

(C) Relative expression of *Kindr* in Ab10 and different *smd* haplotypes. The FPKM of the wild type Ab10 samples has been adjusted to 1.0 with others corrected by the same ratio. Groups of statistical significance as determined by cuffdiff are listed above each bar in lowercase letters. Error bars indicate confidence intervals provided by cuffdiff.
(D) Relative expression of individual copies of *Kindr* in Ab10, *smd8*, and *smd12*. Colors correspond to the bars located below each copy name in 1B. Copies E9 & B9 and B1 & G11 are indistinguishable from one another and combined in this analysis.

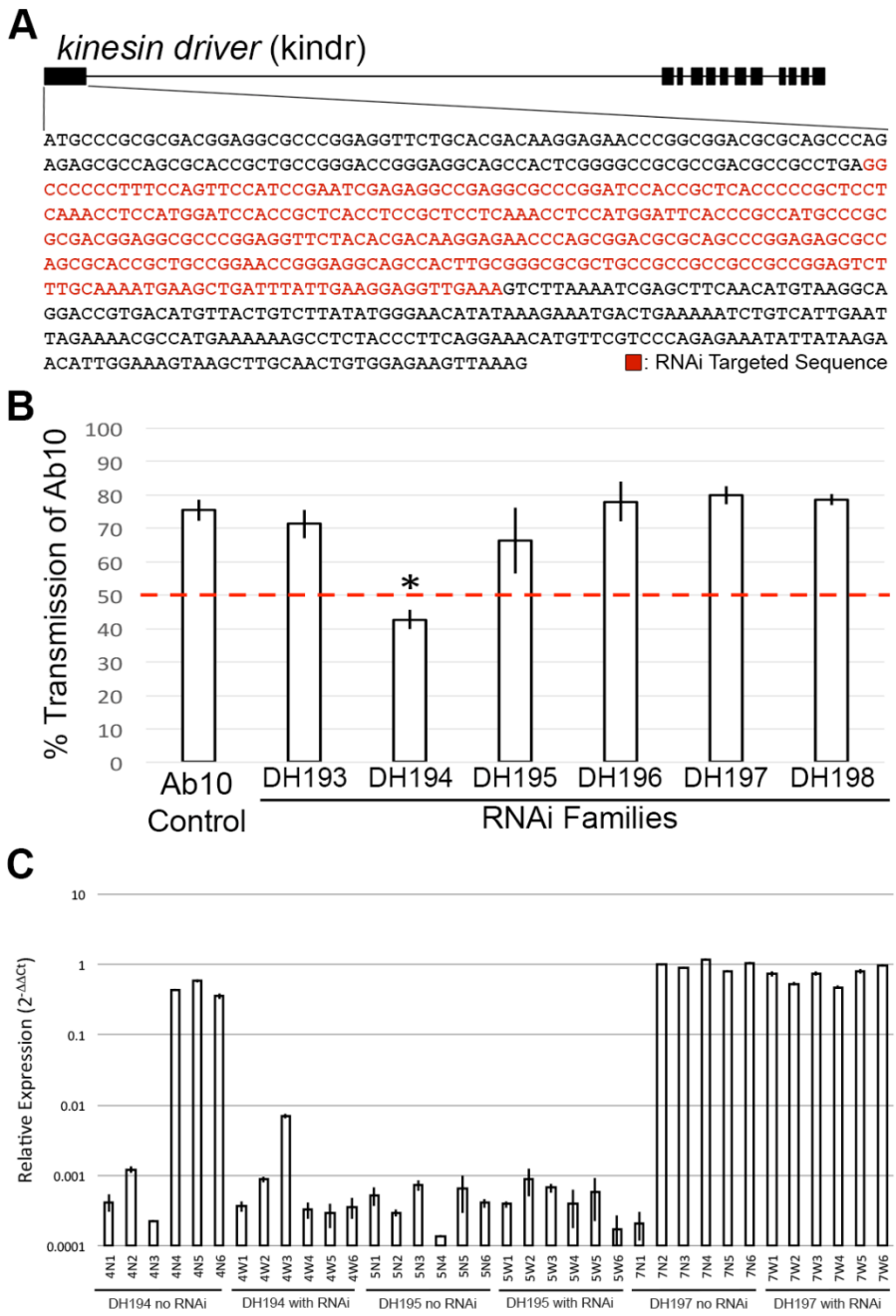

Figure 3.2 RNAi knockdown of Kindr results in loss of meiotic drive.

(A) Gene model of *Kindr* with the sequence of the first exon presented. The sequence targeted by the RNAi construct is given in red.

(B) Transmission rates of Ab10 in six different RNAi families. 50% transmission is expected of a typical heterozygous locus (red dashed line). DH194 (*) is significantly

lower than the expected Mendelian inheritance rate as determined by chi-squared analysis (a=0.01).

(C) Relative expression of *Kindr* in RNAi families. DH197, a family showing no change in drive frequency, also shows no reduction in *Kindr* expression. DH194 and DH195 both show complete loss of *Kindr* expression (greater than 99% reduction) in the presence of the RNAi construct. *Kindr* expression is variable in DH194 and DH195 after the RNAi construct is crossed out of the background, suggesting that the transgene is capable of inducing a stable epimutation which silences the *Kindr* complex.

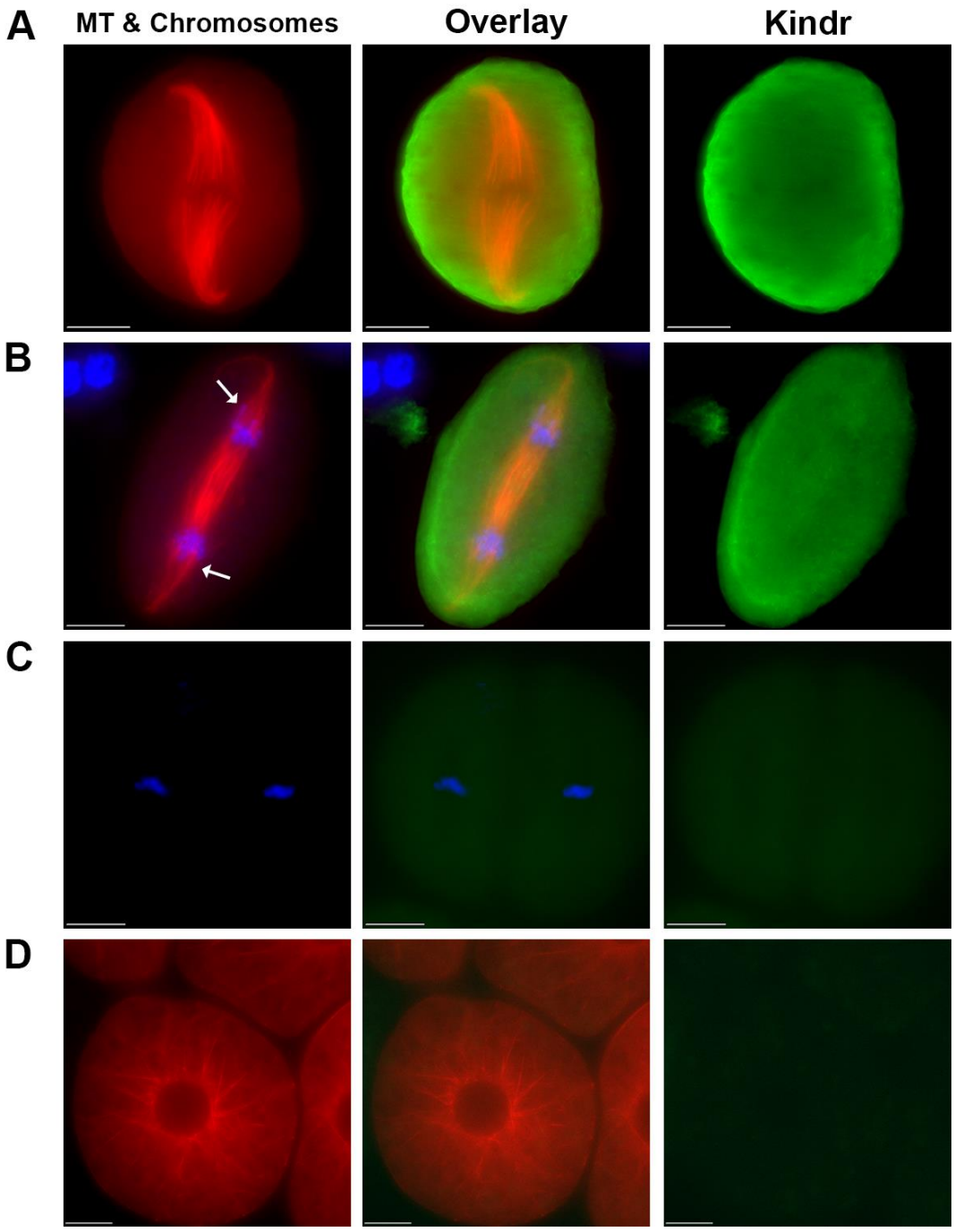

Figure 3.3 Cellular localization of *Kindr*.

The left-most column represents fluorescence channels associated with either microtubules (red), chromatin (blue), or both. The right-most column represents

fluorescence from a *Kindr*-associated source (green). An overlay is presented in the middle column.

(A) Meiocyte in metaphase showing focused spindle poles stained with a *Kindr* antibody.

(B) Meiocyte in anaphase, displaying neocentromere activity (arrows), stained with the same *Kindr* antibody.

(C) Meiocyte in metaphase II carrying a *KindrX1-YFP* transgene.

(D) Post-meiotic pollen cell displaying a fluorescent tubulin transgene driven by the same promoter as *KindrX1-YFP*.

CHAPTER 4

DIVERSITY AND FITNESS COSTS ASSOCIATED WITH THE ABNORMAL CHROMOSOME 10 MEIOTIC DRIVE SYSTEM IN ZEA MAYS[3]

[3] Higgins, D.M.; Becraft, P.W. and R.K. Dawe. To be submitted to *Genetics*.

ABSTRACT

Meiotic drive describes a process whereby selfish genetic elements are transmitted at levels greater than Mendelian expectations. Abnormal chromosome 10 (Ab10) in *Zea mays* (maize) is a variant of normal chromosome 10 (N10) that exhibits meiotic drive, being transmitted to ~75% of the female gametes from Ab10/N10 individuals. Despite this strong driving pressure, Ab10 is only present at low frequencies in natural populations, indicating that there are negative fitness consequences associated with Ab10. We found no evidence that Ab10 transmission is reduced through male parents. However, Ab10 confers a disadvantage as a homozygote, including decreased pollen viability, decreased seed set, and decreased seed weight. We observed an enrichment of nucleotide variants within the inverted regions of the haplotype that may contribute to decreased fitness. In addition, we identified seven new Ab10 chromosomes from landraces and teosinte lines, and measured their diversity at the molecular and phenotypic levels. The data reveal significant variation in the levels of meiotic drive as well as evidence of historic recombination among haplotypes.

INTRODUCTION

The fact that phenotypes are transmitted from parent to offspring was well known before the days of Gregor Mendel and his research on pea plants. In the years since, we have discovered that chromosomes, complex macromolecules made of DNA and protein, contain the units of genetic inheritance. Following DNA replication, chromosomes consist of two identical sister chromatids connected at the centromere. In cells destined to undergo meiosis, homologous chromosomes align and exchange material with one another before the chromatids are faithfully segregated into four daughter cells that will become gametes. In most meiotic events, each allele has an equal (50-50%) chance of being passed on to the next generation. However, a number of systems have been identified in which specific alleles or chromosomes are preferentially inherited at a rate greater than 50% - a process known as meiotic drive (Sandler and Novitski, 1957).

Meiotic drive systems have independently arisen multiple times and involve widely diverse mechanisms. One of best understood meiotic drive systems is the *Segregation Distorter* (*SD*) system in *Drosophila melanogaster* (reviewed in Larracuente and Presgraves, 2012). The *Sd* locus encodes two elements in linkage: a truncated form of RanGAP, a protein involved in nuclear transport (Merrill et al., 1999) and *Responder* (*Rsp*) a region of satellite DNA (Wu et al., 1988). *Sd-RanGAP* is mislocalized in developing spermatocytes and is associated with errors in chromatin condensation, ultimately resulting in sperm cells lacking *Rsp* and failing to mature properly (Kusano et al., 2001). As *Rsp* and *Sd-RanGAP* are in tight linkage, the *Sd* locus selfishly eliminates wild type chromosomes (*Sd+*) causing 95% of offspring of *Sd*/*Sd+* males to carry the *Sd* chromosome. The *Spore killer* (*Sk*) locus of the fungus *Neurospora intermedia* carries out

meiotic drive using a similar mechanism. The *Sk* locus encodes two elements, a killer element (*Sk*) and a resistance gene (*rsk)*. *Sk* eliminates spores lacking *rsk,* which is hypothesized to act through binding and neutralization of the killer element (Hammond et al., 2012). Meiotic drive systems have also been identified in plants, including the *D* locus in *Mimulus* (Fishman and Willis, 2005) and the abnormal chromosome 10 system in *Zea mays* (maize), the subject of this study.

The maize genome, typical of monocots, is heavily enriched with repetitive sequences which account for much of its DNA content. These include transposable elements, the mobile sequences identified by Barbara McClintock which copy themselves throughout the genome, as well as tandem repeats – repetitive sequences unrelated to transposable elements which form arrays that expand and contract due unequal crossing over. There are three major types of tandem repeats in the maize genome, each with their own unique sequence. The 156 bp-long CentC repeat is associated with centromeres (Zhong et al., 2002). Two other so-called knob repeats, the 350 bp TR1 repeat and the 180-bp repeat are found along chromosome arms (Peacock et al., 1981; Ananiev et al., 1998). Because arrays of knob repeats can be quite large and are typically gene-poor, they remain tightly condensed during interphase, appearing as darkly staining balls of heterochromatin (McClintock, 1930). Knobs are easily distinguishable using a light microscope and were an early indicator of genetic diversity in maize and its undomesticated relative teosinte (Longley, 1937).

Maize is a diploid grass with a karyotype comprised of ten pairs of homologous chromosomes (2n = 2x = 20). The tenth chromosome, the smallest of the set, can be found in two forms: a common form without any knobs referred to as “normal

chromosome 10" (N10) and a rarer, abnormal form with large knobs at the end of its long arm known as "abnormal chromosome 10" (Ab10) (Longley, 1938). The heterochromatic knobs at the end of the long arm of Ab10 flank a set of genes which are shared with N10 (Figure 4.1A). It was later discovered that while the gene content in this "shared region" is the same, the gene order is inverted on Ab10, preventing recombination between the two versions of chromosome 10 in this region (Rhoades and Dempsey, 1985). An early mapping study on Ab10 identified it as a meiotic driver – offspring that are created from a heterozygote for Ab10 (Ab10/N10) preferentially inherit the abnormal chromosome at a rate of approximately 70-75% (Rhoades, 1942). The drive phenotype is observed only when Ab10 is crossed as a female (Rhoades, 1942). Further studies demonstrated that Ab10 not only causes the preferential segregation of itself, but all other loci linked to knobs, as long as the knob is heterozygous and Ab10 is present (Longley, 1945). Population surveys have shown that Ab10 is present in 18-22% of landraces of maize across North, Central, and South America while within those populations, the average number of individuals carrying Ab10 is 6-13% (McClintock et al., 1981; Kanizay et al., 2013b). The low frequency of individuals carrying Ab10 is surprising, given its meiotic drive phenotype leads to 70-75% transmission as a heterozygote through the female parent. While Ab10 is a strong driver in a single cross, there must deleterious consequences associated with Ab10 that lowers fitness and prevents it from driving to fixation.

Cytology on meiocytes carrying Ab10 allowed Marcus Rhoades to develop his hypothesis for the mechanism responsible for the drive phenotype. While typically inert during cell division, when Ab10 is present knobs become "neocentromeres" that actively

move along meiotic spindles ahead of centromeres (Rhoades and Vilkomerson, 1942). Neocentromere activity drives knobs to spindle poles, creating an orientation that persists through meiosis II, and causes knobs to be preferentially pulled to the bottom daughter cell of the linear stack. As this cell is the only one which will become a fertile egg cell (the other three abort shortly after meiosis), and Ab10 itself contains a knob, Ab10 is inherited at a rate greater than typically expected (Rhoades, 1952). Although they are called neocentromeres, activated knobs do not recruit typical centromere/kinetochore proteins such as CENP-C (Dawe et al., 1999). Genetics studies revealed that knobs containing 180 bp repeats and knobs containing TR1 repeats are activated to form neocentromeres by separate factors on different parts of the Ab10 chromosome (Hiatt et al., 2002). Recent results show that a novel kinesin motor protein on Ab10 called *kinesin driver* (*Kindr*) is responsible for 180-bp neocentromere activity and meiotic drive (Dawe et al., *Submitted*).

One of the most attractive aspects of maize as a model organism is the vast amount of genetic diversity within domesticated maize and its teosinte relatives (as reviewed in Nannas and Dawe, 2015). Prior data show that Ab10 chromosomes from different accessions can be visibly different in the abundance and locations of knob repeats (Figure 4.1A, 4.1B). Haplotypes of Ab10 are characterized into three major "cytotypes" based on their knob patterning – Ab10-I, Ab10-II, and Ab10-III. In addition, there is another chromosome 10 variant called K10L2 that displays TR1 knob neocentromere activity, but not meiotic drive (Kanizay et al., 2013a). In order to better understand the diversity and fitness consequences associated with Ab10, we used a collection of nine Ab10 haplotypes (Figure 4.1C) to measure phenotypic and genetic

diversity associated with Ab10. In addition we measured fitness traits associated with male and female gametes, as well as pollen viability and seed set. The results reveal a dynamic system where Ab10 haplotypes are actively recombining with each other and showing strong segregation advantages as a heterozygous condition. However, when Ab10 is homozygous, pollen is less viable and seed set is severely reduced. The data suggest that homozygous disadvantage may partially explain the overall low frequency of Ab10 in natural populations.

MATERIALS AND METHODS

Seeds Stocks and Fluorescent in situ *hybridization*

The reference forms of Ab10-I and Ab10-II (Ab10-I-MMR and Ab10-II-MMR) were originally obtained from Marcus M. Rhoades. The K10L2 chromosome was originally isolated from the inbred CI66 (Kanizay et al., 2013a). Additional Ab10 isolates were extracted from landraces and teosintes obtained from the North Central Plant Introduction Research Station (Ames, Iowa) based on the results of Kanizay et al. (2013b). We identified Ab10 by PCR in a set of different lines and crossed and backcrossed the Ab10 chromosome at least four times into standard maize tester stocks. The chromosomes were then named based on their place of origin: Ab10-I-Jal (PI 628445, Jalisco, Mexico), Ab10-II-Sal (Ames 21826, El Salado Guerrero, Mexico), Ab10-II-Tel (Ames 21826, Teloloapan-Arcelia Road, Guerrero, Mexico), Ab10-III–Hui (PI 444834, Huila, Colombia), Ab10-III-Caq (PI 444296, Caqueta, Colombia), Ab10-III-Oax (Ames 19980, Oaxaca, Mexico).

Fluorescent in situ hybridization (FISH) was carried out using the protocol (Kato et al., 2004) and oligonucleotide-tags (Kanizay et al., 2013b) described previously. Slides were imaged using a Zeiss Axio Imager M1 fluorescence microscope with a 63x Plan-APO Chromat oil objective. Images were collected using the Slidebook software package (Intelligent Imaging Innovations, Denver, CO).

Measuring transmission rates, pollen viability, seed counts

The transmission rate of Ab10 was inferred using the marker gene *colored1* (*R1*). *R1* is located near the end of the long arm of maize chromosome 10 and is in tight linkage with the Ab10 haplotype (Rhoades, 1942). Kernels homozygous for the recessive allele (*r1*) are yellow while those with one or more copies of the dominant allele (*R1*) are purple. The Ab10 haplotype linked to *R1* (*R*-Ab10) was crossed to plants homozygous for normal chromosome 10 carrying *r1* (*r*-N10). Heterozygotes (*R*-Ab10/*r*-N10) plants were crossed to a recessive tester (*r*-N10/*r*-N10). The transmission of Ab10 was determined by manually counting the number of kernels of each color from the resulting crosses.

All plants measured for transmission rates were grown in Athens, Georgia, USA. The experiment quantifying the transmission of Ab10 as a male parent was conducted during the summer of 2014 (n=2416-4269 kernels per genotype). The experiment quantifying the transmission of Ab10 as a female parent was conducted during the summer of 2016 (n=421-2966 kernels per genotype).

Pollen viability of Ab10 was calculated using a modified version (Peterson et al., 2010) of the Alexander's stain protocol (Alexander, 1969) as described previously

(Higgins et al., 2016). 500 pollen grains from each plant were scored for viability based on staining color.

The effect of Ab10 on seed set was measured using an Ab10-I-MMR line backcrossed into the B73 background for six generations. Sibling plants either wild type *(r*-N10/*r*-N10), homozygous *(R*-N10/*R*-N10), or heterozygous for Ab10 *(R*-N10/*r*-N10), were pollinated by wild type pollen (n = 43-86 ears per genotype). All plants were grown in Ames, Iowa, USA during the summer of 2016. The number of seeds per ear was counted manually and the mass of seeds from each ear was measured using a balance.

Transcriptome Library Synthesis

Whole transcriptome sequencing (RNA-Seq) from young anthers was employed to identify variants between Ab10 haplotypes and characterize differences in gene expression. Meiotically-staged anthers were dissected from tassels and RNA extracted as described previously (Dawe et al., *Submitted*). Sequencing libraries were generated using the KAPA Stranded RNA-Seq Kit (Kapa Biosystems, Wilmington, MA). Paired-end 75bp sequencing was completed on an Illumina NextSeq at the Georgia Genomics Facility (Athens, GA).

SNP Mapping & PROVEAN Analysis

Reads were cleaned using Trimmomatic to remove adapters and 5' and 3' ends with low-quality scores less than Phred 5 (Bolger et al., 2014). Cleaned reads were aligned to the maize reference genome (B73 AGPv4) using the program STAR under the default settings (Dobin et al., 2012). Variants were called using the software package

Genome Analysis Toolkit (GATK) (McKenna et al., 2010) following the Best Practices Work Flow using HaplotypeCaller (Van der Auwera et al., 2013). SNPs which were not present in each of the replicates (n=2-5) were filtered out using vcftools (Danecek et al., 2011). In addition, variants present in the maize HapMap2 (Chia et al., 2012) and Panzea 2.7 genotyping-by-sequencing (http://www.panzea.org) datasets were removed from analysis in order to focus on Ab10-specific variants. The shared region was defined as the sequence between the *R1* gene and the end of the chromosome 10L (coordinates 10:139,790,276-150,982,314 on B73 RefGen_v4).

The effects of Ab10-specific SNPs were identified using Variant Effect Predictor (McLaren et al., 2016) using the default settings. Those variants that resulted in either gain of a stop codon, a frameshift, or a missense substitution within the shared region distal to *R* were analyzed using PROVEAN Protein webtool to identify the effects of these substitutions (Choi and Chan, 2015).

Expression of Kindr

To quantify the expression of *Kindr* in the ten different accessions (all heterozygous for Ab10), mRNA extraction, cDNA generation, high-throughput sequencing, and read processing was carried out as described above on plants heterozygous for the different Ab10 haplotypes. Reads were aligned to the maize reference genome (B73 AGPv4) using TopHat and expression of transcripts was quantified with Cufflinks using the published protocol (Trapnell et al., 2012).

Phylogeny

Sequence variants were used to generate alternate references representing genomic sequences along the shared region for each haplotype using the FastaAlternateReferenceMaker tool in GATK. Predicted cDNA sequences for each gene in each haplotype were extracted using the gffread utility in Cufflinks (Trapnell et al., 2010). The closest homologs of each of these genes were identified in *Sorghum bicolor* using the Gramene Plant Compara tool (http://ensembl.gramene.org/). The complete set of maize haplotypes as well as the *S. bicolor* homolog were individually aligned using MUSCLE (Edgar, 2004) under the default settings. Gene trees were assembled using RAxML with 500 bootstrap replicates (Stamatakis, 2006). A species tree representing all of the genes from each of the haplotypes was estimating using ASTRAL v4.10.0 (Mirarab and Warnow, 2015; Sayyari and Mirarab, 2016).

Data Availability

Transcriptome reads are available for download on the NCBI Sequence Read Archive (ncbi.nlm.nih.gov/sra) under project accession numbers SRP082328, SRP058857, and SRP082329.

RESULTS

Ab10 shows no evidence of decreased transmission through pollen

We began our study by extracting seven new Ab10 chromosomes from maize landraces and teosintes from across Central and South America (Figure 4.1C). These were initially identified by Kanizay et al. (2013b) in tropical or teosinte backgrounds, and

crossed into standard corn belt maize lines. This new collection of Ab10 chromosomes dramatically expands the available types, as prior to this only the reference forms (Ab10-I-MMR and Ab10-II-MMR) had been studied. Our collection includes new forms of Ab10-I, Ab10-II, and Ab10-III (Figure 4.1A).

Using these lines we tested two hypotheses which could explain the low frequency of Ab10 within populations. The first hypothesis is that the transmission of Ab10 is reduced through the male parent. As meiotic drive only occurs when Ab10 is crossed as a female, it is possible that the fitness advantage through females is counterbalanced by fitness disadvantages in the male, resulting in a lower overall frequency in freely outcrossing populations. The original study by Rhoades (1942) provides support for this, in which he showed that the transmission of Ab10-I-MMR through pollen was 42%, significantly below the expected 1:1 ratio. An alternative finding appeared in a later study which indicated male transmission of Ab10-II-MMR was roughly Mendelian (Rhoades and Dempsey, 1988).

To expand these analyses, we tested male transmission for Ab10-I-MMR, Ab10-II-MMR, and three new isolates of Ab10-III (-Hui, -Caq, and -Oax) by crossing each of these as heterozygotes to recessive tester ears. The presence of Ab10 was scored using alleles of the linked marker gene *colored1* (*R1*) (Figure 4.2A). The average male transmission rates for all five haplotypes were above 50% (x=50.4% - 57.1%) (Figure 4.2B, Table 4.1) and four of the five were significantly higher than the expected 1:1 ratio as determined using chi-squared tests (II-MMR at $p<0.05$, III-Caq, III-Hui, III-Oax at $p<0.01$). This is in contrast to the Rhoades (1942) finding but consistent with Rhoades and Dempsey's more recent finding (1988). Although male transmission is presumably

influenced by genetic background and environment, our data suggest that transmission of Ab10 through pollen is not necessarily worse than what would be expected through traditional Mendelian inheritance.

In plants, the products of meiosis known as gametophytes undergo mitotic divisions before they mature. The gametophyte represents a challenge to cells, as their genomes are haploid but they must still grow, divide, and develop in order to produce functional gametes. It is possible that, after being segregated into pollen mother cells, those cells carrying Ab10 are less able to fully develop into mature pollen and less likely to be transmitted (Figure 4.2C). We screened pollen viability in plants heterozygous and homozygous for Ab10 using a modified version of Alexander's stain. The data showed no differences in average pollen viability between N10 homozygotes ($x=0.97$) and Ab10 heterozygotes ($x=0.96$) as determined by a t-test ($p=0.195$) (Figure 4.2D, Table 4.2). However, pollen viability in Ab10 homozygotes ($x=0.91$) was significantly lower than both N10 homozygotes ($p=0.049$) and Ab10 heterozygotes ($p=0.009$). Mutants that affect pollen viability can act on the haploid gametophytes following meiosis or through the paternal (diploid) sporophyte which contributes to pollen wall development (as reviewed in Scott et al., 2004). If Ab10 was causing errors in pollen development after meiosis, we would expect pollen viability to be lower in the heterozygote, which was not observed. Instead, these data suggest that homozygous Ab10 plants may be partially defective in completing pollen maturation during late anther development.

Ab10 homozygotes produce fewer, smaller seeds than wild type siblings

The homozygous Ab10 genotype may also confer fitness disadvantages at the level of female gametophyte development, fertilization, or seed maturation. To measure these effects, we first backcrossed Ab10-I-MMR to the standard B73 inbred for six generations, and self-crossed to generate seeds that were heterozygous and homozygous for Ab10. For N10 controls, we used the standard B73 inbred. Ears from N10/N10 (B73), Ab10/N10, and Ab10/Ab10 plants were pollinated by B73 (N10) pollen (Figure 4.2E). Seeds produced were then counted and weighed.

Ab10 homozygotes showed a 64.9% reduction in seed count compared to wild type (Figure 4.2F, Table 4.3, $p < 0.001$). In addition, the mass per hundred seeds showed a 23.7% reduction from wild type (Figure 4.2G, Table 4.3, $p < 0.001$). Ab10 heterozygotes showed an intermediate phenotype more similar to wild type with a 13.8% reduction in seed count ($p = 0.023$) and 5.9% reduction in seed mass ($p = 0.013$). Taken together, our data on pollen viability, seed count, and seed mass suggest that Ab10 contains deleterious alleles that negatively impact gamete and seed production.

Unique, deleterious variants have arisen in genes in the shared region between Ab10 and N10

The shared region is conserved between N10 and Ab10 and contains essential genes necessary for plant growth and development. However, several inversions (Mroczek et al., 2006) prevent the two haplotypes from actively recombining in this region (Figure 4.1A). Deleterious alleles that would normally be selected out of

populations might accumulate in the shared region of Ab10 due to limited recombination and strong meiotic drive.

To test this hypothesis, we identified SNPs in the Ab10 shared region using RNA-seq data from meiotic anthers derived from plants heterozygous for the Ab10-I-MMR haplotype. Sequence variants were first identified by comparing RNA-seq reads to maize reference genome (B73 v4). We then filtered out common SNPs observed in other studies, leaving only rare SNPs and those unique to our lines. When the density of variants was mapped across the entire maize genome, a significant enrichment was observed at the end of chromosome 10 corresponding to the shared region (Figure 4.3A). A clear peak of variants can be seen starting from the *R1* locus and extending to the end of chromosome 10 (Figure 4.3B). A total of 13.6% of all SNPs identified (279/2059) were in this region, even though it represents only 0.5% of the genome. Of the 279 SNP variants identified in the shared region, 77 were missense mutations and 1 encoded a premature stop codon.

In order to assess the effects these variants on the proteins they encode, we used Variant Effect Predictor and the PROVEAN Protein software tools. PROVEAN estimates the effect of mutations in proteins based on conservation between related species and the nature of the substitution, assigning a score from 4, corresponding to a substitution with no predicted impact on protein function, to -12, corresponding to a highly deleterious substitution (Choi et al., 2012). Analysis using PROVEAN indicates 13 of the 78 missense substitutions are likely to have deleterious effects on protein function (Table 4.4). In contrast, only 6 of a total of 60 missense mutations identified on the remaining 93% of the length of chromosome 10 were estimated as deleterious by PROVEAN. A

review of the list of genes with deleterious mutations provided no clear candidates which might directly explain the pollen or seed phenotypes observed.

Rates of meiotic drive are largely uniform across haplotypes

To assess diversity between the different haplotypes of Ab10, we first looked for variation in the meiotic drive phenotype. Previously published estimates of drive at approximately 70% are based on the Ab10-I-MMR haplotype (Rhoades, 1942). In order to determine if there is phenotypic variation for meiotic drive among our haplotypes, we generated plants heterozygous for Ab10 and N10 linked to different alleles of the *R1* gene and crossed them to a recessive tester as described previously (Figure 4.2A), this time as a female parent. The data reveal that while all Ab10 haplotypes show meiotic drive, they do not all do so at the same level (Figure 4.2A, Table 4.5). Many of the samples are not significantly different as determined by ANOVA and Tukey's HSD test (α=0.05) from the Ab10-I-MMR haplotype (x=74.9%). However, two haplotypes, Ab10-I-Jal (x=61.6%) and Ab10-III-Hui (x=60.0%) displayed significantly lower levels of meiotic drive than other haplotypes (but were significantly higher than N10 control (x=48.9%)).

Kinesin driver (*Kindr*) is a kinesin motor protein discovered on the distal tip of the Ab10-I-MMR haplotype that has been implicated in neocentromere activity and meiotic drive (Dawe et al., *Submitted*). In order to determine whether variation in the expression of *Kindr* might explain the observed variation in meiotic drive, we calculated *Kindr* expression using RNA-Seq. *Kindr* expression was generally consistent with the Ab10-I-MMR haplotype (Figure 4.4B). Two samples varied, with the Ab10-II-Tel haplotype having approximately twice the *Kindr* expression of Ab10-I-MMR, and Ab10-

III-Gua having approximately half the *Kindr* expression of Ab10-I-MMR. K10L2, the Ab10 variant that lacks the large 180 bp knob (Figure 4.1A) and fails to show strong meiotic drive (Kanizay et al., 2013a), showed no *Kindr* expression. Among the haplotypes that do show meiotic drive, there was no correlation between *Kindr* expression and the degree of preferential segregation ($R^2 = 0.0787$, Figure 4.4C).

Phylogeny of haplotypes suggests recombination between cytotypes in nature

The shared region represents a unique opportunity to assess the evolutionary history of Ab10, as the genes present in this region are conserved between N10 and Ab10, but generally do not recombine with each other. Using the RNA-seq data from the *Kindr* quantification experiment, we identified sequences for each gene present in the shared region for all ten Ab10 haplotypes, K10L2, and paired N10 controls. The sequences were aligned and gene trees assembled using the closest homolog from *Sorghum bicolor* as an outgroup. To best account for all genes in this region, we used the software ASTRAL to combine the gene trees into a single, coalescent-based estimated species tree (Figure 4.5).

Three major clades emerged, including two with Ab10 haplotypes and one with N10 haplotypes. The first major clade includes the Ab10-I-MMR and Ab10-II-MMR haplotypes which were first isolated 80 and 36 years ago, respectively. It is unclear what pedigree these haplotypes have followed since their collection from Mexico, and Rhoades and Dempsey (1985) conducted a number of experiments measuring recombination between the two, which may help to explain their apparent separation from other Ab10 haplotypes. The second major clade includes the N10 haplotypes tested as controls. The

K10L2 haplotype clusters into this clade consistent with prior data (Kanizay et al., 2013b). The final clade contains the rest of the Ab10 haplotypes. The haplotypes do not cluster by cytotype, suggesting there is free exchange of genes in the shared region between Ab10s with different knob contents. Some of the subclades within this group are organized by geography including Ab10-III-Caq and Ab10-III-Hui (both from Columbia) as well as Ab10-II-Tel, Ab10-II-Sal, Ab10-III-Oax, Ab10-III-Gua and Ab10-I-Jal (from Mexico), but overall there are no obvious relationships based on geography or knob content.

DISCUSSION

Abnormal chromosome 10 is a strong meiotic driver in single crosses but fails to reach high frequencies in open-pollinated landraces. Through assessing the diversity of Ab10, we sought to better understand why Ab10 is observed at low frequencies. We found no evidence indicating that the transmission of Ab10 is reduced in male crosses. Quantification across multiple haplotypes indicated no values less than 50% transmission, the level expected by traditional Mendelian inheritance (Figure 4.2B). Indeed, four of the haplotypes showed transmission slightly higher than would be anticipated, a result which has not been indicated in previous Ab10 studies. Furthermore, pollen viability was not significantly different between wild type and heterozygous lines (Figure 4.2D), suggesting Ab10 does not have negative effects on the gametophytic divisions of pollen development as seen in other genetic mutants such as *sidecar pollen* in *Arabidopsis thaliana* (Chen and McCormick, 1996).

Although Ab10 does not appear to affect gamete viability, we observed a number of clear defects at the sporophytic level in Ab10 homozygotes, including pollen maturation, seed set and seed mass (Figure 4.2D, 4.2F, 4.2G). It has been previously shown in other systems that deleterious alleles linked to meiotic drive elements negatively impact their frequency within populations (Cotton et al., 2014). The *D* locus in *Mimulus*, another female-specific meiotic drive system in plants, displays a mild but significant reduction of pollen viability in homozygotes (Fishman and Saunders, 2008). Pollen viability is a sensitive phenotype, affected by physical (Herrero and Johnson, 1980) and chemical (Sharma et al., 1991) stresses, and there are over 20 known genetic loci that cause a male sterile phenotype in maize (reviewed in Coe et al., 1988). The observed defects in seed set could be caused by failures at any level of pollination and fertilization, including silk development and the capacity of the silk to support pollen tube development. The observed reduction in seed mass suggests that there may also be defects in the conducting tissue that supplies seeds with carbohydrates. Low seed weight is correlated with low seedling emergence and plant size in next generation (Hunter and Kannenberg, 1972; El-Abady, 2015).

As it contains essential genes but cannot recombine with the N10 haplotype, the inverted shared region is a likely place for deleterious mutations to accumulate. By screening the shared region for missense mutations, we identified an enrichment of SNPs (Figure 4.3B) which are predicted to cause deleterious effects on their protein products (Table 4.4). The data suggests there are multiple mutations in essential genes along the shared region each with their own small, but not insignificant, effects on fitness, including pollen and seed production. We hypothesize that the sum of these effects

reduces the relative fitness of individuals and populations containing Ab10, particularly as it reaches high frequencies.

Our studies of different Ab10 haplotypes indicate that most exhibit drive at rates between 70 and 80% (Figure 4.4A). We observed no trends in level of drive based on cytotype, indicating that knob size is not a good predictor of drive as was previously suggested (Kanizay et al., 2013b). Likewise, expression of the *Kindr* gene implicated in meiotic drive is largely uniform (Figure 4.4B). Ab110-II-Tel represents a strong outlier, with approximately two- to four-fold higher levels of *Kindr* expression than other haplotypes, but its rate of meiotic drive is not significantly different from other haplotypes (Figure 4.4C). Two samples from Columbia (Ab10-III-Caq and Ab10-III-Hui) show significantly different rates of meiotic drive (Figure 4.4A, x= 79.2% and 60.0% respectively) yet their phylogeny indicates they are closely related (Figure 4.5) and their *Kindr* expression is similar (Figure 4.4B). These results indicate that there are factors other than knob size and *Kindr* expression that impact meiotic drive.

It has been previously hypothesized that different haplotypes recombine with each other in nature (Rhoades and Dempsey, 1985) and controlled experiments have demonstrated recombination between Ab10-I-MMR and Ab10-II-MMR in human-assisted crosses (Kanizay et al., 2013a). Our phylogeny provides evidence in support of this view, as the Ab10 clade does not show distinct subclades associated with different cytotypes (Figure 4.5). The K10L2 haplotype clustered with the N10 clade, supporting previous findings that K10L2 readily recombines with N10 but not Ab10 (Kanizay et al., 2013a). However, our molecular analyses should be viewed as first estimates, as they are based on RNA-seq data from anthers, and are limited to the genes expressed in this

tissue. The construction of a complete genomic reference for Ab10 will reveal more about the molecular nature of the inversions that define the Ab10 haplotype and make it possible to identify additional, novel elements that impact meiotic drive and the frequency of Ab10 in populations.

WORKS CITED

Alexander, M. (1969). Differential staining of aborted and nonaborted pollen. *Stain technology* 44**,** 117-122.

Allen, C., and Borisy, G.G. (1974). Structural polarity and directional growth of microtubules of *Chlamydomonas* flagella. *J. Cell Sci.* 14**,** 523-549.

Amaratunga, A., Morin, P.J., Kosik, K.S., and Fine, R.E. (1993). Inhibition of Kinesin Synthesis and Rapid Anterograde Axonal Transport *in Vivo* by an Antisense Oligonucleotide. *Journal of Biological Chemistry* 268**,** 17427-17430.

Ambrose, J.C., and Cyr, R. (2007). The kinesin ATK5 functions in early spindle assembly in Arabidopsis. *The Plant Cell* 19**,** 226-236.

Ambrose, J.C., Li, W., Marcus, A., Ma, H., and Cyr, R. (2005). A minus-end-directed kinesin with plus-end tracking protein activity is involved in spindle morphogenesis. *Mol Biol Cell* 16**,** 1584-1592.

Ananiev, E., Phillips, R., and Rines, H. (1998). A knob-associated tandem repeat in maize capable of forming fold-back DNA segments: Are chromosome knobs megatransposons? *Proceedings of the National Academy of Sciences* 95**,** 10785-10790.

Ardlie, K.G., and Silver, L.M. (1996). Low Frequency of Mouse t Haplotypes in Wild Populations Is Not Explained by Modifiers of Meiotic Drive. *Genetics* 144**,** 1787-1797.

Asai, D.J., Thompson, W.C., Wilson, L., and Brokaw, C.J. (1982). Two different monoclonal antibodies to alpha-tubulin inhibit the bending of reactivated sea urchin spermatozoa. *Cell motility* 2**,** 599-614.

Austin, B., and Trivers, R. (2006). *Genes in Conflict.* Harvard University Press.

Azimzadeh, J., Nacry, P., Christodoulidou, A., Drevensek, S., Camilleri, C., Amiour, N., Parcy, F., Pastuglia, M., and Bouchez, D. (2008). Arabidopsis TONNEAU1 Proteins Are Essential for Preprophase Band Formation and Interact with Centrin. *The Plant Cell Online* 20**,** 2146-2159.

Bannigan, A., Lizotte-Waniewski, M., Riley, M., and Baskin, T.I. (2008). Emerging molecular mechanisms that power and regulate the anastral mitotic spindle of flowering plants. *Cell motility and the cytoskeleton* 65**,** 1-11.

Berchowitz, L.E., and Copenhaver, G.P. (2008). Fluorescent Arabidopsis tetrads: a visual assay for quickly developing large crossover and crossover interference data sets. *Nat. Protocols* 3**,** 41-50.

Bolger, A.M., Lohse, M., and Usadel, B. (2014). Trimmomatic: a flexible trimmer for Illumina sequence data. *Bioinformatics***,** btu170.

Brouhard, G.J., and Hunt, A.J. (2005). Microtubule movements on the arms of mitotic chromosomes: polar ejection forces quantified in vitro. *Proceedings of the National Academy of Sciences of the United States of America* 102**,** 13903-13908.

Brown, R.C., and Lemmon, B.E. (1997). The quadripolar microtubule system in lower land plants. *Journal of Plant Research* 110**,** 93-106.

Brown, R.C., and Lemmon, B.E. (2001). Sporogenesis in Eusporangiate Ferns: I. monoplastidic Meiosis in Angiopteris (Marattiales). *Journal of Plant Research* 114**,** 223-235.

Cai, S., Weaver, L.N., Ems-Mcclung, S.C., and Walczak, C.E. (2009). Kinesin-14 family proteins HSET/XCTK2 control spindle length by cross-linking and sliding microtubules. *Mol Biol Cell* 20**,** 1348-1359.

Cande, W.Z., and Freeling, M. (2011). Inna Golubovskaya: the life of a geneticist studying meiosis. *Genetics* 188**,** 491-498.

Carlson, W. (1988). The Cytogenetics of Corn. *Corn and Corn Improvement. Third Edition.***,** 259-343.

Chan, J., Calder, G.M., Doonan, J.H., and Lloyd, C.W. (2003). EB1 reveals mobile microtubule nucleation sites in Arabidopsis. *Nat Cell Biol* 5**,** 967-971.

Chen, C., Marcus, A., Li, W., Hu, Y., Calzada, J.-P.V., Grossniklaus, U., Cyr, R.J., and Ma, H. (2002). The *Arabidopsis ATK1* gene is required for spindle morphogenesis in male meiosis. *Development* 129**,** 2401-2409.

Chen, Y., and Mccormick, S. (1996). sidecar pollen, an Arabidopsis thaliana male gametophytic mutant with aberrant cell divisions during pollen development. *Development* 122**,** 3243-3253.

Chia, J.-M., Song, C., Bradbury, P.J., Costich, D., De Leon, N., Doebley, J., Elshire, R.J., Gaut, B., Geller, L., Glaubitz, J.C., Gore, M., Guill, K.E., Holland, J., Hufford, M.B., Lai, J., Li, M., Liu, X., Lu, Y., Mccombie, R., Nelson, R., Poland, J., Prasanna, B.M., Pyhäjärvi, T., Rong, T., Sekhon, R.S., Sun, Q., Tenaillon, M.I., Tian, F., Wang, J., Wang, J., Xu, X., Zhang, Z., Kaeppler, S.M., Ross-Ibarra, J., Mcmullen, M.D., Buckler, E.S., Zhang, G., Xu, Y., and Ware, D. 2012. Maize HapMap2 identifies extant variation from a genome in flux. *Nature genetics* [Online], 44.

Choi, Y., and Chan, A.P. (2015). PROVEAN web server: a tool to predict the functional effect of amino acid substitutions and indels. *Bioinformatics* 31**,** 2745-2747.

Choi, Y., Sims, G.E., Murphy, S., Miller, J.R., and Chan, A.P. (2012). Predicting the Functional Effect of Amino Acid Substitutions and Indels. *PLoS ONE* 7**,** e46688.

Clark, F.J. (1940). Cytogenetic Studies of Divergent Meiotic Spindle Formation in Zea Mays. *American Journal of Botany* 27**,** 547-559.

Clark, F.J. (1943). The Germination Capacity of Maize Pollen Having Aberrant Nuclei. *Bulletin of the Torrey Botanical Club* 70**,** 449-456.

Clarke, J.D. (2009). Cetyltrimethyl ammonium bromide (CTAB) DNA miniprep for plant DNA isolation. *Cold Spring Harbor Protocols* 2009**,** pdb. prot5177.

Coe, E.H., Neuffer, M.G., and Hoisington, D.A. (1988). The Genetics of Corn. *Corn and Corn improvement. Third Edition.***,** 81-258.

Collins, E., Mann, B.J., and Wadsworth, P. (2014). Eg5 restricts anaphase B spindle elongation in mammalian cells. *Cytoskeleton* 71**,** 136-144.
Conduit, P.T., Wainman, A., and Raff, J.W. (2015). Centrosome function and assembly in animal cells. *Nat Rev Mol Cell Biol* 16**,** 611-624.
Cotton, A., Földvári, M., Cotton, S., and Pomiankowski, A. (2014). Male eyespan size is associated with meiotic drive in wild stalk-eyed flies (Teleopsis dalmanni). *Heredity* 112**,** 363-369.
Danecek, P., Auton, A., Abecasis, G., Albers, C.A., Banks, E., Depristo, M.A., Handsaker, R.E., Lunter, G., Marth, G.T., and Sherry, S.T. (2011). The variant call format and VCFtools. *Bioinformatics* 27**,** 2156-2158.
Davis, D. (1969). Chromosome behavior under the influence of claret-nondisjunctional in Drosophila melanogaster. *Genetics* 61**,** 577.
Dawe, R.K., and Cande, W.Z. (1996). Induction of centromeric activity in maize by suppressor of meiotic drive 1. *Proceedings of the National Academy of Sciences* 93**,** 8512-8517.
Dawe, R.K., and Hiatt, E.N. (2004). Plant neocentromeres: fast, focused, and driven. *Chromosome Research* 12**,** 655-669.
Dawe, R.K., Lowry, E.G., Gent, J.I., Stitzer, M.C., Higgins, D.M., Ross-Ibarra, J., Wallace, J.G., Kanizay, L.B., Alabady, M., Wang, N., Gao, Z., Birchler, J.A., Harkess, A.E., Hodges, A.L., and Hiatt, E.N. (Submitted). A novel maize kinesin causes neocentromere activity and meiotic drive, altering inheritance across the genome.
Dawe, R.K., Reed, L.M., Yu, H.-G., Muszynski, M.G., and Hiatt, E.N. (1999). A maize homolog of mammalian CENPC is a constitutive component of the inner kinetochore. *The Plant Cell* 11**,** 1227-1238.
De La Peña, A. (1986). 'In vitro' culture of isolated meiocytes of rye, Secale cereale L. *Environmental and Experimental Botany* 26**,** 17-23.
De Mendiburu, F. (2014). Agricolae: statistical procedures for agricultural research. *R package version* 1**,** 1-6.
Delgehyr, N., Sillibourne, J., and Bornens, M. (2005). Microtubule nucleation and anchoring at the centrosome are independent processes linked by ninein function. *Journal of Cell Science* 118**,** 1565-1575.
Dobin, A., Davis, C.A., Schlesinger, F., Drenkow, J., Zaleski, C., Jha, S., Batut, P., Chaisson, M., and Gingeras, T.R. (2012). STAR: ultrafast universal RNA-seq aligner. *Bioinformatics* 29**,** 15-21.
Duroc, Y., Lemhemdi, A., Larchevêque, C., Hurel, A., Cuacos, M., Cromer, L., Horlow, C., Armstrong, S.J., Chelysheva, L., and Mercier, R. (2014). The kinesin AtPSS1 promotes synapsis and is required for proper crossover distribution in meiosis. *PLoS Genet* 10**,** e1004674.
Dutcher, S.K., and Trabuco, E.C. (1998). The UNI3 Gene Is Required for Assembly of Basal Bodies of Chlamydomonas and Encodes δ-Tubulin, a New Member of the Tubulin Superfamily. *Molecular Biology of the Cell* 9**,** 1293-1308.
Edgar, R.C. (2004). MUSCLE: multiple sequence alignment with high accuracy and high throughput. *Nucleic Acids Research* 32**,** 1792-1797.
El-Abady, M. (2015). Influence of Maize Seed Size/Shape, Planted at Different Depths and Temperatures on Seed Emergence and Seedling Vigor.

Elliott, S., Knop, M., Schlenstedt, G., and Schiebel, E. (1999). Spc29p is a component of the Spc110p subcomplex and is essential for spindle pole body duplication. *Proceedings of the National Academy of Sciences* 96**,** 6205-6210.

Endow, S., and Higuchi, H. (2000). A mutant of the motor protein kinesin that moves in both directions on microtubules. *Nature* 406**,** 913-916.

Endow, S.A., Henikoff, S., and Soler-Niedziela, L. (1990). Mediation of meiotic and early mitotic chromosome segregation in Drosophilia by a protein related to kinesin. *Nature* 345**,** 81.

Enos, A.P., and Morris, N.R. (1990). Mutation of a gene that encodes a kinesin-like protein blocks nuclear division in A. nidulans. *Cell* 60**,** 1019-1027.

Fink, G., Hajdo, L., Skowronek, K.J., Reuther, C., Kasprzak, A.A., and Diez, S. (2009). The mitotic kinesin-14 Ncd drives directional microtubule-microtubule sliding. *Nat Cell Biol* 11**,** 717-723.

Fishman, L., and Saunders, A. (2008). Centromere-associated female meiotic drive entails male fitness costs in monkeyflowers. *Science* 322**,** 1559-1562.

Fishman, L., and Willis, J.H. (2005). A novel meiotic drive locus almost completely distorts segregation in Mimulus (monkeyflower) hybrids. *Genetics* 169**,** 347-353.

Golubovskaya, I., Avalkina, N.A., and Sheridan, W.F. (1992). Effects of several meiotic mutations on female meiosis in maize. *genesis* 13**,** 411-424.

Gould, R.R., and Borisy, G.G. (1977). The pericentriolar material in Chinese hamster ovary cells nucleates microtubule formation. *Journal of Cell Biology* 73**,** 601-615.

Gruneberg, U., Campbell, K., Simpson, C., Grindlay, J., and Schiebel, E. (2000). Nud1p links astral microtubule organization and the control of exit from mitosis. *The EMBO Journal* 19**,** 6475-6488.

Hammond, T.M., Rehard, D.G., Xiao, H., and Shiu, P.K.T. (2012). Molecular dissection of Neurospora Spore killer meiotic drive elements. *Proceedings of the National Academy of Sciences* 109**,** 12093-12098.

Hatsumi, M., and Endow, S. (1992). Mutants of the microtubule motor protein, nonclaret disjunctional, affect spindle structure and chromosome movement in meiosis and mitosis. *Journal of Cell Science* 101**,** 547-559.

Hepperla, A.J., Willey, P.T., Coombes, C.E., Schuster, B.M., Gerami-Nejad, M., Mcclellan, M., Mukherjee, S., Fox, J., Winey, M., and Odde, D.J. (2014). Minus-End-Directed Kinesin-14 Motors Align Antiparallel Microtubules to Control Metaphase Spindle Length. *Developmental cell* 31**,** 61-72.

Herrero, M.P., and Johnson, R.R. (1980). High Temperature Stress and Pollen Viability of Maize. *Crop Science* 20**,** 796-800.

Herrmann, B.G., Koschorz, B., Wertz, K., Mclaughlin, K.J., and Kispert, A. (1999). A protein kinase encoded by the t complex responder gene causes non-mendelian inheritance. *Nature* 402**,** 141-146.

Hiatt, E.N., and Dawe, R.K. (2003). The meiotic drive system on maize abnormal chromosome 10 contains few essential genes. *Genetica* 117**,** 67-76.

Hiatt, E.N., Kentner, E.K., and Dawe, R.K. (2002). Independently regulated neocentromere activity of two classes of tandem repeat arrays. *The Plant Cell Online* 14**,** 407-420.

Higgins, D.M., Nannas, N.J., and Dawe, R.K. (2016). The maize Divergent spindle-1 (dv1) gene encodes a kinesin-14A motor protein required for meiotic spindle pole organization. *Frontiers in Plant Science* 7.

Hirokawa, N., and Noda, Y. (2008). Intracellular transport and kinesin superfamily proteins, KIFs: structure, function, and dynamics. *Physiological reviews* 88**,** 1089-1118.

Hirokawa, N., Noda, Y., Tanaka, Y., and Niwa, S. (2009). Kinesin superfamily motor proteins and intracellular transport. *Nat Rev Mol Cell Biol* 10**,** 682-696.

Hirokawa, N., Pfister, K.K., Yorifuji, H., Wagner, M.C., Brady, S.T., and Bloom, G.S. (1989). Submolecular domains of bovine brain kinesin identified by electron microscopy and monoclonal antibody decoration. *Cell* 56**,** 867-878.

Howard, J., and Hyman, A.A. (2003). Dynamics and mechanics of the microtubule plus end. *Nature* 422**,** 753-758.

Howard, J., and Hyman, A.A. (2009). Growth, fluctuation and switching at microtubule plus ends. *Nature Reviews Molecular Cell Biology* 10**,** 569-574.

Howe, E.S., Clemente, T.E., and Bass, H.W. (2012). Maize histone H2B-mCherry: a new fluorescent chromatin marker for somatic and meiotic chromosome research. *DNA and cell biology* 31**,** 925-938.

Hunter, R.B., and Kannenberg, L. (1972). Effects of seed size on emergence, grain yield, and plant height in corn. *Canadian Journal of Plant Science* 52**,** 252-256.

Jaspersen, S.L., Martin, A.E., Glazko, G., Giddings, T.H., Morgan, G., Mushegian, A., and Winey, M. (2006). The Sad1-UNC-84 homology domain in Mps3 interacts with Mps2 to connect the spindle pole body with the nuclear envelope. *The Journal of Cell Biology* 174**,** 665-675.

Kanizay, L.B., Albert, P.S., Birchler, J.A., and Dawe, R.K. (2013a). Intragenomic conflict between the two major knob repeats of maize. *Genetics* 194**,** 81-89.

Kanizay, L.B., Pyhajarvi, T., Lowry, E.G., Hufford, M.B., Peterson, D.G., Ross-Ibarra, J., and Dawe, R.K. (2013b). Diversity and abundance of the abnormal chromosome 10 meiotic drive complex in Zea mays. *Heredity* 110**,** 570-577.

Kashina, A., Baskin, R., Cole, D., Wedaman, K., Saxton, W., and Scholey, J.M. (1996). A bipolar kinesin. *Nature* 379**,** 270.

Kato, A., Lamb, J.C., and Birchler, J.A. (2004). Chromosome painting using repetitive DNA sequences as probes for somatic chromosome identification in maize. *Proceedings of the National Academy of Sciences of the United States of America* 101**,** 13554-13559.

Kilmartin, J.V. (2014). Lessons from yeast: the spindle pole body and the centrosome. *Philosophical Transactions of the Royal Society of London B: Biological Sciences* 369**,** 20130456.

Kim, D., Pertea, G., Trapnell, C., Pimentel, H., Kelley, R., and Salzberg, S.L. (2013). TopHat2: accurate alignment of transcriptomes in the presence of insertions, deletions and gene fusions. *Genome biology* 14**,** 1.

Knop, M., and Schiebel, E. (1997). Spc98p and Spc97p of the yeast γ-tubulin complex mediate binding to the spindle pole body via their interaction with Spc110p. *The EMBO Journal* 16**,** 6985-6995.

Knop, M., and Schiebel, E. (1998). Receptors determine the cellular localization of a γ-tubulin complex and thereby the site of microtubule formation. *The EMBO journal* 17**,** 3952-3967.

Komarova, Y.A., Akhmanova, A.S., Kojima, S., Galjart, N., and Borisy, G.G. (2002). Cytoplasmic linker proteins promote microtubule rescue *in vivo*. *Journal of Cell Biology* 159.

Kops, G.J.P.L., Weaver, B.a.A., and Cleveland, D.W. (2005). On the road to cancer: aneuploidy and the mitotic checkpoint. *Nat Rev Cancer* 5**,** 773-785.

Kull, F.J., Sablin, E.P., Lau, R., Fletterick, R.J., and Vale, R.D. (1996). Crystal structure of the kinesin motor domain reveals a structural similarity to myosin. *Nature* 380**,** 550.

Kusano, A., Staber, C., and Ganetzky, B. (2001). Nuclear Mislocalization of Enzymatically Active RanGAP Causes Segregation Distortion in Drosophila. *Developmental Cell* 1**,** 351-361.

Larracuente, A.M., and Presgraves, D.C. (2012). The selfish Segregation Distorter gene complex of Drosophila melanogaster. *Genetics* 192**,** 33-53.

Lawrence, C.J., Dawe, R.K., Christie, K.R., Cleveland, D.W., Dawson, S.C., Endow, S.A., Goldstein, L.S., Goodson, H.V., Hirokawa, N., Howard, J., Malmberg, R.L., Mcintosh, J.R., Miki, H., Mitchison, T.J., Okada, Y., Reddy, A.S., Saxton, W.M., Schliwa, M., Scholey, J.M., Vale, R.D., Walczak, C.E., and Wordeman, L. (2004). A standardized kinesin nomenclature. *J Cell Biol* 167**,** 19-22.

Lawrence, C.J., Malmberg, R.L., Muszynski, M.G., and Dawe, R.K. (2002). Maximum likelihood methods reveal conservation of function among closely related kinesin families. *J Mol Evol* 54**,** 42-53.

Lawrence, C.J., Morris, N.R., Meagher, R.B., and Dawe, R.K. (2001). Dyneins Have Run Their Course in Plant Lineage. *Traffic* 2**,** 362-363.

Ledbetter, M.C., and Porter, K.R. (1963). A"Microtubule" in Plant Cell Fine Structure. *Journal of Cell Biology* 19**,** 239-250.

Li, X., and Dawe, R.K. (2009). Fused sister kinetochores initiate the reductional division in meiosis I. *Nat Cell Biol* 11**,** 1103-1108.

Liu, B., Hotta, T., Ho, C.-M.K., and Lee, Y.-R.J. (2011a). "Microtubule Organization in the Phragmoplast," in *The Plant Cytoskeleton*, ed. B. Liu. (New York, NY: Springer New York), 207-225.

Liu, B., Marc, J., Joshi, H.C., and Palevitz, B.A. (1993). A gamma-tubulin-related protein associated with the microtubule arrays of higher plants in a cell cycle-dependent manner. *J Cell Sci* 104 (Pt 4)**,** 1217-1228.

Liu, H., Jin, F., Liang, F., Tian, X., and Wang, Y. (2011b). The Cik1/Kar3 Motor Complex Is Required for the Proper Kinetochore–Microtubule Interaction After Stressful DNA Replication. *Genetics* 187**,** 397-407.

Livak, K.J., and Schmittgen, T.D. (2001). Analysis of relative gene expression data using real-time quantitative PCR and the 2− ΔΔCT method. *methods* 25**,** 402-408.

Lloyd, C.W., and Chan, J. (2006). Not so divided: the common basis of plant and animal cell division. *Nature Reviews Molecular Cell Biology* 7**,** 147-152.

Longley, A. (1937). Morphological characters of teosinte chromosomes. *J. agric. Res* 54**,** 836-862.

Longley, A.E. (1938). Chromosomes of maize from Native American Indians. *J. Agric. Res.* 56**,** 177-195.
Longley, A.E. (1945). Abnormal Segregation during Megasporogenesis in Maize. *Genetics* 30**,** 100-113.
Lowry, E.G. (2015). *The meiotic drive mechanism of a selfish chromosome in Zea mays.* Doctor of Philosophy, University of Georgia.
Luck, D.J.L. (1984). Genetic and Biochemical Dissection of the Eucaryotic Flagellum. *Journal of Cell Biology* 98**,** 789-794.
Lyon, M.F. (1991). The genetic basis of transmission-ratio distortion and male sterility due to the t complex. *The American Naturalist* 137**,** 349-358.
Maddox, P., Chin, E., Mallavarapu, A., Yeh, E., Salmon, E.D., and Bloom, K. (1999). Microtubule Dynamics from Mating through the First Zygotic Division in the Budding Yeast Saccharomyces cerevisiae. *The Journal of Cell Biology* 144**,** 977-987.
Manning, B.D., Barrett, J.G., Wallace, J.A., Granok, H., and Snyder, M. (1999). Differential regulation of the Kar3p kinesin-related protein by two associated proteins, Cik1p and Vik1p. *The Journal of cell biology* 144**,** 1219-1233.
Manoli, A., Sturaro, A., Trevisan, S., Quaggiotti, S., and Nonis, A. (2012). Evaluation of candidate reference genes for qPCR in maize. *Journal of Plant Physiology* 169**,** 807-815.
Marshall, W.F. (2009). Centriole Evolution. *Current Opinion in Cell Biology* 21**,** 14-19.
Matthies, H.J., Mcdonald, H.B., Goldstein, L.S., and Theurkauf, W.E. (1996). Anastral meiotic spindle morphogenesis: role of the non-claret disjunctional kinesin-like protein. *The Journal of Cell Biology* 134**,** 455-464.
Mazumdar, M., Sundareshan, S., and Misteli, T. (2004). Human chromokinesin KIF4A functions in chromosome condensation and segregation. *The Journal of cell biology* 166**,** 613-620.
Mcclintock, B. (1930). A cytological demonstration of the location of an interchange between two non-homologous chromosomes of Zea mays. *Proceedings of the National Academy of Sciences* 16**,** 791-796.
Mcclintock, B., Yamakake, T.a.K., and Blumenschein, A. (1981). *Chromosome constitution of races of maize: its significance in the interpretation of relationships between races and varieties in the Americas.* Colegio de Postgraduados Mexico.
Mcdonald, H.B., Stewart, R.J., and Goldstein, L.S. (1990). The kinesin-like ncd protein of Drosophila is a minus end-directed microtubule motor. *Cell* 63**,** 1159-1165.
Mckenna, A., Hanna, M., Banks, E., Sivachenko, A., Cibulskis, K., Kernytsky, A., Garimella, K., Altshuler, D., Gabriel, S., Daly, M., and Depristo, M.A. (2010). The Genome Analysis Toolkit: A MapReduce framework for analyzing next-generation DNA sequencing data. *Genome Research* 20**,** 1297-1303.
Mclaren, W., Gil, L., Hunt, S.E., Riat, H.S., Ritchie, G.R.S., Thormann, A., Flicek, P., and Cunningham, F. (2016). The Ensembl Variant Effect Predictor. *Genome Biology* 17**,** 122.
Mcmichael, C.M., and Bednarek, S.Y. (2013). Cytoskeletal and membrane dynamics during higher plant cytokinesis. *New Phytologist* 197**,** 1039-1057.

Meluh, P.B., and Rose, M.D. (1990). KAR3, a kinesin-related gene required for yeast nuclear fusion. *Cell* 60**,** 1029-1041.
Merrill, C., Bayraktaroglu, L., Kusano, A., and Ganetzky, B. (1999). Truncated RanGAP encoded by the Segregation Distorter locus of Drosophila. *Science* 283**,** 1742-1745.
Miki, H., Okada, Y., and Hirokawa, N. (2005). Analysis of the kinesin superfamily: insights into structure and function. *Trends in Cell Biology* 15**,** 467-476.
Mineyuki, Y. (1999). "The Preprophase Band of Microtubules: Its Function as a Cytokinetic Apparatus in Higher Plants," in *International Review of Cytology*, ed. W.J. Kwang. Academic Press), 1-49.
Mirarab, S., and Warnow, T. (2015). ASTRAL-II: coalescent-based species tree estimation with many hundreds of taxa and thousands of genes. *Bioinformatics* 31**,** i44-i52.
Mitsui, H., Yamaguchi-Shinozaki, K., Shinozaki, K., Nishikawa, K., and Takahashi, H. (1993). Identification of a gene family (kat) encoding kinesin-like proteins in Arabidopsis thaliana and the characterization of secondary structure of KatA. *Molecular and General Genetics MGG* 238**,** 362-368.
Mohanty, A., Luo, A., Deblasio, S., Ling, X., Yang, Y., Tuthill, D.E., Williams, K.E., Hill, D., Zadrozny, T., Chan, A., Sylvester, A.W., and Jackson, D. (2009). Advancing cell biology and functional genomics in maize using fluorescent protein-tagged lines. *Plant Physiol* 149**,** 601-605.
Mroczek, R.J., Melo, J.R., Luce, A.C., Hiatt, E.N., and Dawe, R.K. (2006). The Maize Ab10 Meiotic Drive System Maps to Supernumerary Sequences in a Large Complex Haplotype. *Genetics* 174**,** 145.
Muller, E.G.D., Snydsman, B.E., Novik, I., Hailey, D.W., Gestaut, D.R., Niemann, C.A., O'toole, E.T., Giddings, T.H., Sundin, B.A., and Davis, T.N. (2005). The Organization of the Core Proteins of the Yeast Spindle Pole Body. *Molecular Biology of the Cell* 16**,** 3341-3352.
Murphy, S.P., Gumber, H.K., Mao, Y., and Bass, H.W. (2014). A dynamic meiotic SUN belt includes the zygotene-stage telomere bouquet and is disrupted in chromosome segregation mutants of maize (Zea mays L.). *Frontiers in Plant Science* 5**,** 314.
Naito, H., and Goshima, G. (2015). NACK kinesin is required for metaphase chromosome alignment and cytokinesis in the moss Physcomitrella patens. *Cell structure and function* 40**,** 31-41.
Nannas, N.J., and Dawe, R.K. (2015). Genetic and Genomic Toolbox of Zea mays. *Genetics* 199**,** 655-669.
Nguyen-Ngoc, T., Afshar, K., and Gonczy, P. (2007). Coupling of cortical dynein and G[alpha] proteins mediates spindle positioning in Caenorhabditis elegans. *Nat Cell Biol* 9**,** 1294-1302.
Nicklas, R.B., Lee, G.M., Rieder, C.L., and Rupp, G. (1989). Mechanically cut mitotic spindles: clean cuts and stable microtubules. *Journal of Cell Science* 94**,** 415-423.
Nogales, E., Wolf, S.G., and Downing, K.H. (1998). Structure of the alpha-beta tubulin dimer by electron crystallography. *Nature* 391**,** 199-203.

O'toole, E.T., Winey, M., and Mcintosh, J.R. (1999). High-Voltage Electron Tomography of Spindle Pole Bodies and Early Mitotic Spindles in the Yeast Saccharomyces cerevisiae. *Molecular Biology of the Cell* 10**,** 2017-2031.

Olds-Clarke, P., and Johnson, L.R. (1993). t Haplotypes in the Mouse Compromise Sperm Flagellar Function. *Developmental Biology* 155**,** 14-25.

Olmsted, Z.T., Colliver, A.G., Riehlman, T.D., and Paluh, J.L. (2014). Kinesin-14 and kinesin-5 antagonistically regulate microtubule nucleation by γ-TuRC in yeast and human cells. *Nature Communications* 5.

Olmsted, Z.T., Riehlman, T.D., Branca, C.N., Colliver, A.G., Cruz, L.O., and Paluh, J.L. (2013). Kinesin-14 Pkl1 targets γ-tubulin for release from the γ-tubulin ring complex (γ-TuRC). *Cell Cycle* 12**,** 842.

Osborn, M., and Weber, K. (1976). Cytoplasmic microtubules in tissue culture cells appear to grow from an organizing structure towards the plasma membrane. *Proc Natl Acad Sci U S A* 73**,** 867-871.

Page, B.D., Satterwhite, L.L., Rose, M.D., and Snyder, M. (1994). Localization of the Kar3 kinesin heavy chain-related protein requires the Cik1 interacting protein. *The Journal of Cell Biology* 124**,** 507-519.

Paredez, A.R., Somerville, C.R., and Ehrhardt, D.W. (2006). Visualization of Cellulose Synthase Demonstrates Functional Association with Microtubules. *Science* 312**,** 1491-1495.

Pastuglia, M., Azimzadeh, J., Goussot, M., Camilleri, C., Belcram, K., Evrard, J.L., Schmit, A.C., Guerche, P., and Bouchez, D. (2006). Gamma-tubulin is essential for microtubule organization and development in Arabidopsis. *Plant Cell* 18**,** 1412-1425.

Peacock, W., Dennis, E., Rhoades, M., and Pryor, A. (1981). Highly repeated DNA sequence limited to knob heterochromatin in maize. *Proceedings of the National Academy of Sciences* 78**,** 4490-4494.

Peterson, R., Slovin, J.P., and Chen, C. (2010). A simplified method for differential staining of aborted and non-aborted pollen grains. *International Journal of Plant Biology* 1.

Pickett-Heaps, J.D. (1969). The evolution of the mitotic apparatus: an attempt at comparative ultrastructural cytology in dividing plant cells. *Cytobios* 3**,** 257-280.

Quan, L., Xiao, R., Li, W., Oh, S.A., Kong, H., Ambrose, J.C., Malcos, J.L., Cyr, R., Twell, D., and Ma, H. (2008). Functional divergence of the duplicated AtKIN14a and AtKIN14b genes: critical roles in Arabidopsis meiosis and gametophyte development. *Plant J* 53**,** 1013-1026.

Reddy, A.S., and Day, I.S. (2001). Kinesins in the Arabidopsis genome: a comparative analysis among eukaryotes. *BMC genomics* 2**,** 2.

Rhoades, M., and Dempsey, E. (1988). Structure of K10-II chromosome and comparison with K10-I. *Maize Genet. Coop. News Lett* 62**,** 33.

Rhoades, M., and Vilkomerson, H. (1942). On the anaphase movement of chromosomes. *Proceedings of the National Academy of Sciences* 28**,** 433-436.

Rhoades, M.M. (1942). Preferential Segregation in Maize. *Genetics* 27**,** 395-407.

Rhoades, M.M. (1952). "Preferential Segregation in Maize", in: *Heterosis.* (ed.) J.W. Gowen. Iowa State College Press).

Rhoades, M.M., and Dempsey, E. (1985). "Structural heterogeneity of chromosome 10 in races of maize and teosinte.," in *Plant Genetics : proceedings of the Third Annual ARCO Plant Cell Research Institute-UCLA Symposium on Plant Biology, April 13-19, 1985,* ed. M. Freeling. New York : A.R. Liss, 1985.), 1-18.

Sablin, E.P., Kull, F.J., Cooke, R., Vale, R.D., and Fletterick, R.J. (1996). Crystal structure of the motor domain of the kinesin-related motor ncd. *Nature* 380**,** 555-559.

Salisbury, J.L., Suino, K.M., Busby, R., and Springett, M. (2002). Centrin-2 is required for centriole duplication in mammalian cells. *Curr Biol* 12**,** 1287-1292.

Sandler, L., and Novitski, E. (1957). Meiotic drive as an evolutionary force. *The American Naturalist* 91**,** 105-110.

Saunders, A.M., Powers, J., Strome, S., and Saxton, W.M. (2007). Kinesin-5 acts as a brake in anaphase spindle elongation. *Current Biology* 17**,** R453-R454.

Sayyari, E., and Mirarab, S. (2016). Fast Coalescent-Based Computation of Local Branch Support from Quartet Frequencies. *Molecular Biology and Evolution* 33**,** 1654-1668.

Schnable, P.S., Ware, D., Fulton, R.S., Stein, J.C., Wei, F., Pasternak, S., Liang, C., Zhang, J., Fulton, L., Graves, T.A., Minx, P., Reily, A.D., Courtney, L., Kruchowski, S.S., Tomlinson, C., Strong, C., Delehaunty, K., Fronick, C., Courtney, B., Rock, S.M., Belter, E., Du, F., Kim, K., Abbott, R.M., Cotton, M., Levy, A., Marchetto, P., Ochoa, K., Jackson, S.M., Gillam, B., Chen, W., Yan, L., Higginbotham, J., Cardenas, M., Waligorski, J., Applebaum, E., Phelps, L., Falcone, J., Kanchi, K., Thane, T., Scimone, A., Thane, N., Henke, J., Wang, T., Ruppert, J., Shah, N., Rotter, K., Hodges, J., Ingenthron, E., Cordes, M., Kohlberg, S., Sgro, J., Delgado, B., Mead, K., Chinwalla, A., Leonard, S., Crouse, K., Collura, K., Kudrna, D., Currie, J., He, R., Angelova, A., Rajasekar, S., Mueller, T., Lomeli, R., Scara, G., Ko, A., Delaney, K., Wissotski, M., Lopez, G., Campos, D., Braidotti, M., Ashley, E., Golser, W., Kim, H., Lee, S., Lin, J., Dujmic, Z., Kim, W., Talag, J., Zuccolo, A., Fan, C., Sebastian, A., Kramer, M., Spiegel, L., Nascimento, L., Zutavern, T., Miller, B., Ambroise, C., Muller, S., Spooner, W., Narechania, A., Ren, L., Wei, S., Kumari, S., Faga, B., Levy, M.J., Mcmahan, L., Van Buren, P., Vaughn, M.W., et al. (2009). The B73 Maize Genome: Complexity, Diversity, and Dynamics. *Science* 326**,** 1112-1115.

Scott, R.J., Spielman, M., and Dickinson, H.G. (2004). Stamen Structure and Function. *The Plant Cell* 16**,** S46-S60.

Sekhon, R.S., Lin, H., Childs, K.L., Hansey, C.N., Buell, C.R., De Leon, N., and Kaeppler, S.M. (2011). Genome-wide atlas of transcription during maize development. *The Plant Journal* 66**,** 553-563.

Shamina, N., Dorogova, N., and Trunova, S. (2000). Radial Spindle and the Phenotype of the Maize Meiotic Mutant, DV. *Cell Biology International* 24**,** 729-736.

Shamina, N.V. (2005). Formation of division spindles in higher plant meiosis. *Cell Biology International* 29**,** 307-318.

Sharma, C.P., Sharma, P.N., Chatterjee, C., and Agarwala, S.C. (1991). Manganese deficiency in maize affects pollen viability. *Plant and Soil* 138**,** 139-142.

Sharp, D.J., Rogers, G.C., and Scholey, J.M. (2000). Microtubule motors in mitosis. *Nature* 407**,** 41-47.

Shaw, S.L., Kamyar, R., and Ehrhardt, D.W. (2003). Sustained Microtubule Treadmilling in Arabidopsis Cortical Arrays. *Science* 300**,** 1715-1718.
Sobel, S.G., and Snyder, M. (1995). A highly divergent gamma-tubulin gene is essential for cell growth and proper microtubule organization in Saccharomyces cerevisiae. *The Journal of Cell Biology* 131**,** 1775-1788.
Soeda, S., Yamada-Nomoto, K., and Ohsugi, M. (2016). The microtubule-binding and coiled-coil domains of Kid are required to turn off the polar ejection force at anaphase. *J Cell Sci* 129**,** 3609-3619.
Southworth, D., and Cresti, M. (1997). Comparison of flagellated and nonflagellated sperm in plants. *American Journal of Botany* 84**,** 1301.
Spielman, M., Preuss, D., Li, F.-L., Browne, W.E., Scott, R.J., and Dickinson, H.G. (1997). TETRASPORE is required for male meiotic cytokinesis in Arabidopsis thaliana. *Development* 124**,** 2645-2657.
Staiger, C.J., and Cande, W.Z. (1990). Microtubule Distribution in dv, a Maize Meiotic Mutant Defective in the Prophase to Metaphase Transition. *Developmental Biology* 138**,** 231-242.
Stamatakis, A. (2006). RAxML-VI-HPC: maximum likelihood-based phylogenetic analyses with thousands of taxa and mixed models. *Bioinformatics* 22**,** 2688-2690.
Stearns, T., Evans, L., and Kirschner, M. (1991). gamma-Tubulin is a highly conserved component of the centrosome. *Cell* 65.
Stoppin, V., Vantard, M., Schmit, A.C., and Lambert, A.M. (1994). Isolated Plant Nuclei Nucleate Microtubule Assembly: The Nuclear Surface in Higher Plants Has Centrosome-like Activity. *The Plant Cell Online* 6**,** 1099-1106.
Strompen, G., El Kasmi, F., Richter, S., Lukowitz, W., Assaad, F.F., Jürgens, G., and Mayer, U. (2002). The Arabidopsis HINKEL gene encodes a kinesin-related protein involved in cytokinesis and is expressed in a cell cycle-dependent manner. *Current Biology* 12**,** 153-158.
Sturtevant, A.H. (1929). The claret mutant type of Drosophila simulans: a study of chromosome elimination and of cell-lineage. *Z. wiss. Zool* 135**,** 323-356.
Sunkel, C., Gomes, R., Sampaio, P., Perdigao, J., and Gonzalez, C. (1995). Gamma-tubulin is required for the structure and function of the microtubule organizing centre in Drosophila neuroblasts. *The EMBO journal* 14**,** 28.
Takahashi, M., Wakai, T., and Hirota, T. (2016). Condensin I-mediated mitotic chromosome assembly requires association with chromokinesin KIF4A. *Genes & Development* 30**,** 1931-1936.
Takahashi, Y., Soyano, T., Kosetsu, K., Sasabe, M., and Machida, Y. (2010). HINKEL kinesin, ANP MAPKKKs and MKK6/ANQ MAPKK, which phosphorylates and activates MPK4 MAPK, constitute a pathway that is required for cytokinesis in Arabidopsis thaliana. *Plant and cell physiology* 51**,** 1766-1776.
Temin, R.G., Ganetzky, B., Powers, P.A., Lyttle, T.W., Pimpinelli, S., Dimitri, P., Chung, I.W., and Hiraizumi, Y. (1991). Segregation Distortion in Drosophila melanogaster: Genetic and Molecular Analyses. *The American Naturalist* 137**,** 287-331.

Thorvaldsdóttir, H., Robinson, J.T., and Mesirov, J.P. (2013). Integrative Genomics Viewer (IGV): high-performance genomics data visualization and exploration. *Briefings in bioinformatics* 14**,** 178-192.

Tokai-Nishizumi, N., Ohsugi, M., Suzuki, E., and Yamamoto, T. (2005). The chromokinesin Kid is required for maintenance of proper metaphase spindle size. *Molecular biology of the cell* 16**,** 5455-5463.

Tokai, N., Fujimoto-Nishiyama, A., Toyoshima, Y., Yonemura, S., Tsukita, S., Inoue, J., and Yamamota, T. (1996). Kid, a novel kinesin-like DNA binding protein, is localized to chromosomes and the mitotic spindle. *The EMBO journal* 15**,** 457.

Trapnell, C., Roberts, A., Goff, L., Pertea, G., Kim, D., Kelley, D.R., Pimentel, H., Salzberg, S.L., Rinn, J.L., and Pachter, L. (2012). Differential gene and transcript expression analysis of RNA-seq experiments with TopHat and Cufflinks. *Nat. Protocols* 7**,** 562-578.

Trapnell, C., Williams, B.A., Pertea, G., Mortazavi, A., Kwan, G., Van Baren, M.J., Salzberg, S.L., Wold, B.J., and Pachter, L. (2010). Transcript assembly and quantification by RNA-Seq reveals unannotated transcripts and isoform switching during cell differentiation. *Nature biotechnology* 28**,** 511-515.

Troxell, C.L., Sweezy, M.A., West, R.R., Reed, K.D., Carson, B.D., Pidoux, A.L., Cande, W.Z., and Mcintosh, J.R. (2001). pkl1(+)and klp2(+): Two kinesins of the Kar3 subfamily in fission yeast perform different functions in both mitosis and meiosis. *Mol Biol Cell* 12**,** 3476-3488.

Vale, R.D., Reese, T.S., and Sheetz, M.P. (1985). Identification of a novel force-generating protein, kinesin, involved in microtubule-based motility. *Cell* 42**,** 39-50.

Van Der Auwera, G.A., Carneiro, M.O., Hartl, C., Poplin, R., Del Angel, G., Levy-Moonshine, A., Jordan, T., Shakir, K., Roazen, D., Thibault, J., Banks, E., Garimella, K.V., Altshuler, D., Gabriel, S., and Depristo, M.A. (2013). "From FastQ Data to High-Confidence Variant Calls: The Genome Analysis Toolkit Best Practices Pipeline," in *Current Protocols in Bioinformatics*. John Wiley & Sons, Inc.).

Walczak, C., Verma, S., and Mitchison, T. (1997). XCTK2: A Kinesin-related Protein That Promotes Mitotic Spindle Assembly in *Xenopus laevis* Egg Extracts. *Journal of Cell Biology* 136**,** 859-870.

Walczak, C.E., Vernos, I., Mitchison, T.J., Karsenti, E., and Heald, R. (1998). A model for the proposed roles of different microtubule-based motor proteins in establishing spindle bipolarity. *Current biology* 8**,** 903-913.

Walker, R.A., Salmon, E.D., and Endow, S.A. (1990). The Drosophila Claret Segregation Protein Is a Minus-End Directed Motor Molecule. *Nature* 347**,** 780-782.

Wang, S.-Z., and Adler, R. (1995). Chromokinesin: a DNA-binding, kinesin-like nuclear protein. *Journal of Cell Biology* 128**,** 761-768.

Wu, C.-I., Lyttle, T.W., Wu, M.-L., and Lin, G.-F. (1988). Association between a satellite DNA sequence and the Responder of Segregation Distorter in D. melanogaster. *Cell* 54**,** 179-189.

Yang, C.Y., Spielman, M., Coles, J., Li, Y., Ghelani, S., Bourdon, V., Brown, R., Lemmon, B., Scott, R.J., and Dickinson, H. (2003). TETRASPORE encodes a

kinesin required for male meiotic cytokinesis in Arabidopsis. *The Plant Journal* 34**,** 229-240.

Yang, J.T., Laymon, R.A., and Goldstein, L.S. (1989). A three-domain structure of kinesin heavy chain revealed by DNA sequence and microtubule binding analyses. *Cell* 56**,** 879-889.

Yu, H.-G., Hiatt, E.N., Chan, A., Sweeney, M., and Dawe, R.K. (1997). Neocentromere-mediated Chromosome Movement in Maize. *The Journal of Cell Biology* 139**,** 831-840.

Zhang, D., and Nicklas, R.B. (1995). The impact of chromosomes and centrosomes on spindle assembly as observed in living cells. *Journal of Cell Biology* 129**,** 1287-1300.

Zhang, H., and Dawe, R.K. (2011). Mechanisms of plant spindle formation. *Chromosome research* 19**,** 335-344.

Zhang, H., Phan, B.H., Wang, K., Artelt, B.J., Jiang, J., Parrott, W.A., and Dawe, R.K. (2012). Stable integration of an engineered megabase repeat array into the maize genome. *The Plant Journal* 70**,** 357-365.

Zhong, C.X., Marshall, J.B., Topp, C., Mroczek, R., Kato, A., Nagaki, K., Birchler, J.A., Jiang, J., and Dawe, R.K. (2002). Centromeric Retroelements and Satellites Interact with Maize Kinetochore Protein CENH3. *The Plant Cell* 14**,** 2825-2836.

Table 4.1 Transmission of Ab10 as a male parent

Male Parent	Ab10 Offspring	N10 Offspring	Sum	% Ab10
I-MMR	164	126	290	0.565517241
I-MMR	147	116	263	0.558935361
I-MMR	169	149	318	0.531446541
I-MMR	163	161	324	0.50308642
I-MMR	159	160	319	0.498432602
I-MMR	216	250	466	0.463519313
I-MMR	202	234	436	0.463302752
TOTAL I-MMR	**1220**	**1196**	**2416**	**0.504966887**
II-MMR	202	124	326	0.619631902
II-MMR	206	161	367	0.561307902
II-MMR	253	206	459	0.551198257
II-MMR	69	59	128	0.5390625
II-MMR	301	264	565	0.532743363
II-MMR	252	223	475	0.530526316
II-MMR	329	299	628	0.52388535
II-MMR	100	102	202	0.495049505
II-MMR	196	206	402	0.487562189
II-MMR	190	204	394	0.482233503
II-MMR	155	168	323	0.479876161
II-MMR	38	43	81	0.469135802
II-MMR	190	216	406	0.467980296
II-MMR	91	142	233	0.39055794
TOTAL II-MMR	**2572**	**2417**	4989	0.515534175
III-Caq	221	144	365	0.605479452
III-Caq	215	164	379	0.567282322
III-Caq	254	206	460	0.552173913
III-Caq	248	211	459	0.540305011
III-Caq	224	190	414	0.541062802
III-Caq	238	203	441	0.53968254
III-Caq	139	114	253	0.549407115
III-Caq	130	113	243	0.534979424
III-Caq	190	173	363	0.523415978
III-Caq	162	158	320	0.50625
TOTAL III-Caq	**2021**	**1676**	3697	0.546659454

III-Hui	190	85	275	0.690909091
III-Hui	252	144	396	0.636363636
III-Hui	255	184	439	0.580865604
III-Hui	225	160	385	0.584415584
III-Hui	164	120	284	0.577464789
III-Hui	144	104	248	0.580645161
III-Hui	207	161	368	0.5625
III-Hui	106	83	189	0.560846561
III-Hui	112	89	201	0.55721393
III-Hui	144	119	263	0.547528517
III-Hui	179	165	344	0.520348837
III-Hui	58	51	109	0.532110092
III-Hui	158	148	306	0.516339869
III-Hui	34	38	72	0.472222222
III-Hui	105	101	206	0.509708738
TOTAL III-Hui	**2333**	**1752**	4085	0.571113831
III-Oax	301	229	530	0.567924528
III-Oax	151	110	261	0.578544061
III-Oax	105	78	183	0.573770492
III-Oax	95	75	170	0.558823529
III-Oax	140	118	258	0.542635659
III-Oax	127	108	235	0.540425532
III-Oax	129	110	239	0.539748954
III-Oax	232	216	448	0.517857143
III-Oax	175	182	357	0.490196078
III-Oax	137	133	270	0.507407407
III-Oax	306	302	608	0.503289474
III-Oax	236	238	474	0.497890295
III-Oax	118	118	236	0.5
TOTAL III-Oax	**2252**	**2017**	4269	0.52752401

Table 4.2 Pollen viability of Ab10 plants

Pollen Source	Viable Pollen	Aborted Pollen	% Viable
N10/N10	477	23	0.954
N10/N10	495	5	0.99
N10/N10	470	1	0.997876858
N10/N10	478	22	0.956
TOTAL N10/N10	**1920**	**51**	**0.97412481**
Ab10/N10	487	13	0.974
Ab10/N10	496	14	0.97254902
Ab10/N10	495	5	0.99
Ab10/N10	481	19	0.962
Ab10/N10	467	33	0.934
Ab10/N10	489	14	0.972166998
Ab10/N10	462	38	0.924
Ab10/N10	470	30	0.94
Ab10/N10	485	15	0.97
Ab10/N10	493	7	0.986
Ab10/N10	483	17	0.966
Ab10/N10	487	13	0.974
TOTAL Ab10/N10	**5795**	**218**	**0.963745219**
Ab10/Ab10	478	22	0.956
Ab10/Ab10	476	24	0.952
Ab10/Ab10	452	48	0.904
Ab10/Ab10	400	100	0.8
Ab10/Ab10	473	27	0.946
Ab10/Ab10	480	20	0.96
Ab10/Ab10	500	100	0.833333333
Ab10/Ab10	479	21	0.958
TOTAL Ab10/Ab10	**3738**	**362**	**0.911707317**

Table 4.3 Seed count and seed weight of Ab10 plants

Female Parent	Seed Count	Total Mass of Seeds (g)	Mass per 100 Seeds (g)
N10/N10	287	75.97	26.47038328
N10/N10	53	14.93	28.16981132
N10/N10	311	94.99	30.54340836
N10/N10	64	11.4	17.8125
N10/N10	195	60.19	30.86666667
N10/N10	186	49.75	26.74731183
N10/N10	245	68.2	27.83673469
N10/N10	301	85.47	28.39534884
N10/N10	294	69.52	23.6462585
N10/N10	274	81.07	29.58759124
N10/N10	57	12.22	21.43859649
N10/N10	271	84.88	31.32103321
N10/N10	294	74.78	25.43537415
N10/N10	280	73.89	26.38928571
N10/N10	243	75.24	30.96296296
N10/N10	68	17.89	26.30882353
N10/N10	315	87.81	27.87619048
N10/N10	57	15.79	27.70175439
N10/N10	268	71.81	26.79477612
N10/N10	320	83.85	26.203125
N10/N10	292	82.56	28.2739726
N10/N10	371	90.55	24.40700809
N10/N10	142	35.54	25.02816901
N10/N10	254	74.16	29.19685039
N10/N10	330	93.48	28.32727273
N10/N10	313	92.03	29.40255591
N10/N10	357	104.75	29.34173669
N10/N10	213	61.12	28.69483568
N10/N10	204	53.7	26.32352941
N10/N10	355	88.52	24.93521127
N10/N10	292	76.16	26.08219178
N10/N10	307	86.69	28.23778502
N10/N10	263	77.2	29.35361217
N10/N10	329	88.63	26.93920973
N10/N10	318	87.25	27.43710692
N10/N10	334	90.79	27.18263473
N10/N10	400	111.39	27.8475
N10/N10	320	97.96	30.6125
N10/N10	314	99.27	31.61464968
N10/N10	347	87.33	25.16714697

N10/N10	389	102.92	26.45758355
N10/N10	305	90	29.50819672
N10/N10	215	59.96	27.88837209
N10/N10	371	105.64	28.47439353
N10/N10	387	102.8	26.56330749
N10/N10	347	95.95	27.65129683
N10/N10	272	62.64	23.02941176
AVERAGE N10/N10	**270.7234043**	**74.65191489**	**27.57497642**
Ab10/N10	155	34.54	22.28387097
Ab10/N10	305	79.3	26
Ab10/N10	86	12.33	14.3372093
Ab10/N10	81	20.88	25.77777778
Ab10/N10	277	74.57	26.92057762
Ab10/N10	169	43.77	25.89940828
Ab10/N10	288	76.28	26.48611111
Ab10/N10	89	19.69	22.12359551
Ab10/N10	86	19.51	22.68604651
Ab10/N10	290	76.58	26.40689655
Ab10/N10	323	84.43	26.13931889
Ab10/N10	234	71.44	30.52991453
Ab10/N10	92	23.25	25.27173913
Ab10/N10	79	16.67	21.10126582
Ab10/N10	263	64.62	24.57034221
Ab10/N10	435	76.93	17.68505747
Ab10/N10	271	71.64	26.43542435
Ab10/N10	229	55.29	24.1441048
Ab10/N10	348	94.45	27.1408046
Ab10/N10	236	61.28	25.96610169
Ab10/N10	262	71.28	27.20610687
Ab10/N10	282	78.29	27.76241135
Ab10/N10	131	36.23	27.65648855
Ab10/N10	223	62.51	28.03139013
Ab10/N10	232	64.85	27.95258621
Ab10/N10	314	60.64	19.31210191
Ab10/N10	295	73.81	25.02033898
Ab10/N10	113	31.72	28.07079646
Ab10/N10	271	58.19	21.47232472
Ab10/N10	224	63.91	28.53125
Ab10/N10	286	86.16	30.12587413
Ab10/N10	288	55.81	19.37847222
Ab10/N10	126	37.3	29.6031746
Ab10/N10	141	40.2	28.5106383
Ab10/N10	366	75.54	20.63934426
Ab10/N10	236	66.97	28.37711864
Ab10/N10	111	28.35	25.54054054

Ab10/N10	369	90.07	24.40921409
Ab10/N10	331	80.33	24.26888218
Ab10/N10	325	86.99	26.76615385
Ab10/N10	240	49.15	20.47916667
Ab10/N10	264	67.58	25.59848485
Ab10/N10	287	89.64	31.23344948
Ab10/N10	343	91.4	26.64723032
Ab10/N10	267	81.82	30.64419476
Ab10/N10	237	39.25	16.56118143
Ab10/N10	233	61.32	26.31759657
Ab10/N10	293	87.54	29.87713311
Ab10/N10	172	48.16	28
Ab10/N10	190	50.18	26.41052632
Ab10/N10	295	65.99	22.36949153
Ab10/N10	242	55.49	22.92975207
Ab10/N10	117	33.8	28.88888889
Ab10/N10	105	21.65	20.61904762
Ab10/N10	291	81.76	28.09621993
Ab10/N10	273	86.05	31.52014652
Ab10/N10	114	33.83	29.6754386
Ab10/N10	205	58.77	28.66829268
Ab10/N10	248	69.07	27.85080645
Ab10/N10	245	64.32	26.25306122
Ab10/N10	66	11.39	17.25757576
Ab10/N10	331	89.53	27.04833837
Ab10/N10	210	62.88	29.94285714
Ab10/N10	131	31.75	24.23664122
Ab10/N10	330	65.02	19.7030303
Ab10/N10	316	92.59	29.30063291
Ab10/N10	169	50.6	29.9408284
Ab10/N10	387	102	26.35658915
Ab10/N10	329	88.65	26.94528875
Ab10/N10	283	79.29	28.01766784
Ab10/N10	261	76.35	29.25287356
Ab10/N10	206	55.22	26.80582524
Ab10/N10	138	38.76	28.08695652
Ab10/N10	254	72.38	28.49606299
Ab10/N10	83	12.2	14.69879518
Ab10/N10	137	37.84	27.62043796
Ab10/N10	177	55.78	31.51412429
Ab10/N10	251	67.15	26.75298805
Ab10/N10	176	34.24	19.45454545
Ab10/N10	351	93.65	26.68091168
Ab10/N10	211	65.4	30.99526066
Ab10/N10	330	64.97	19.68787879
Ab10/N10	327	98.53	30.13149847
AVERAGE Ab10/N10	**233.4578313**	**60.35590361**	**25.85302162**

Ab10/Ab10	158	44.12	27.92405063
Ab10/Ab10	117	21	17.94871795
Ab10/Ab10	62	10.26	16.5483871
Ab10/Ab10	97	23.84	24.57731959
Ab10/Ab10	66	15.75	23.86363636
Ab10/Ab10	132	33.25	25.18939394
Ab10/Ab10	139	19.06	13.71223022
Ab10/Ab10	83	13.5	16.26506024
Ab10/Ab10	66	13.58	20.57575758
Ab10/Ab10	91	17.5	19.23076923
Ab10/Ab10	85	17.08	20.09411765
Ab10/Ab10	96	17.44	18.16666667
Ab10/Ab10	44	4.95	11.25
Ab10/Ab10	109	19.81	18.17431193
Ab10/Ab10	154	45.66	29.64935065
Ab10/Ab10	135	36.02	26.68148148
Ab10/Ab10	87	20.38	23.42528736
Ab10/Ab10	38	5.58	14.68421053
Ab10/Ab10	55	6.59	11.98181818
Ab10/Ab10	92	16.54	17.97826087
Ab10/Ab10	63	13.27	21.06349206
Ab10/Ab10	95	21.82	22.96842105
Ab10/Ab10	163	44.19	27.11042945
Ab10/Ab10	160	40.45	25.28125
Ab10/Ab10	60	13.18	21.96666667
Ab10/Ab10	121	26.7	22.0661157
Ab10/Ab10	91	25.43	27.94505495
Ab10/Ab10	109	28.79	26.41284404
Ab10/Ab10	68	13.77	20.25
Ab10/Ab10	73	14.56	19.94520548
Ab10/Ab10	137	40.69	29.70072993
Ab10/Ab10	26	3.4	13.07692308
Ab10/Ab10	54	12.44	23.03703704
Ab10/Ab10	18	2.15	11.94444444
Ab10/Ab10	156	43.35	27.78846154
Ab10/Ab10	96	18.46	19.22916667
Ab10/Ab10	75	18.91	25.21333333
Ab10/Ab10	76	10.49	13.80263158
Ab10/Ab10	90	18.85	20.94444444
Ab10/Ab10	49	3.29	6.714285714
Ab10/Ab10	140	33.76	24.11428571
Ab10/Ab10	145	36.68	25.29655172
Ab10/Ab10	151	37.26	24.67549669
Ab10/Ab10	100	22.72	22.72
Ab10/Ab10	91	18.13	19.92307692
Ab10/Ab10	54	9.65	17.87037037
AVERAGE Ab10/Ab10	**94.93478261**	**21.18043478**	**22.31051065**

Table 4.4 Complete list of SNPs which cause missense mutations in the shared region of Ab10

Gene ID	Substitution	PROVEAN	Prediction	Closest Arabidopsis Homolog, Predicted Gene Function
Zm00001d026563_T001	R55C	-7.833	Deleterious	ERF7; ethylene-responsive transcription factor; ABA sensitive
Zm00001d026651_T001	P83R	-5.4	Deleterious	unknown function; single exon, monocot-specific
Zm00001d026381_T001	H235Y	-5.258	Deleterious	DUF572; unknown function
Zm00001d026573_T001	R441I	-4.322	Deleterious	MTK1; methylthioribose kinase; sulfur-sensitive
Zm00001d026548_T001	P54H	-4.307	Deleterious	KCBP; kinesin-like calmodulin binding protein; binds to phragmoplast
Zm00001d026425_T001	K67N	-4.306	Deleterious	AT1G14340; RNA-binding; oxidoreductase
Zm00001d026351_T001	Q451H	-4.015	Deleterious	ATML1; homeobox-leucine zipper protein; stomata & leaf development
Zm00001d026669_T001	S274Y	-3.949	Deleterious	FTSZ2-2; plastid division
Zm00001d026647_T001	D794N	-3.687	Deleterious	MSH3; DNA mismatch repair protein
Zm00001d026536_T001	L201F	-3.55	Deleterious	AT1G19860; Zinc finger CCCH domain-containing protein 6
Zm00001d026391_T001	F120S	-3.321	Deleterious	NAA10; embryo development
Zm00001d026334_T001	V432A	-2.993	Deleterious	PAO2; polyamine oxidase
Zm00001d026633_T001	V329A	-2.768	Deleterious	AIRP2; ubiquitin ligase, induced by ABA; ABA hyposensitive
Zm00001d026362_T001	R747Q	-2.389	Neutral	ALY3; essential for spermatogenesis
Zm00001d026326_T001	E347V	-2.307	Neutral	FBX2; phosphate sensing
Zm00001d026587_T001	V400D	-2.13	Neutral	AT2G02160; Zinc finger CCCH domain-containing protein 17
Zm00001d026587_T001	D612G	-2.109	Neutral	AT2G02160; Zinc finger CCCH domain-containing protein 17
Zm00001d026261_T001	N320H	-1.876	Neutral	AT4G31350; Cre-2/I-branching beta-1,6-N-acetylglucosaminyltransferase family protein
Zm00001d026270_T001	G1121D	-1.68	Neutral	EMB1135; RING/FYVE/PHD zinc finger superfamily protein
Zm00001d026477_T001	G211R	-1.461	Neutral	TIFY3B; unknown function
Zm00001d026590_T001	Q426R	-1.397	Neutral	ARF8; auxin response factor
Zm00001d026587_T001	R282G	-1.311	Neutral	AT2G02160; Zinc finger CCCH domain-containing protein 17
Zm00001d026307_T001	Q236*	-1.27	Neutral	MORF3; multiple organellar RNA editing factor 3
Zm00001d026487_T001	R26S	-1.194	Neutral	KAKU4; affects nuclear envelope
Zm00001d026630_T001	Q300H	-1.093	Neutral	CLC2; clathrin light chain 2; localizes to cell plate
Zm00001d026632_T001	A165V	-1.042	Neutral	AT4G27450; aluminum-induced protein with YGL and LRDR motifs
Zm00001d026452_T001	N877D	-0.95	Neutral	AT2G23360; filament-like plant protein 7
Zm00001d026511_T001	M950T	-0.789	Neutral	M3KE1; MAP3K epsilon protein kinase 1
Zm00001d026223_T001	A78E	-0.656	Neutral	AT3G03150; unknown function
Zm00001d026536_T001	S290L	-0.65	Neutral	AT1G19860; Zinc finger CCCH domain-containing protein 6
Zm00001d026271_T001	P124A	-0.622	Neutral	ERF4; ethylene-responsive transcription factor
Zm00001d026439_T001	V1292A	-0.609	Neutral	AT1G15290; Tetratricopeptide repeat (TPR)-like superfamily protein
Zm00001d026452_T001	P610R	-0.581	Neutral	AT2G23360; filament-like plant protein 7
Zm00001d026452_T001	L668V	-0.581	Neutral	AT2G23360; filament-like plant protein 7
Zm00001d026668_T001	L696F	-0.581	Neutral	TMK2; receptor-like kinase
Zm00001d026452_T001	N877S	-0.567	Neutral	AT2G23360; filament-like plant protein 7
Zm00001d026586_T001	S176T	-0.564	Neutral	LDL1; lysine-specific demethylase1
Zm00001d026662_T001	A41V	-0.56	Neutral	YLS9; leaf senescence-associated
Zm00001d026511_T001	D336G	-0.55	Neutral	M3KE1; MAP3K epsilon protein kinase 1
Zm00001d026396_T001	E167K	-0.542	Neutral	MIC60; mitochondia-targeted
Zm00001d026452_T001	I131V	-0.467	Neutral	AT2G23360; filament-like plant protein 7
Zm00001d026333_T001	R106Q	-0.465	Neutral	GTE7; transcription factor
Zm00001d026537_T001	S96N	-0.383	Neutral	WUS; stem-cell maintenance of meristems
Zm00001d026280_T001	R283G	-0.381	Neutral	AT4G19610; unknown function
Zm00001d026537_T001	S225R	-0.367	Neutral	WUS; stem-cell maintenance of meristems
Zm00001d026452_T001	L844V	-0.344	Neutral	AT2G23360; filament-like plant protein 7
Zm00001d026280_T001	A203S	-0.324	Neutral	AT4G19610; unknown function
Zm00001d026535_T001	E672A	-0.19	Neutral	IQD32; microtubule-associated protein
Zm00001d026630_T001	A35G	-0.189	Neutral	CLC2; clathrin light chain 2; localizes to cell plate
Zm00001d026280_T001	N284K	-0.015	Neutral	AT4G19610; unknown function
Zm00001d026587_T001	V400I	0	Neutral	AT2G02160; Zinc finger CCCH domain-containing protein 17
Zm00001d026359_T001	F435L	0.021	Neutral	AT3G20720; unknown function
Zm00001d026452_T001	I212L	0.044	Neutral	AT2G23360; filament-like plant protein 7
Zm00001d026213_T001	D319N	0.115	Neutral	Translation elongation factor EF1A/initiation factor IF2gamma family protein
Zm00001d026511_T001	L499M	0.135	Neutral	M3KE1; MAP3K epsilon protein kinase 1
Zm00001d026477_T001	G199D	0.139	Neutral	TIFY3B; unknown function
Zm00001d026535_T001	I671V	0.157	Neutral	IQD32; microtubule-associated protein
Zm00001d026326_T001	Q268K	0.174	Neutral	FBX2; phosphate sensing
Zm00001d026283_T001	P29A	0.289	Neutral	AT1G30630; coatomer epsilon subunit
Zm00001d026501_T001	G33V	0.313	Neutral	GLN2; glutamine synthetase

Zm00001d026351_T001	S175A	0.415	Neutral	ATML1; homeobox-leucine zipper protein; stomata & leaf development
Zm00001d026668_T001	M852L	0.484	Neutral	TMK2; receptor-like kinase
Zm00001d026684_T001	G259A	0.529	Neutral	AT1G75710; C2H2-like zinc finger protein
Zm00001d026193_T001	T581A	0.589	Neutral	AT1G65010; putative WEB family protein
Zm00001d026600_T001	R321K	0.62	Neutral	PAT11; protein S-acyltransferase 11
Zm00001d026668_T001	S265G	0.648	Neutral	TMK2; receptor-like kinase
Zm00001d026351_T001	L355M	0.66	Neutral	ATML1; homeobox-leucine zipper protein; stomata & leaf development
Zm00001d026495_T001	R522K	0.685	Neutral	AT5G20600; unknown function
Zm00001d026630_T001	V33G	0.725	Neutral	CLC2; clathrin light chain 2; localizes to cell plate
Zm00001d026649_T001	A152V	0.895	Neutral	AAE3; oxalate-CoA ligase
Zm00001d026649_T001	A135T	0.895	Neutral	AAE3; oxalate-CoA ligase
Zm00001d026627_T001	A128G	1.226	Neutral	AT3G15470; Transducin/WD40 repeat-like superfamily protein
Zm00001d026346_T001	T36M	1.296	Neutral	RBP45C; polyadenylate-binding protein
Zm00001d026439_T001	H1220Q	1.44	Neutral	AT1G15290; Tetratricopeptide repeat (TPR)-like superfamily protein
Zm00001d026311_T001	L472H	1.459	Neutral	MEE25; NAD(P)-binding Rossmann-fold superfamily protein
Zm00001d026577_T001	A146G	1.558	Neutral	RD21B; cysteine protease
Zm00001d026333_T001	I429T	1.658	Neutral	GTE7; transcription factor

Table 4.5 Rates of meiotic drive in different Ab10 haplotypes

Female Parent	Ab10 Offspring	N10 Offspring	Sum	% Ab10
I-MMR	323	113	436	0.740825688
I-MMR	382	122	504	0.757936508
I-MMR	436	141	577	0.755632582
I-MMR	432	162	594	0.727272727
I-MMR	289	106	395	0.73164557
I-MMR	359	101	460	0.780434783
TOTAL I-MMR	**2221**	**745**	**2966**	**0.74881996**
I-Jal	271	144	415	0.653012048
I-Jal	208	158	366	0.568306011
I-Jal	156	87	243	0.641975309
I-Jal	366	201	567	0.645502646
I-Jal	282	198	480	0.5875
I-Jal	219	113	332	0.659638554
I-Jal	300	239	539	0.556586271
TOTAL I-Jal	**1802**	**1140**	**2942**	**0.612508498**
II-MMR	224	83	307	0.729641694
II-MMR	262	76	338	0.775147929
II-MMR	149	65	214	0.696261682
TOTAL II-MMR	**635**	**224**	**859**	**0.739231665**
II-Tel	130	42	172	0.755813953
II-Tel	192	57	249	0.771084337
TOTAL II-Tel	**322**	**99**	**421**	**0.764845606**
II-Sal	114	29	143	0.797202797
II-Sal	182	80	262	0.694656489
II-Sal	115	47	162	0.709876543
II-Sal	229	94	323	0.708978328
TOTAL II-Sal	**640**	**250**	**890**	**0.719101124**
III-Caq	388	72	460	0.843478261
III-Caq	295	89	384	0.768229167
III-Caq	265	66	331	0.80060423
III-Caq	337	80	417	0.808153477
III-Caq	332	133	465	0.713978495
III-Caq	248	56	304	0.815789474
TOTAL III-Caq	**1865**	**496**	**2361**	**0.789919526**
III-Gua	140	39	179	0.782122905
III-Gua	315	63	378	0.833333333
III-Gua	427	97	524	0.814885496
III-Gua	370	110	480	0.770833333
III-Gua	367	133	500	0.734
TOTAL III-Gua	**1619**	**442**	**2061**	**0.785541**

III-Hui	281	202	483	0.581780538
III-Hui	251	140	391	0.641943734
III-Hui	288	168	456	0.631578947
III-Hui	291	139	430	0.676744186
III-Hui	186	137	323	0.575851393
TOTAL III-Hui	**1297**	**786**	**2083**	**0.622659626**
III-Oax	246	53	299	0.822742475
III-Oax	314	51	365	0.860273973
III-Oax	329	83	412	0.798543689
III-Oax	175	84	259	0.675675676
III-Oax	322	88	410	0.785365854
III-Oax	258	55	313	0.82428115
TOTAL III-Oax	**1644**	**414**	**2058**	**0.798833819**
N10	342	337	679	0.503681885
N10	274	283	557	0.491921005
N10	234	262	496	0.471774194
TOTAL N10	**850**	**882**	**1732**	**0.490762125**

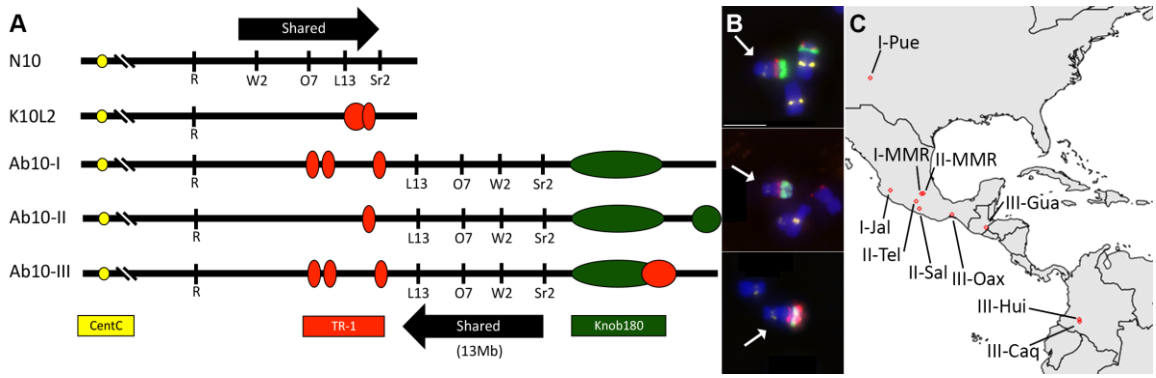

Figure 4.1 The abnormal chromosome 10 haplotype in *Zea mays*.

(A) Chromosome models of different haplotypes of chromosome 10 in *Zea mays*. The locations of CentC (yellow), TR-1 (red), and Knob-180 (green) repeats are colored as listed. The locations of marker loci *colored1* (R1), *white seedling2* (W2), *opaque endosperm7* (O7), *luteus13* (L13), and *striate leaves2* (Sr2) are listed below their relative positions. Note that in Ab10-I, Ab10-II, and Ab10-III haplotypes, the relative ordering of W2, O7, and L13 is inverted in what is known as the "shared region." K10L2 contains these same genes but their order and position relative to its knob is unknown.

(B) Fluorescent in situ hybridization of maize repeats. Haplotypes I-MMR, II-MMR, III-Caq are shown from top to bottom (arrows). Color of stains correspond to colors in Figure 4.1A. Scale is the equivalent for all images. Scalebar = 10 um.

(C) Map of locations haplotypes were originally collected from across North and South America.

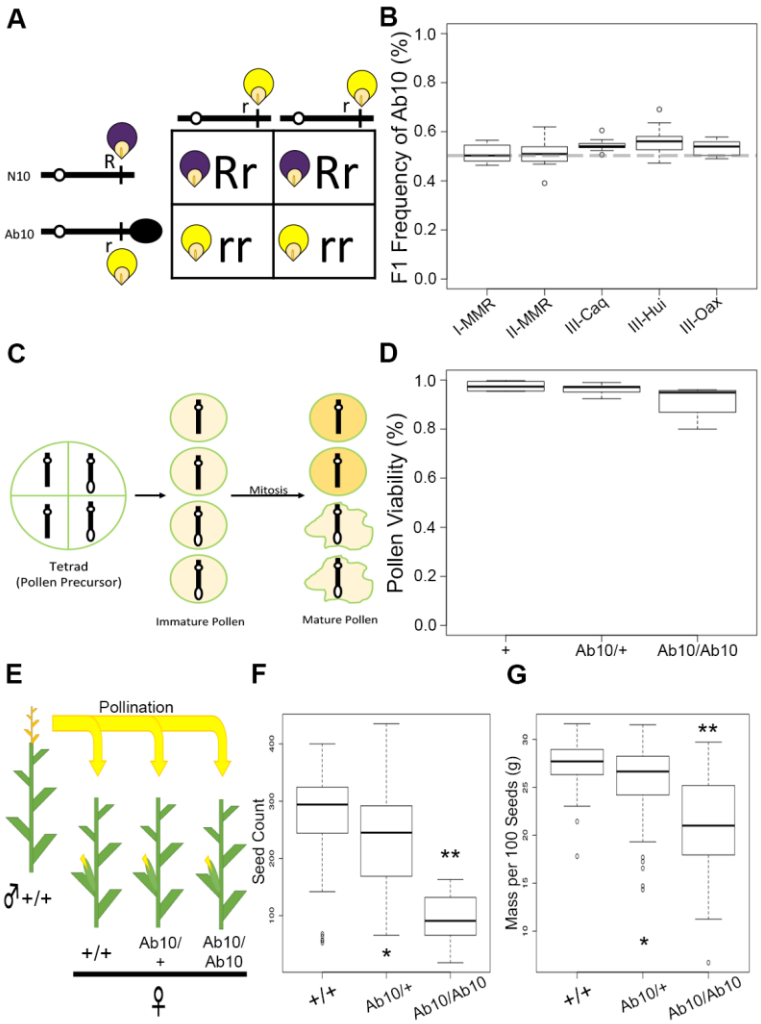

Figure 4.2 Transmission of Ab10 is not inhibited through the male gametophyte though seed count and weight are reduced in homozygotes.

(A) Punnett square model diagramming the crossing scheme used to measure inheritance of Ab10. The Ab10 haplotype (represented as a dark oval on the chromosome diagram) is linked to the recessive allele of *r1*, resulting in yellow kernels. The dominant allele *R1*, causing a purple kernel phenotype, is linked to the N10 haplotype. Plants heterozygous for these two alleles (*R*-N10/*r*-Ab10) were crossed to a recessive tester (*r*-N10/*r*-N10). Kernels in the resulting F1 generation were counted by color, representing the inheritance

of either N10 (purple) or Ab10 (yellow). If Mendelian inheritance is occurring, an equal, 50:50 ratio would be observed.

(B) Quantification of the transmission rates of five Ab10 haplotypes as a male parent. None of the medians were lower than 50%. Transmission in 4 of the haplotypes was significantly higher than expected as determined by chi-squared analysis at a=0.05 (labeled *) or a=0.01 (labeled **).

(C) Model demonstrating the hypothesis that Ab10 may be affecting development of male gametophytes. In plants, the products of meiosis must undergo mitotic divisions before being capable of fertilization. It is possible that after meiosis, those gametophytes carrying Ab10 (chromosomes with white ovals) fail to fully mature and are unable to fertilize seeds.

(D) Pollen viability from dehiscent anthers in different Ab10-I-MMR genotypes. Pollen viability in maize homozygous for N10 (x=0.97) and N10/I-MMR heterozygotes (x=0.96) are not significantly different as determined by a t-test (p=0.195). The Ab10 homozygote had significantly lower pollen viability (x=0.91) than both N10 and I-MMR/N10 (x=0.96) (p=0.049 and 0.009, respectively).

(E) The effect of the Ab10 on seed count was measured through pollination of a I-MMR haplotype backcrossed into the B73 inbred background. Sibling plants carrying either N10, Ab10, or heterozygotes were pollenated by N10 pollen.

(F) Seed count in Ab10 homozygotes (x=95) and Ab10 heterozygotes (x=233) is significantly reduced compared to N10 wild types (x=271). Statistical significance as determined by a t-test is indicated with asterisk (*: $p<0.05$, **: $p<0.001$).

(G) Mass per hundred seeds in Ab10 homozygotes (x=20.8g) and Ab10 heterozygotes (x=25.7g) is significantly reduced compared to N10 wild types (x=27.3g). Statistical significance as determined by a t-test is indicated as in Figure 4.2F.

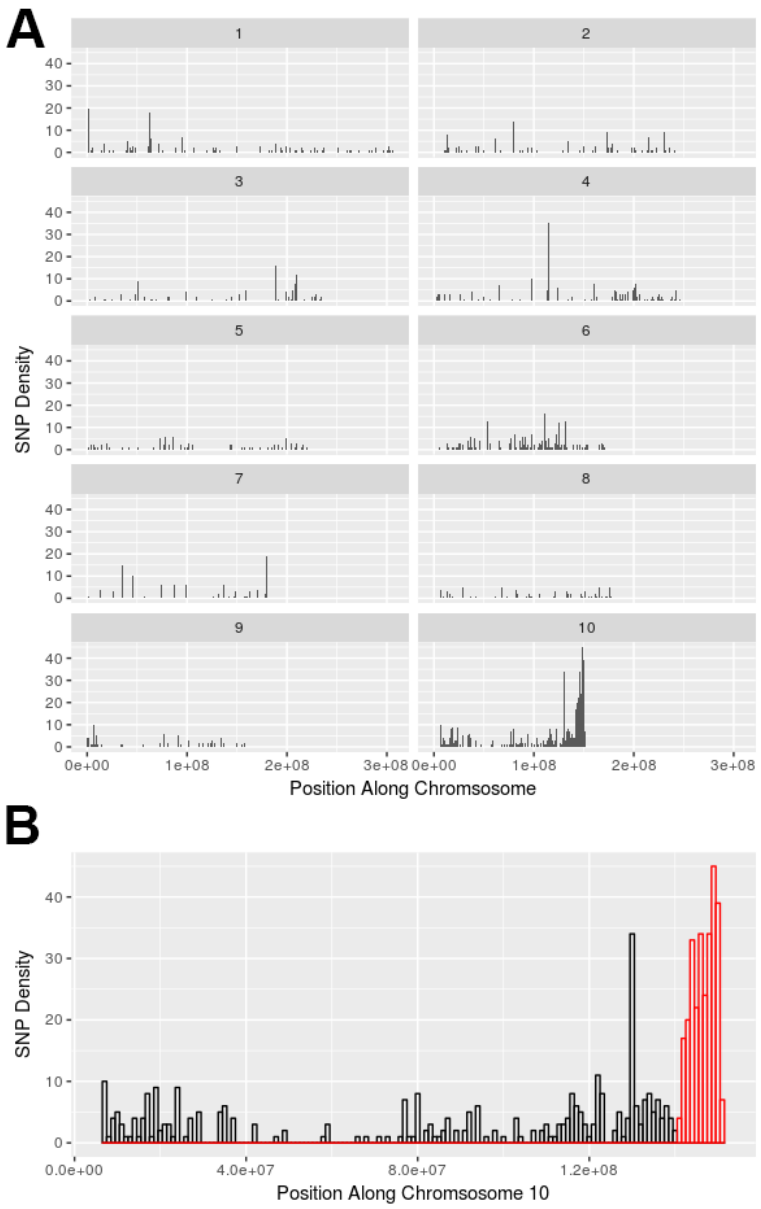

Figure 4.3 An enrichment of variation exists in the shared region between N10 and Ab10.

SNPs were identified through transcriptome sequencing on meiotic anthers.

(A) Histogram showing the location of SNPs in the maize genome. The height of each bar represents the number of SNPs in each 1 million basepair window.

(B) Histogram showing the location of SNPs, as above, on chromosome 10. The shared region downstream of the *R1* locus is highlighted in red. 13.6% of SNPs identified map to this region which only represents 0.5% of the total genome size.

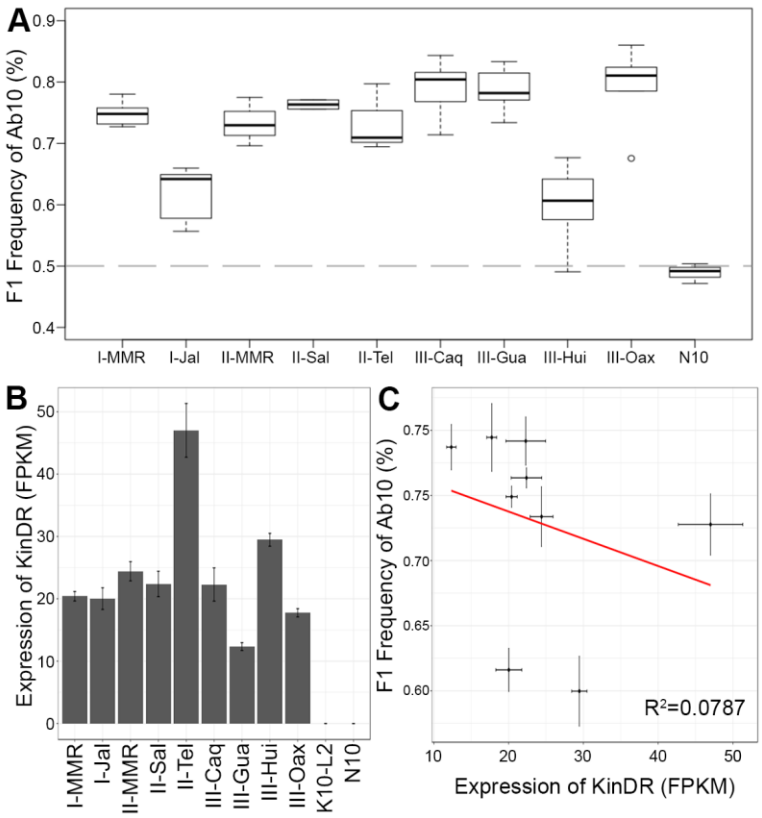

Figure 4.4 Rates of meiotic drive and Kindr expression are largely conserved across haplotypes.

(A) The F1 frequency of Ab10 as transmitted through female parents was calculated using the same crossing scheme as diagrammed in Figure 4.2A. Rates of meiotic drive are largely consistent with the I-MMR haplotype used for prior studies of Ab10. Groups of statistical significance are listed with letters as determined by ANOVA and Tukey's HSD.

(B) Expression of *Kindr* in each Ab10 haplotype is measured in fragments per kilobase of transcript per million mapped reads (FPKM) as calculated using Cufflinks. Groups of statistical significance are listed with letters as determined by Cuffdiff.

(C) When plotted against one another, the two variables of *Kindr* expression and meiotic drive show no correlation (R^2=0.0787). Error bars represent standard error for both variables.

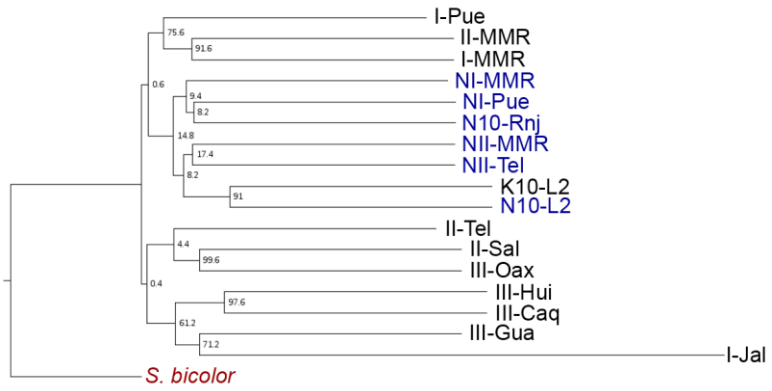

Figure 4.5 Phylogeny of Ab10 haplotypes.

This estimated species tree was generated from 190 individual gene trees derived from genes in the shared region combined using the software ASTRAL (Mirarab and Warnow, 2015). Ab10 haplotypes are listed in black while N10 haplotypes are listed in black. The closest homolog for each gene was identified in the Sorghum bicolor genome and used as an outgroup, shown in red. Numbers at the base of node represent a measure of support out of a maximum of 100 called "local posterior probability" (Sayyari and Mirarab, 2016).

CHAPTER 5

CONCLUSIONS AND DIRECTIONS FOR FUTURE STUDY

The transition of life from prokaryotic to eukaryotic brought new challenges for cells, including larger cytoplasm, compartmentalization of cellular processes, and specialized cell shapes. Microtubules and microfilaments are the two components of the cytoskeleton which provide cell structure as well as a network for shuttling molecular cargo to necessary locations. Kinesins are the microtubule motor proteins that carry out these functions in plants. The kinesin gene family has undergone a massive expansion, consistent with the diverse functions its members carry out (as reviewed in Miki et al., 2005; Hirokawa et al., 2009), but its members have the same general structure. The typical kinesin molecule consists of three domains, a highly conserved motor domain responsible for binding to microtubules and hydrolyzing adenosine triphosphate (ATP), a coiled-coil linker domain that allows kinesins to dimerize, and a highly specialized cargo-binding tail.

The kinesin superfamily is organized into 14 distinct subfamilies, each with different molecular cargoes specific to their cellular function. While several families are implicated in microtubule organization and chromosome segregation, members of the kinesin-14A subfamily are unique in having motor domains located on the C-terminal end of the protein. Consistent with this changing of the motor position is a change in the directionality of these enzymes: this class of kinesins moves in a minus-end directed

fashion in contrast to the other 13 plus-end directed families (McDonald et al., 1990; Ambrose et al., 2005).

The goal of this study was to further understand the role members of the kinesin-14A subfamily play in spindle assembly and chromosome segregation in *Zea mays*. In the following sections, the major findings of Chapters 2, 3, and 4 are presented with a discussion of their context as well as future directions to be examined in subsequent work.

THE ROLE OF KINESIN-14A IN SPINDLE ASSEMBLY AND CHROMOSOME ORGANIZATION

In Chapter 2, we identified the classic *Zea mays* (maize) mutant *divergent spindle1* (*dv1*) to be the gene *ZmKin6* (GRMZM2G114861). The *dv1* mutant was first isolated over 75 years ago due to its effects on pollen viability; when pollen mother cells were screened, the spindle poles at metaphase were found to be highly unfocused and disorganized (Clark, 1940). Given that this phenotype is consistent with mutants of other members of the kinesin-14A subfamily (McDonald et al., 1990; Meluh and Rose, 1990; Mitsui et al., 1993; Walczak et al., 1997), we undertook a candidate gene approach to identify *dv1*, sequencing the two members of the 14A subfamily in the *dv1* background. We identified a premature stop codon in *ZmKin6*, upstream of the motor domain which we predict would result in a nonfunctional protein. Expression of *ZmKin6* is decreased in the *dv1* background, likely due to nonsense mediated decay. Additionally, a second allele of *dv1* was identified which produces a similar phenotype and the two mutants fail to

complement one another. Given together, we concluded from this evidence that *dv1* is encoded by *ZmKin6*.

We further characterized the role *dv1* plays in spindle formation through fixed-cell immunolocalization as well as live-cell fluorescent imaging. Quantification of spindle shape demonstrated that *dv1* mutants have longer half-spindle lengths as well as wider metaphase plates in meiosis. Live cell imaging of the prophase-metaphase transition in *dv1* mutants showed widely dispersed chromosomes at the moment of nuclear envelope breakdown; three small spindles formed around each set of chromosomes which were then brought together as the microtubules folded into a parallel arrangement.

Our observation that *dv1* mutants show chromosome segregation defects at both prometaphase and metaphase suggests that kinesin-14As may play a role in chromosome organization in addition to spindle organization. Kinesin-1s are capable of transferring force across the nuclear envelope through a direct interaction with the SUN-KASH complex, affecting rates of recombination (Duroc et al., 2014). The potential for kinesin-14A to carry out a similar function is corroborated by the mislocalization of *ZmSUN2* in the *dv1* background (Murphy et al., 2014) as well as observed defects in nuclear envelope breakdown in *dv1* using electron microscopy (Shamina et al., 2000). Future experiments should be directed at better characterizing the interaction between members of the kinesin-14A and SUN protein families. A direct interaction between the cargo domain of kinesin-14A and *ZmSun2* can be carried out using a yeast 2-hybrid system, or an alternative protein binding test such as bimolecular fluorescence complementation or protein co-immunoprecipitation. If a similar interaction as members of the kinesin-1

subfamily is shown, it is possible that kinesin-14A knockouts will have the same effects on recombination rates (Duroc et al., 2014). Rates of recombination in the *dv1* background have never been measured but crosses to the B73 inbred line were made in the completion of this project. As the source of the reference genome, B73 is highly characterized but the genetic background of *dv1* is more ambiguous. Novel genetic markers could be identified in the *dv1* using a genotyping by sequencing assay, but a more accessible approach may be to carry out these experiments in *Arabidopsis thaliana* where rates of recombination can be estimated by observing different fluorescent protein constructs in the products of meiosis in the TETRASPORE background (Berchowitz and Copenhaver, 2008).

THE ROLE OF KINESIN-14A IN THE ABNORMAL CHROMOSOME 10 MEIOTIC DRIVE SYSTEM

In Chapter 3, we characterized *Kindr*, a novel kinesin-14A implicated in the abnormal chromosome 10 (Ab10) meiotic drive system in maize. In meiosis, the four sister chromatids are segregated into a separate daughter cell in a random fashion, allowing the two alleles to be passed on to the next generation at a 50:50 ratio. That each allele gets an equal chance at inheritance is important for the forces of natural selection to act effectively (Austin and Trivers, 2006), but there exist a number of "selfish elements" that are transmitted at a rate greater than 50%, a process known as meiotic drive (Sandler and Novitski, 1957).

Ab10 was first identified as a meiotic drive element by Marcus Rhoades who observed preferential transmission of a kernel color allele linked to the knobbed Ab10

haplotype (Rhoades, 1942). Cytogenetic studies of this maize line identified a novel phenomenon in which normally inert heterochromatic knobs become activated "neocentromeres" which move to the spindle poles ahead of the normal centromeres (Rhoades and Vilkomerson, 1942). Rhoades went on to hypothesize that these neocentromeres are responsible for the drive phenotype – by pulling knobbed chromosome arms ahead of the centromeres, a knobbed chromosome will preferentially end in the single product of female meiosis which comes a fertile egg, allowing it to be inherited at a higher rate than 50:50 (Rhoades, 1952). Recent sequencing projects identified *Kindr*, a novel gene located in the distal tip of Ab10. *Kindr* is most closely related to the maize gene *ZmKin11*, a class 14A kinesin, sharing a C-terminal kinesin motor domain with a unique, derived cargo-binding tail (Lowry, 2015). As a member of the minus-end directed kinesin family, *Kindr* represents an ideal candidate for the neocentromere-activating gene, potentially binding to knobs and moving them toward the spindle pole (microtubule minus-end).

Transcriptome sequencing of Ab10 mutants deficient for meiotic drive demonstrated that expression of *Kindr* is disrupted in three of the five mutants tested, indicating it plays a role in the drive phenotype. Two of the mutants, *smd8* and *smd13* showed no significant decrease in *Kindr* expression although they do not exhibit meiotic drive, indicating that *Kindr* alone is not sufficient for meiotic drive to occur. An RNAi knockdown targeting *Kindr* showed a loss of drive associated with a loss of *Kindr* expression, indicating it is necessary for the drive phenotype. Attempts at imaging *Kindr* using both fixed-cell immunolocalization and live-cell fluorescent protein tags failed to identify protein localization within meiocytes.

The conclusion that *Kindr* is necessary but not sufficient for drive indicates that there are additional factors present in Ab10 which have not yet been identified. It is already known that there are two genes responsible for neocentromere movement, one for each of the major knob repeats in maize (Hiatt et al., 2002). Rather than recognizing the DNA sequence itself, it is possible that *Kindr* binds with another factor which interacts with the knob specifically. Kinesins are capable of binding DNA directly (Wang and Adler, 1995; Tokai et al., 1996), though such an interaction has never been shown in the 14A subfamily. In fact, many of the kinesins which bind DNA are also capable of binding chromatin proteins *in vivo* (Soeda et al., 2016; Takahashi et al., 2016), suggesting this may be a method of *Kindr* activity. In order to identify the cargo of *Kindr,* the tail could be used as the bait for a yeast 2-hybrid library derived from Ab10 transcripts. This would account for any novel genes unique to Ab10 present elsewhere on the distal tip although such a gene could also be present in the inverted shared region linked to the Ab10 haplotype. Future efforts to characterize the sub-cellular localization of *Kindr* should be focused on capturing images of the female meiocyte rather than using male meiocytes as a proxy. The female meiocyte, the site of the phenotype, is a highly elongated cell which undergoes asymmetric cell division and does not resemble pollen mother cells (Golubovskaya et al., 1992). It is possible that *Kindr* does not bind knobs at all, and is instead acting through an alternative mechanism to alter spindle position in the female meiocyte as dynein does in other organisms (Nguyen-Ngoc et al., 2007). Direct visualization of KINDR in female meiocytes is likely to provide important clues about how the protein acts to promote meiotic drive.

ABNORMAL CHROMOSOME 10 MEIOTIC DRIVE

In Chapter 4, we studied the evolutionary consequences of the Ab10 meiotic drive system. As a heterozygote, Ab10 preferentially segregates at a rate of approximately 70% through the female parent (Rhoades, 1942). Given this huge advantage in inheritance, it would be assumed that Ab10 should quickly reach fixation in open pollinated maize populations. To the contrary, assessments of chromosome diversity in maize land races indicate that the frequency of Ab10 within populations is quite low – only 6 - 13% (McClintock et al., 1981; Kanizay et al., 2013b).

We tested two different hypotheses for why Ab10 is maintained at low frequencies in populations. The first was based specifically on Ab10 transmission as a male. As the drive phenotype is observed exclusively through the female, it is possible that there are negative impacts of Ab10 on transmission through pollen. No evidence was found to support this hypothesis: transmission through pollen was measured in five different Ab10 genotypes and none were found to transmit below the expected level of 50%. Additionally, pollen viability in plants heterozygous for Ab10 was found to not be significantly different from wild type, indicating Ab10 does not affect male fertility as a heterozygote. Pollen viability in the Ab10 homozygous genotype was significantly lower (91% viable), leading us to our second hypothesis regarding homozygous disadvantage. The Ab10 chromosome carries an inversion in which essential genes are unable to recombine with the normal chromosome 10 (N10). It is possible that deleterious mutations have arisen in these genes which are maintained by the inversion and meiotic drive. Without a functional copy from N10, Ab10 homozygotes have decreased fitness, keeping their frequency in populations low. In addition to the pollen data above, Ab10

homozygotes were measured to have significantly reduced seed count (64.9% fewer seeds) and seed mass (23.7% smaller seeds). Furthermore, transcriptome sequencing of genes in the shared region identified an enrichment of variants in the shared region including a number which result in predicted deleterious substitutions. These results indicate that there are strong fitness costs associated with Ab10 homozygosity, helping to explain the overall low frequency of Ab10 in nature.

Drive rates in a diversity panel of Ab10 from North, Central, and South America were measured and determined to be largely consistent, driving between 70-80% inheritance. Drive rates do not correlate with knob size nor do they correlate with expression of *Kindr*, further supporting the conclusions of Chapter 3 that additional meiotic drive factors have yet to be identified. A phylogeny of variants in the shared region indicates recombination of the haplotypes, suggesting genetic material within the shared region is freely exchanged between them within open pollenated land races.

While providing the first phenotyping of homozygous Ab10 and the detection of deleterious variants linked to the driver, a limit of the study is the nature by which the variants were identified. Transcripts from meiotic anthers were sequenced and mapped to the B73 reference genome, preventing the detection of variants in genes with poor expression and the identification of novel genes which might be unique to Ab10. A future direction should be to complete a genomic reference of an Ab10 haplotype. This would allow several further experiments, including a comprehensive list of variants in this region, identification of any novel transcripts including other factors which may be implicated in drive. If supported by BioNano optical mapping, the new reference could

also be used to identify the exact locations of knob repeats as well as the breakpoints of the inversion, offering a full characterization of Ab10.

WORKS CITED

Ambrose, J.C., Li, W., Marcus, A., Ma, H., and Cyr, R. (2005). A minus-end-directed kinesin with plus-end tracking protein activity is involved in spindle morphogenesis. *Mol Biol Cell* 16**,** 1584-1592.

Austin, B., and Trivers, R. (2006). *Genes in Conflict.* Harvard University Press.

Berchowitz, L.E., and Copenhaver, G.P. (2008). Fluorescent Arabidopsis tetrads: a visual assay for quickly developing large crossover and crossover interference data sets. *Nat. Protocols* 3**,** 41-50.

Clark, F.J. (1940). Cytogenetic Studies of Divergent Meiotic Spindle Formation in Zea Mays. *American Journal of Botany* 27**,** 547-559.

Duroc, Y., Lemhemdi, A., Larchevêque, C., Hurel, A., Cuacos, M., Cromer, L., Horlow, C., Armstrong, S.J., Chelysheva, L., and Mercier, R. (2014). The kinesin AtPSS1 promotes synapsis and is required for proper crossover distribution in meiosis. *PLoS Genet* 10**,** e1004674.

Golubovskaya, I., Avalkina, N.A., and Sheridan, W.F. (1992). Effects of several meiotic mutations on female meiosis in maize. *genesis* 13**,** 411-424.

Hiatt, E.N., Kentner, E.K., and Dawe, R.K. (2002). Independently regulated neocentromere activity of two classes of tandem repeat arrays. *The Plant Cell Online* 14**,** 407-420.

Hirokawa, N., Noda, Y., Tanaka, Y., and Niwa, S. (2009). Kinesin superfamily motor proteins and intracellular transport. *Nat Rev Mol Cell Biol* 10**,** 682-696.

Kanizay, L.B., Pyhajarvi, T., Lowry, E.G., Hufford, M.B., Peterson, D.G., Ross-Ibarra, J., and Dawe, R.K. (2013). Diversity and abundance of the abnormal chromosome 10 meiotic drive complex in Zea mays. *Heredity* 110**,** 570-577.

Lowry, E.G. (2015). *The meiotic drive mechanism of a selfish chromosome in Zea mays.* Doctor of Philosophy, University of Georgia.

Mcclintock, B., Yamakake, T.a.K., and Blumenschein, A. (1981). *Chromosome constitution of races of maize: its significance in the interpretation of relationships between races and varieties in the Americas.* Colegio de Postgraduados Mexico.

Mcdonald, H.B., Stewart, R.J., and Goldstein, L.S. (1990). The kinesin-like ncd protein of Drosophila is a minus end-directed microtubule motor. *Cell* 63**,** 1159-1165.

Meluh, P.B., and Rose, M.D. (1990). KAR3, a kinesin-related gene required for yeast nuclear fusion. *Cell* 60**,** 1029-1041.

Miki, H., Okada, Y., and Hirokawa, N. (2005). Analysis of the kinesin superfamily: insights into structure and function. *Trends in Cell Biology* 15**,** 467-476.

Mitsui, H., Yamaguchi-Shinozaki, K., Shinozaki, K., Nishikawa, K., and Takahashi, H. (1993). Identification of a gene family (kat) encoding kinesin-like proteins in

Arabidopsis thaliana and the characterization of secondary structure of KatA. *Molecular and General Genetics MGG* 238**,** 362-368.
Murphy, S.P., Gumber, H.K., Mao, Y., and Bass, H.W. (2014). A dynamic meiotic SUN belt includes the zygotene-stage telomere bouquet and is disrupted in chromosome segregation mutants of maize (Zea mays L.). *Frontiers in Plant Science* 5**,** 314.
Nguyen-Ngoc, T., Afshar, K., and Gonczy, P. (2007). Coupling of cortical dynein and G[alpha] proteins mediates spindle positioning in Caenorhabditis elegans. *Nat Cell Biol* 9**,** 1294-1302.
Rhoades, M., and Vilkomerson, H. (1942). On the anaphase movement of chromosomes. *Proceedings of the National Academy of Sciences* 28**,** 433-436.
Rhoades, M.M. (1942). Preferential Segregation in Maize. *Genetics* 27**,** 395-407.
Rhoades, M.M. (1952). "Preferential Segregation in Maize", in: *Heterosis.* (ed.) J.W. Gowen. Iowa State College Press).
Sandler, L., and Novitski, E. (1957). Meiotic drive as an evolutionary force. *The American Naturalist* 91**,** 105-110.
Shamina, N., Dorogova, N., and Trunova, S. (2000). Radial Spindle and the Phenotype of the Maize Meiotic Mutant, DV. *Cell Biology International* 24**,** 729-736.
Soeda, S., Yamada-Nomoto, K., and Ohsugi, M. (2016). The microtubule-binding and coiled-coil domains of Kid are required to turn off the polar ejection force at anaphase. *J Cell Sci* 129**,** 3609-3619.
Takahashi, M., Wakai, T., and Hirota, T. (2016). Condensin I-mediated mitotic chromosome assembly requires association with chromokinesin KIF4A. *Genes & Development* 30**,** 1931-1936.
Tokai, N., Fujimoto-Nishiyama, A., Toyoshima, Y., Yonemura, S., Tsukita, S., Inoue, J., and Yamamota, T. (1996). Kid, a novel kinesin-like DNA binding protein, is localized to chromosomes and the mitotic spindle. *The EMBO journal* 15**,** 457.
Walczak, C., Verma, S., and Mitchison, T. (1997). XCTK2: A Kinesin-related Protein That Promotes Mitotic Spindle Assembly in *Xenopus laevis* Egg Extracts. *Journal of Cell Biology* 136**,** 859-870.
Wang, S.-Z., and Adler, R. (1995). Chromokinesin: a DNA-binding, kinesin-like nuclear protein. *Journal of Cell Biology* 128**,** 761-768.